THE CRYSTAL STRUCTURES OF SOME ORGANIC ACIDS

THESIS
PRESENTED FOR THE DEGREE OF
DOCTOR OF PHILOSOPHY
IN THE
UNIVERSITY OF GLASGOW
BY

GEORGE A. SIM, B.Sc.

SEPTEMBER, 1955.

PREFACE

This thesis describes the investigation by X-ray diffraction methods, of the crystal structures of benzoic acid, 11-amino-undecanoic acid hydrobromide hemihydrate, and isopalmitic acid. It also contains a description of attempts to solve some other crystal structures. An introductory chapter on some of the methods used in the thesis is included.

I wish to thank Professor J.M. Robertson, Dr. V. Vand, and Dr. W. Cochran, who have been my supervisors at various stages of the work described here. My gratitude to other colleagues, in particular Dr. M.M. Woolfson and Dr. T.H. Goodwin, for discussion and advice must also be acknowledged.

I am grateful to Dr. M.V. Wilkes and the computing staff of the Mathematical Laboratory of the University of Cambridge for the evaluation of Fourier series on the Hollerith machine, and for various calculations performed on E.D.S.A.C., the electronic computer in the Mathematical Laboratory. To my wife who undertook many calculations for me, I am also grateful.

I wish to express my thanks to Professor N.F. Mott and Dr. W.H. Taylor for provision of research facilities during a year spent in the Cavendish Laboratory, Cambridge.

I am indebted to the Department of Scientific and Industrial Research for a maintenance grant, and later to the Ramsay Memorial Fellowships Trust for the award of a Fellowship, which enabled me to undertake this work.

Summary

The crystal structures of some organic acids have been examined by X-ray diffraction methods.

Benzoic acid is monoclinic, space group $P2_1/c$, with four molecules per unit cell. The crystal structure has been accurately determined from a study of projections of ρ_o and $(\rho_o-\rho_c)$ along the a and b axes. The molecules occur as planar, centrosymmetrical dimers, with hydrogen bonds of length 2.64 Å between the adjacent carboxyl groups. The hydrogen atoms bonded to the benzene carbon atoms have been clearly revealed in difference syntheses but the carboxyl hydrogen has proved difficult to locate. Corrections have been made for the anisotropic thermal vibration of many of the atoms. Bond length variations in the benzene ring have been found and are discussed. The analysis has been carried out with both visually estimated and Geiger-counter measured intensities and the results obtained with each are compared.

11-amino-undecanoic acid hydrobromide is monoclinic, space group A2/a, with eight molecules per unit cell. The atomic coordinates have been derived from a study of projections of ρ_o and $(\rho_o-\rho_c)$ along the a and b axes. Dimeric association between adjacent carboxyl groups occurs and the water molecules, situated on twofold axes, are involved in hydrogen bonding with the Br^- and NH_3^+ ions. The average distance between two

alternate carbon atoms in the hydrocarbon chain is 2.563 Å, and the average C-C bond length is 1.539 Å, the estimated standard deviation of these values being 0.013 Å. The hydrocarbon chain is planar but the terminal nitrogen atom is displaced from this plane. Alternate hydrocarbon chains are inclined in opposite directions and cross each other.

Expressions have been derived giving the fraction of reflexions for any particular structure which are determined in sign by a heavy atom or by a group of atoms. In the case of 11-amino-undecanoic acid hydrobromide hemihydrate it was found possible to make an accurate prediction of the fraction of reflexions which have the same sign as the appropriate bromine contribution.

Isopalmitic acid is triclinic, space group $P\bar{1}$, with two molecules in the unit cell. Electron-density projections along the a axis have been prepared and approximate coordinates for the oxygen and carbon atoms have been estimated.

CONTENTS

GENERAL INTRODUCTION

A very wide range of chemical information can be obtained from the X-ray analyses of organic compounds, depending both on the accuracy of the experimental data and on the techniques used in interpreting that data.

If only the stereochemistry of the molecule as a whole is required, that is, the order in which individual atoms are bonded together, atomic positions need not be known more precisely than within 0.1 Å. In this case highly accurate intensity data is not necessary, and it is not essential to use a very elaborate model for the calculation of structure factors.

If, on the other hand, bond lengths accurate to about a hundredth of an Angstrom unit are required to discuss some problem in valency, or if interest is centred on obtaining information about the location of hydrogen atoms or the distribution of bonding electrons, then use must be made of the developments which have taken place in recent years in improving both experimental and interpretative techniques.

The important advance in experimental technique was the introduction of the Geiger-counter for the measurement of

intensities, which has enabled structure factors to be estimated with a standard deviation of about 1%. In order to make full use of the accuracy available in this way very elaborate refinement of the structure is necessary, with allowance for the effects of anisotropic vibration, termination of series, and the presence of hydrogen atoms. The question of the scattering factors to be used is also important.

In the study of the crystal structure of benzoic acid described in this thesis, an attempt has been made to make use of these recent techniques in order to obtain information about the distribution of hydrogen atoms, and about possible bond length variations in the benzene ring.

The analysis of the hydrobromide of 11-amino-undecanoic acid has not been carried out quite so thoroughly as that of benzoic acid, since the presence of the bromide ions in the structure limits the accuracy which may be obtained. In this structure the main points of interest are the hydrogen bonding systems which are present, and the type of packing of the hydrocarbon chains. Although the final coordinates are not of such a high degree of accuracy as those of benzoic acid, it is still possible to obtain interesting results.

The third compound to be described in this thesis, isopalmitic acid, was chosen for study because no detailed structural analysis of a branched chain fatty acid has yet been reported. As it has only been possible to investigate one projection of the structure no detailed information about interatomic distances is available, but nonetheless information about the type of packing of the branched chains has been obtained.

There are now a very large number of methods by which a crystal structure may be solved and the choice of method depends on individual circumstances. A survey of some of the methods used in solving the crystal structures described in this thesis is given in Chapter 1, with the chief emphasis being given to the Fourier Transform method, for this is undoubtedly the most fundamental and elegant introduction to diffraction problems.

CHAPTER I

SOME METHODS OF CRYSTAL STRUCTURE ANALYSIS

1. THE FOURIER TRANSFORM IN CRYSTAL STRUCTURE ANALYSIS

1.1. Introduction

The diffraction properties of a distribution of scattering matter in space are described most directly not in terms of the function representing the distribution, but in terms of another function derived from the first, and known as its Fourier transform. Diffraction experiments measure essentially the transform of the structure, and it is from this transform that the structure must be deduced.

Let $\rho(\underline{r})$ be the density of scattering matter at a point (xyz) in space, and let $\underline{r}$ be the vector from the origin to the point (xyz). Let the directions of incident and scattered waves be defined by the unit vectors $\underline{s}_0$ and $\underline{s}$ respectively and let $\underline{R}$ be the vector $(\underline{s} - \underline{s}_0)/\lambda$, so that $\underline{R}$ has the dimensions of the reciprocal of length. Then the amplitude scattered by the distribution of scattering matter is given by the expression

$$T(\underline{R}) = \int \rho(\underline{r}) \exp.(2\pi i \underline{R}.\underline{r}) d\underline{r} \quad \ldots\ldots\ldots\ldots\ldots (1)$$

$T(\underline{R})$ may be plotted as a distribution in the space, known as reciprocal space, of a vector drawn from the origin and having the magnitude and direction of $\underline{R}$.

1.2. Structure Factors and Scattering Factors

The function $T(\underline{R})$, which is the Fourier transform of $\rho(\underline{r})$,

is known as the structure factor (F) of the distribution $\rho(\underline{r})$, or if $\rho(\underline{r})$ is the electron density in an atom then $T(\underline{R})$ is the scattering factor (f). In the latter case it is possible to calculate values of f for the various atoms by putting $\rho(\underline{r}) = \Sigma|\psi_n|^2$, where ψ_n is the wave-function of the nth electron in the atom. For some atoms values of ψ have been calculated by Hartree and by later workers using the self-consistent field method. The labour involved in the calculation, especially for the heavier atoms, is such that there is not nearly a complete list of f values calculated in this way. Tables of f values calculated by a method of interpolation, based on the accurate calculations for ten different atoms by the self-consistent field method, have been prepared by James and Brindley[1].

More accurate values for some of the lighter atoms have been calculated by McWeeny[2], and recently still more accurate f curves for carbon, nitrogen, and oxygen atoms have been computed from Hartree - Fock radial wave-functions by Hoerni and Ibers[3].

1.3. Expression for $\rho(\underline{r})$

If Fourier's integral theorem is applied to equation (1), the expression

$$\rho(\underline{r}) = \int T(\underline{R}) \exp.(-2\pi i \underline{r} . \underline{R}) d\underline{R} \quad \ldots\ldots\ldots\ldots \quad (2)$$

is obtained. This allows us to calculate the distribution of scattering matter $\rho(\underline{r})$ from a knowledge of its Fourier transform.

1.4. Finite Wave-Length Errors in the Evaluation of $\rho(r)$

In X-ray diffraction experiments only points not further than $2/\lambda$ from the origin of reciprocal space are available for observation, and this introduces errors into the values of $\rho(\underline{r})$ calculated by means of equation (2). This limitation on the knowledge of $T(\underline{R})$ affects the resolving power of the method, for ignorance of the transform outside the sphere of radius $2/\lambda$ drawn from the origin of reciprocal space means that structural details whose dimensions are much smaller than $\lambda/2$ in real space cannot be distinguished[4]. Two peaks in direct space cannot be distinguished if they are closer together than $0.61\lambda/2$, so that for copper $K\alpha$ radiation with $\lambda = 1.54$ Å, the minimum resolvable separation is about 0.47 Å. This should not impair resolution of atoms if full three dimensional data are used, but in projection resolution may be impaired.

1.5. The Transform of a Periodic Distribution

The Fourier transform of a periodically repeating distribution with a large number of repetitions has appreciable values only at certain points known as the reciprocal lattice.

Let the density distribution be contained in a parallelopiped with sides represented by vector translations $\underline{a}$, $\underline{b}$, and $\underline{c}$, and let the number of parallelopipeds packed together in directions $\underline{a}$, $\underline{b}$, and $\underline{c}$, be N_1, N_2, and N_3 respectively.

It can then be shown that the total transform $T(\underline{R})$ of the $N_1N_2N_3$ units is the product of the transform $F(\underline{R})$ of one unit, multiplied by the transform $G(\underline{R})$ of the lattice of point scatterers with primitive translations $\underline{a}$, $\underline{b}$, and $\underline{c}$, and N_1, N_2, N_3 points parallel to these directions respectively. The latter transform in turn can be shown to be the product of three transforms, each representing the transform of a line of N_1, N_2, N_3 points parallel to $\underline{a}$, $\underline{b}$, and $\underline{c}$ respectively. Each of these transforms is of the form

$$G_a(\underline{R}) = \exp.\{\pi i(N_1 - 1)\underline{a}.\underline{R}\} \sin(\pi N_1 \underline{a}.\underline{R}) \div \sin(\pi \underline{a}.\underline{R}) \quad \ldots \quad (3)$$

$G_a(\underline{R})$ is a function of $\underline{a}.\underline{R}$, and is constant over any plane perpendicular to the direction of $\underline{a}$.

Let $\underline{a}^*$ be a vector drawn from the origin perpendicular to the $\underline{bc}$ plane, of length $1/a$. Let $\underline{b}^*$, $\underline{c}^*$ be vectors which are defined in a similar manner. Let the triplet of numbers (ξ, η, ζ) not necessarily integers, define a point at a vector distance $(\xi \underline{a}^* + \eta \underline{b}^* + \zeta \underline{c}^*)$ from the origin. Then

$$\underline{R} = (\xi \underline{a}^* + \eta \underline{b}^* + \zeta \underline{c}^*)$$

and since $\underline{a}.\underline{a}^* = 1$, while $\underline{a}^*.\underline{b} = 0$, etc. we have

$$\underline{a}.\underline{R} = \xi \quad , \quad \underline{b}.\underline{R} = \eta \quad , \quad \underline{c}.\underline{R} = \zeta$$

Thus, for equation (3) we can write

$$G_a(\underline{R}) = \exp.\{\pi i(N_1 - 1)\xi\} \sin(\pi N_1 \xi)/\sin(\pi \xi) \quad \ldots\ldots \quad (4)$$

which has appreciable values for large N_1 only when ξ is an integer. Similar considerations apply to $G_b(\underline{R})$ and $G_c(\underline{R})$, and consequently $G(\underline{R})$, the product of these, only has appreciable values for large N_1, N_2, N_3 when ξ, η and ζ are integers. Thus $T(\underline{R})$, the total transform, only has appreciable values when ξ, η and ζ are integers, say h, k and ℓ.

For a periodic distribution, such as molecules in a crystal, the periodicity causes interference so that the transform of the crystal, which is what we observe, gives us values of the transform of the unit cell sampled at the points of the reciprocal lattice only. The transform of the crystal could be represented as the reciprocal lattice weighted at each point ($hk\ell$) with the value of the structure factor appropriate to that point.

1.6. Structure Factor Formulae

For a periodic distribution of electron density in a

crystal, it was shown in the previous section that the vector $\underline{R} = (\xi\underline{a}^* + \eta\underline{b}^* + \zeta\underline{c}^*)$ only has effective values for scattering when ξ, η and ζ are integers h, k and ℓ respectively.

Let (xyz) define a point at a vector distance $\underline{r} = (x\underline{a} + y\underline{b} + z\underline{c})$ from the origin of the unit cell. Then:

$$\underline{R}.\underline{r} = (h\underline{a}^* + k\underline{b}^* + \ell\underline{c}^*).(x\underline{a} + y\underline{b} + z\underline{c})$$

$$= (hx + ky + \ell z)$$

since $\underline{a}^*.\underline{a} = 1$, etc., and $\underline{a}^*.\underline{b} = 0$, etc.

Equation (1), on making these substitutes for $\underline{r}$ and $\underline{R}$ becomes

$$F(hk\ell) = V\iiint_{000}^{111} \rho(xyz)\ \exp.\{2\pi i(hx + ky + \ell z)\}\,dx\,dy\,dz \quad \ldots\ldots (5)$$

If the electron density distribution is assumed to consist of a set of discrete atoms, the transforms of whose electron densities are the scattering factors f_j, then $F(hk\ell)$ can be expressed as a summation over the N atoms in the unit cell. This gives

$$F(hk\ell) = \sum_{j=1}^{N} f_j\ \exp.\{2\pi i(hx_j + ky_j + \ell z_j)\} \quad \ldots\ldots\ldots\ldots (6)$$

If the unit cell possesses a centre of symmetry this expression can be reduced further to

$$F(hk\ell) = \sum_{j=1}^{N/2} f_j\ \cos 2\pi(hx_j + ky_j + \ell z_j) \quad \ldots\ldots\ldots\ldots\ldots (7)$$

The presence of other elements of symmetry, causing the number of independent atoms to become a smaller fraction of N, allows the expression to be modified further. The structure factor equations for the various space groups are to be found in

"International Tables for X-ray Crystallography"[5].

1.7. The Fourier Series Representation of a Crystal Structure

Since the crystal has a periodic structure it can be represented by a three-dimensional Fourier series, as was first suggested by W.H. Bragg in 1915[6]. Let

$$\rho(xyz) = \sum_{-\infty}^{\infty}\sum\sum A(pqr)\ \exp.\{2\pi i(px + qy + rz)\} \quad \ldots\ldots\ldots\ldots (8)$$

On inserting this expression for ρ in equation (5) we obtain

$$F(hk\ell) = V\iiint_{000} \{\sum_{-\infty}^{\infty}\sum\sum A(pqr)\ \exp.\ 2\pi i(px + qy + rz)\}\exp.2\pi i(hx+ky+\ell z)\ dx\ dy\ dz$$

On integrating, every term is zero except that for which $p = -h$, $q = -k$, $r = -\ell$, when

$$F(hk\ell) = V\iiint_{000} A(\bar{h}\bar{k}\bar{\ell})\,dx\ dy\ dz \quad = VA(\bar{h}\bar{k}\bar{\ell})$$

Consequently $A(\bar{h}\bar{k}\bar{\ell}) = F(hk\ell)/V$, and the Fourier series representing the electron density may be written

$$\rho(xyz) = \frac{1}{V}\sum_{-\infty}^{\infty}\sum\sum F(hk\ell)\ \exp.\{-2\pi i(hx + ky + \ell z)\} \quad \ldots\ldots\ldots (9)$$

The zero term of the series, F(000), may be obtained by substituting $h = 0$, $k = 0$, $\ell = 0$ in equation (5), and integrating, when we obtain

$$F(000) = V\iiint_{000}\rho(xyz)\ dx\ dy\ dz = Z \quad \ldots\ldots\ldots\ldots\ldots\ldots (10)$$

where Z is the total number of electrons in the unit cell. Since the structure factors used in the series decrease with increasing values of $\sin\theta/\lambda$, because of the fall off in the scattering factors of the atoms, the series will converge.

The evaluation of a complete electron density function in three dimensions by means of equation (9) is extremely laborious because of the large number of terms in the series. It is usually only used when great accuracy is required, or when the complexity of the structure is such that other methods do not give reliable results. Normally the series which is used to represent the electron density in a crystal is of the form

$$\rho(xy) = \frac{1}{A}\sum_{-\infty}^{\infty}\sum F(hk)\ \exp.\{-2\pi i(hx+ky)\} \quad \ldots\ldots\ldots\ldots\ldots \quad (11)$$

and this gives the electron density projected on a plane. Because of the much smaller number of terms in the series it can be evaluated much more readily. This type of expression for the electron density was first used by W.L. Bragg to represent the diopside structure[7]. The simplest form of the Fourier series is of the form

$$\rho(x) = \frac{1}{a}\sum_{-\infty}^{\infty}F(h)\ \exp.(-2\pi ihx) \quad \ldots\ldots\ldots\ldots\ldots\ldots\ldots \quad (12)$$

which gives the electron density projected on an axis in the crystal. Although easy to evaluate it usually gives little information when even moderately complex structures are being examined.

1.8. The Phase Problem

The transform of an electron density distribution may be real or complex, and if real assumes both positive and negative

values. The physical meaning of this is that the phase of the scattered radiation is a function of the angle of scattering. In general this phase may take any value, but for a great many crystals the phase, for the correct choice of origin, is either 0 or π, corresponding to $F(hk\ell)$ being positive or negative respectively. If the phase can take any angle then the transform, $F(hk\ell)$, is complex.

There is no method by which the phase of the scattered radiation may be observed directly when dealing with X-ray diffraction. All that can be measured is the intensity of the diffracted beam, from which $|F(hk\ell)|^2$ may be derived. The distribution $|F(hk\ell)|^2$ cannot give the actual density distribution $\rho(\underline{r})$, but can often give useful information, enabling us to derive the phases and subsequently $\rho(\underline{r})$.

The expression for an electron density projection may be written in the form

$$\rho(xy) = \frac{1}{A}\sum\sum|F(hk0)|\cos\{2\pi(hx+ky) - \alpha(hk0)\} \quad \ldots\ldots \quad (13)$$

in which $\alpha(hk0)$ is the phase angle of the $(hk0)$ reflexion. By assigning arbitrary values to α, it is possible to derive an infinite number of electron density projections from the measured structure amplitudes of a given crystal. In order to decide on the correct distribution appeal has to be made to additional facts. These facts fall into two main classes.

The first consists of any known chemical facts. Thus, if the correct molecular formula is known, it is often possible to decide on the correct phases by postulating an atomic arrangement and calculating a set of structure factors. If the observed and calculated amplitudes agree then the calculated phases can be assigned to the observed structure factors.

There are besides various physical properties which may be of use. The electron density distribution must be a positive function, that is, any regions of negative density are not allowable, and a set of phases which gives an appreciable amount of negative density must be incorrect. An acceptable electron density distribution must also be composed of a number of atomic functions which are known approximately in advance.

In section 1.5 it was shown that only some points on the Fourier transform of a periodic distribution of scattering matter are observable. If the complete transform could be observed structure analysis would be infinitely easier, for the phase problem would disappear for centrosymmetric crystals. For these the transform must be positive or negative, and a change in sign would be associated with a zero-surface in the transform. The origin of the transform must be positive, so signs could be allotted by inspection, the transform changeing

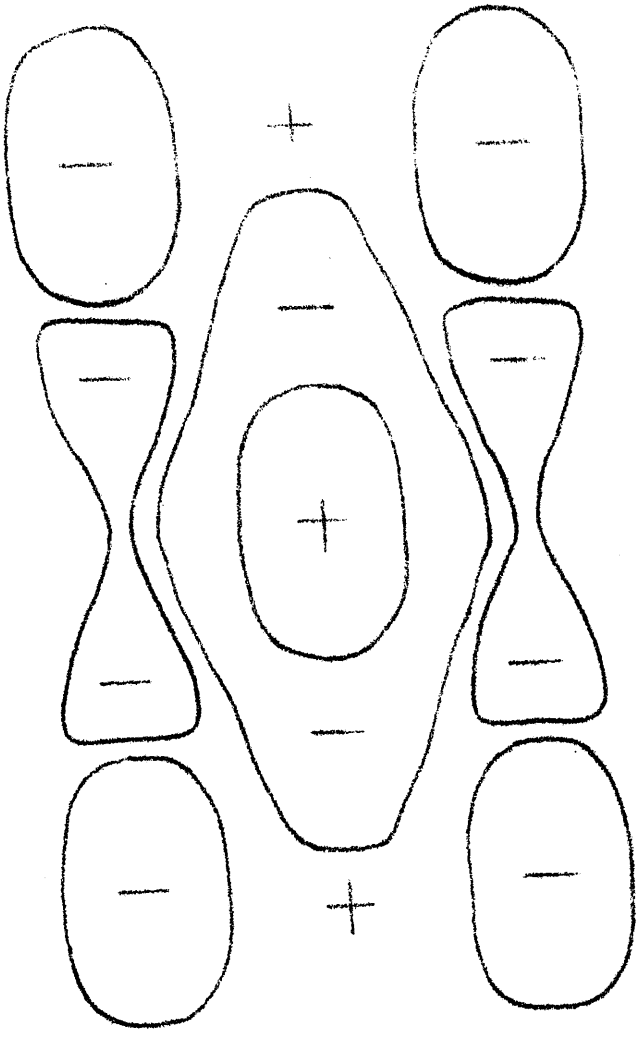

Fig. 1. Transform of a centrosymmetric distribution, illustrating how the lines $T(\underline{R}) = 0$ divide it into regions in which the phase is alternately 0 or π .

sign on passing through zero. This situation is illustrated in Fig. 1 for a two-dimensional case.

This method has recently become of practical value in the study of protein crystals. Horse methaemoglobin[8] forms crystals from which water molecules can be added or removed without much change in the crystal structure apart from small changes in the unit cell dimensions. These changes in the unit cell dimensions cause corresponding changes in the reciprocal lattice, so that intensity data from crystals with different water contents refer to essentially the same transform sampled at different points. This allows the transform to be explored in rather more detail than is usual, and signs can be allotted in some regions of the transform by the above method.

1.9. Application of Molecular Transforms in Structure Analysis

The transform of a crystal structure is the transform of the contents of one unit cell, sampled at the reciprocal lattice points. If the configuration of the contents of the cell is known, the transform of the unit cell could be calculated, and the reciprocal lattice with the same origin as $T(\underline{R})$ rotated about the origin until the values of the transform at the reciprocal lattice points agree with the observed structure amplitudes.[9,10]

Although this seems a straightforward and elegant method of solving crystal structures there are several difficulties to be overcome. Usually the unit cell contains several molecules related by the space-group symmetry, and it would be necessary to calculate first the transform of one molecule, and then to build up the resultant transform of the unit cell for any relative positions and orientations of the molecules. This would normally be a very complicated process. Another difficulty is that in the general case $T(\underline{R})$ will be a three-dimensional function, the evaluation will be arduous, and the representation of $T(\underline{R})$ and the three-dimensional process of fitting a reciprocal lattice to it would be difficult.

Consequently, up to the present time the method has been confined to planar molecules. For these the function $T(\underline{R})$ is cylindrical in character, having the same value along any line perpendicular to the plane of the molecule, and thus only the section in the plane of the molecule need be evaluated. If the molecule possesses a centre of symmetry this is used as origin in calculating the transform, which is everywhere real. If there is no centre of symmetry it is necessary to evaluate both the real and the imaginary parts of the transform and to combine them when calculating structure amplitudes.[10]

For a centrosymmetrical molecule the transform can be expressed as

$$T(\underline{R}) = \sum_{j=1}^{N/2} f_j \cos 2\pi(\xi x_j + \eta y_j) \quad \ldots\ldots\ldots\ldots\ldots (14)$$

where ξ and η may take any value, both integral and non-integral, and where $(x_j\ y_j)$ are the coordinates of the jth atom. Because of the factor f_j the transform is not truly periodic, but if we assume that all the atoms in the molecule have scattering factors of the form $\hat{f}N_j$, where N_j is the number of electrons associated with the jth atom, then the function

$$T(\underline{R})/\hat{f} = \sum_{j=1}^{N/2} N_j \cos 2\pi(\xi x_j + \eta y_j) \quad \ldots\ldots\ldots\ldots\ldots (15)$$

will be truly periodic. If the x and y coordinates are all multiples of p and q Å respectively, the transform will be periodic with repeat distances 1/p and 1/q $Å^{-1}$ respectively.

If we are concerned with a projection of the structure, say on (010), we need consider only the $(h0\ell)$ section of the reciprocal lattice, and the rotation of the reciprocal lattice in space may be accomplished by a suitable distortion of the $(h0\ell)$ reciprocal net on the transform.

The simplest case arises when the molecules in projection are all parallel and have as origin the origin of the unit cell. When the reciprocal-lattice section is fitted properly

to the transform, the values of the transform at the reciprocal-lattice points give directly the structure factors. This is the situation which arises in the analysis of the benzoic acid structure (Chapter III).

2. THE PATTERSON FUNCTION

2.1. Derivation and Meaning

To be able to deduce a set of atomic coordinates from measured intensities it is necessary to know the relative phases of the different reflexions as well as the amplitudes. Patterson[11] showed that the use of a Fourier series employing as coefficients values of $|F(hk\ell)|^2$ yielded information about interatomic vectors.

Let the Fourier transforms of two functions f(x) and h(x) be F(k) and H(k) respectively. Then a result of transform theory is that the transform of the product F(k)H(k) is the convolution[12] of f(x) with h(x).

Transform of $F(k)H(k) = \widehat{f(x)h(x)}$

$$\int_{-\infty}^{\infty} F(k)H(k)\ \exp.(-2\pi ikx)dk = \int_{-\infty}^{\infty} f(y)h(x-y)dy \quad \ldots\ldots\ldots\ (16)$$

Similarly, we have

$$\int_{-\infty}^{\infty} F(\ell)H(k-\ell)d\ell = \int_{-\infty}^{\infty} f(x)h(x)\ \exp.(2\pi ikx)dx \quad \ldots\ldots\ldots\ (17)$$

that is, the transform of f(x)h(x) is the convolution of F(k) with H(k). The process of convolution consists in placing F(k)

with its origin successively at each point of H(k), multiplying it by the value of H(k) at that point, and summing all the results.

It has been shown earlier that the transform of $F(hk\ell)$ is $\rho(xyz)$. Similarly the transform of $F(\bar{h}\bar{k}\bar{\ell})$ is $\rho(\bar{x}\bar{y}\bar{z})$, and the transform of the product $F(hk\ell)F(\bar{h}\bar{k}\bar{\ell})$ will be obtained by convoluting $\rho(xyz)$ with $\rho(\bar{x}\bar{y}\bar{z})$.

$$P(uvw) = \text{Transform of } F(hk\ell)F(\bar{h}\bar{k}\bar{\ell}) = \text{Transform of } |F(hk\ell)|^2$$

$$= V\int_{\circ}^{1}\int_{\circ}^{1}\int_{\circ}^{1} \rho(xyz)\rho(x+u,\ y+v,\ z+w)dx\,dy\,dz \quad \ldots\ldots\ldots(18)$$

If two atoms in a structure are separated by a vector $(\underline{u},\underline{v},\underline{w})$ then the Patterson function P(uvw) will have a peak with coordinates (u,v,w) of weight proportional to the product of the electron densities of the atoms concerned.

2.2. Fourier Series Representation of the Patterson Function

For a periodic crystal $\rho(xyz)$ can be represented in terms of $F(hk\ell)$ by a Fourier series. Similarly P(uvw) can be represented by the Fourier series

$$P(uvw) = \frac{1}{V}\sum_{-\infty}^{\infty}\sum\sum |F(hk\ell)|^2 \exp.\{-2\pi i(hu+kv+\ell w)\} \quad \ldots\ldots\ (19)$$

P(uvw) is real for all values of u,v,w. This can be shown[13] by collecting together the coefficients in pairs $hk\ell$ and $\bar{h}\bar{k}\bar{\ell}$, and then putting $|F(\bar{h}\bar{k}\bar{\ell})|^2 = |F(hk\ell)|^2$.

Consequently equation (19) can be written

$$P(uvw) = \frac{1}{2V}\sum_{-\infty}^{\infty}\sum\sum\left[|F(hk\ell)|^2 \exp.\{-2\pi i(hu+kv+\ell w)\} + |F(\bar{h}\bar{k}\bar{\ell})|^2 \exp.\{2\pi i(hu+kv+\ell w)\}\right]$$

$$= \frac{1}{2V}\sum_{-\infty}^{\infty}\sum\sum |F(hk\ell)|^2 \left[\exp.\{-2\pi i(hu+kv+\ell w)\} + \exp.\{2\pi i(hu+kv+\ell w)\}\right]$$

$$= \frac{1}{V}\sum_{-\infty}^{\infty}\sum\sum |F(hk\ell)|^2 \cos 2\pi(hu+kv+\ell w) \quad \ldots\ldots \quad (20)$$

2.3. Practical Applications

For a crystal of moderate complexity the Patterson function, especially a two-dimensional projection, will be very difficult to interpret. If the unit cell contains N atoms, the Patterson function should contain N^2 peaks. The density of peaks N^2/V (or N^2/A in projection) will increase rapidly as N increases, since V is proportional to N, and in consequence when there are more than about ten atoms in the unit cell it is only rarely that individual peaks will be recognised.

One important case where the Patterson function can be used fairly directly is when the crystal contains a small number of heavy atoms in the unit cell. Vectors between the heavy atoms, and perhaps between heavy atoms and light atoms, then cause Patterson peaks which stand out against the background of peaks due to the light atoms. The coordinates of the heavy atoms can be determined from the Patterson quite

readily, their contributions to each structure factor evaluated, and the remaining atoms then revealed by Fourier methods.

When the structure does not contain a proportion of atoms heavier than the majority it is necessary to know approximately the geometry of the molecule concerned. It may then be possible to explain the Patterson peaks in terms of expected atomic separations, as in the analysis of salicylic acid by Cochran.[31]

3. TRIAL AND ERROR METHODS

The most commonly employed method (until recently at any rate) for molecules which contain no heavy atom, consists of postulating a likely configuration for the molecule, and its position in the unit cell. Structure factors for this set of atomic coordinates are then calculated, and compared with the measured X-ray amplitudes. If there is some measure of agreement it is assumed that the arrangement is approximately correct, and coordinates are changed in order to improve the agreement. When there is a good measure of agreement the process of refinement by successive Fourier syntheses can be undertaken.

In order to postulate a likely set of coordinates the observed intensities must be considered. Low-order reflexions indicate the orientation of the molecule, while high-order reflexions may be used to obtain atomic coordinates.

Abrahams & Robertson[15] in their analysis of the structure of p-nitroaniline made use of the presence of a very strong (202) reflexion to deduce approximate positions for the molecules. In their analysis of the coronene structure Robertson & White[16] employed several outstanding high-order reflexions to give the structure in almost complete detail, since it consists, to a first approximation, of regular hexagons. This type of deduction may be regarded as simply a special case of the use of Fourier transforms, though of course it is impractical to consider the use of these if the molecule is nonplanar.

4. DIRECT METHODS OF SIGN DETERMINATION

4.1. Introduction

The discussion which follows is limited to centrosymmetric crystals or projections.

In recent years a large number of investigations have taken place on the limitations imposed on the signs of the coefficients of a Fourier series representing the electron density ρ, by the condition that ρ must be positive everywhere. Harker & Kasper[17] derived sets of inequality relations between the structure factors, and it is now known that these are based on the positivity of the electron density. Karle & Hauptmann[18] have given a discussion of the limitations imposed by the positivity of the electron density, and from determinant

relations between the Fourier coefficients deduced inequalities.

Unfortunately these inequalities to be applied successfully need large unitary structure factors. (A unitary structure factor $U(hk\ell)$ is defined to be $F(hk\ell)/Z\hat{f}$, where $\hat{f}$ is the unitary scattering factor, and Z is the total number of electrons in the unit cell.) The root-mean-square average unitary structure factor, for a unit cell containing N equal atoms is $1/\sqrt{N}$, and values of $U(hk\ell)$ are distributed approximately according to a Gaussian law. Hence only 10% will exceed $1.7/\sqrt{N}$ and only 0.1% will exceed $3.3/\sqrt{N}$. As N increases, $\{\overline{U^2\{\overline{U^2(hk\ell)}\}}\}^{\frac{1}{2}}$ will be smaller, and in consequence for moderately complex molecules Harker-Kasper inequalities will be of little use.

4.2. Sign Relations between Structure Factors

For a crystal composed of equal, resolved atoms, Sayre[19] has derived an equality relationship between structure factors. Later Cochran,[20] and Zachariasen[21] developed this relationship further, and showed that the signs of three unitary structure factors U(h), U(h'), and U(h+h') tend to be related by the equation

$$S(h)S(h') = S(h+h') \quad \ldots\ldots\ldots\ldots\ldots\ldots \quad (21)$$

where S(h) denotes the sign of U(h). Consequently the product U(h)U(h')U(h+h') will tend to be positive, and Cochran

& Douglas[22] have evolved a method whereby E.D.S.A.C., the electronic computer in the Cambridge University Mathematical Laboratory, selects sets of signs for a given set of unitary structure factors such that

$$\chi = \sum_{h}\sum_{h'} U(h)U(h')U(h+h') \quad \ldots\ldots\ldots\ldots\ldots\ldots \quad (22)$$

will be large and positive. The correct set of signs will give a large value for χ, but in many cases an incorrect set of signs gives a larger value of χ than the correct, so that it is necessary to determine all sets of signs which give a value of $\chi > \chi_e$ where χ_e is a lower limit to the value of χ which we may expect. If the correct set is included in the sets of signs given by the machine, it should be possible to find it by evaluating the Fourier maps corresponding to the sets of signs and examining them for expected features.

CHAPTER II

PROPERTIES OF CARBOXYLIC ACIDS AND HYDROGEN BONDS

1. GENERAL PROPERTIES

Carboxylic acids are weak acids, that is, they are only sparingly dissociated in solution. In the series of normal aliphatic acids from acetic (C_2) to pelargonic (C_9) the dissociation constants k_a range from 1.1×10^{-5} to 1.8×10^{-5}. The substitution of electronegative radicals, such as the halogens, in the chain causes an increase in the dissociation constant, trichloroacetic acid being nearly as strongly acidic as the mineral acids.

The higher members of the aliphatic carboxylic acid series are isolated from fats and waxes. They, and their derivatives possess many interesting properties. The sodium salts form monomolecular layers when added to water and considerably reduce surface tension, or interfacial tension in a liquid-liquid system. The surface tension of water is 73 dynes/cm.[2], while solutions of sodium laurate (C_{12}), myristate (C_{14}), and palmitate (C_{16}), have surface tensions of only from 25 to 30 dynes/cm.[2]

Almost all the long chain fatty acids occurring naturally are straight chain acids with an even number of carbon atoms. The only acid with an odd number of carbon atoms to be isolated from fats is isovaleric acid $(CH_3)_2CHCH_2COOH$.

Monocarboxylic acids of the benzene series are crystalline solids, and all have melting points greater than 100°C. The boiling points are slightly higher and the melting points much higher than those of aliphatic acids of similar molecular weight. Presumably this is because the flat benzene rings, with hydrogen atoms only in the plane of the ring, can pack together more closely than can the aliphatic chains which usually have hydrogen atoms around the chains, causing longer carbon - carbon van der Waals distances. Benzoic acid is somewhat more strongly acidic (k_a 6.8 x 10^{-5}) than acetic acid (k_a 1.8 x 10^{-5}), and most substituents in the ring increase the dissociation constant.

2. HYDROGEN BONDING

2.1. Introduction

The boiling points of the carboxylic acids are much higher than those of hydrocarbons or alkyl chlorides of similar molecular size. Cryoscopic determinations in hydrocarbon solvents and X-ray crystallographic measurements both indicate that the carboxylic acids exist in dimeric form, the association being due to hydrogen bonding.

The first reference to an intermolecular linkage involving hydrogen has been attributed to Oddo & Puxeddu[23]

who suggested that the abnormal properties of o-hydroxyazo compounds were due to a divided hydrogen valency. Later Moore & Winmill[24] made measurements on the conductivity of solutions of substituted ammonium bases, and on their partition coefficients between water and an immiscible solvent at several temperatures, and calculated the true dissociation constants. Their results led to the postulation of the structure of primary, secondary and tertiary alkyl substituted ammonium hydroxides as $R_xH_{3-x}N-H-OH$, with a hydrogen atom forming some kind of bond between the nitrogen and the hydroxyl group.

Since then much information has accumulated about the existence of such linkages and the role of the hydrogen atom involved. Sidgwick[25] has explained the properties of some ortho-substituted phenols on the basis of an intramolecular hydrogen bond causing chelate rings to be formed. Thus certain ortho-substituted phenols have been shown to have lower boiling points and to be more soluble in nonpolar solvents and less soluble in water than their meta and para isomers. Wulf[26] has shown that absorption in the region of the infrared spectrum characteristic of the hydroxyl group is absent for dilute solutions in carbon tetrachloride of phenols containing groups such as CHO, COMe, or NO_2 in the

ortho position. These properties indicate that the hydroxyl group in the ortho-compounds is combined in some way with the ortho substituent and so does not show its usual properties.

Electron diffraction studies, X-ray crystallographic investigations, and spectroscopic studies have also provided further evidence for the existence of hydrogen bonds.

In many organic crystals the bond plays an important role in linking together individual molecules either in pairs to form dimers or in a continuous three-dimensional array throughout the crystal. In such hydrogen-bonded crystals a much more compact type of molecular packing often occurs than in other crystals, such as the aromatic or aliphatic hydrocarbons, with the distances between the hydrogen-bonded atoms being usually about 1 Å less than the normal van der Waals distances. This usually leads to the crystals having higher melting points and being more brittle.

2.2. The Role of the Hydrogen Atom

Much controversy has existed about the nature of the hydrogen bond. It has been shown by Pauling[27] that only the (1s) orbital is available for bond formation; it being energetically impossible to form bonds with the outer orbitals. Thus any formulation of the hydrogen bond which attributes two covalent bonds to the hydrogen atom is incorrect. Gillette

& Sherman[28] postulated a resonance structure of the form

X - H Y ; X H - Y.

The hydrogen atom would require to be situated midway between X and Y or oscillating continually between the two possible positions for it, at a covalent bond distance from X or Y. Taking the case of the carboxylic acids which are known to exist as dimers in crystals, this theory would require resonance to occur between the two structures:

Such resonance would require the two carbon - oxygen bonds to be of equal length, whereas from the many crystal structure analyses of carboxylic acids which have been accomplished, it is known that these two bonds differ significantly in length. The oxygen - oxygen distance along the hydrogen bond in these acids is usually around 2.6 Å, and, consequently, for a symmetrical bond the O - H distance would be 1.3 Å.

Measurements of infrared absorption and Raman spectra show that the characteristic frequency of an O - H bond is only changed slightly on association to form dimers. The change observed can be related to the change in force constant (k) of the O - H bond, and this subsequently to its

change in length by means of Badger's equation:

$$k = A/(R - B)^2 \quad \ldots\ldots\ldots\ldots\ldots\ldots \quad (23)$$

where R is the interatomic distance, and A and B are constants. The small change in length is not nearly large enough to change the normal O - H distance from 1.0 to 1.3 Å, so that the hydrogen must be unsymmetrically placed in the bond.

These results show that the resonance theory is untenable in the case of O - H....O bonds of the length found in carboxylic acid dimers.

It is now generally accepted that the hydrogen bond is essentially electrostatic in nature, being due to the attraction between the positively charged hydrogen and the negative charge on the adjoining oxygen, nitrogen, or halogen atom. This explanation of the bond requires the hydrogen to be at about the normal covalent distance from one of the heavier atoms in the bond, and this agrees with what is known of the position of the hydrogen.

2.3. Location of Hydrogen Atoms by Diffraction Methods

In recent years it has become possible to obtain evidence of the position of the hydrogen atom in a hydrogen bond by means of diffraction methods. Neutron diffraction is probably the most powerful method for this type of investigation and has been used to obtain the distribution of

nuclei in potassium dihydrogen phosphate both at room and at liquid air temperatures by Bacon & Pease.[29] It has also been used recently to locate the hydrogen atoms in α-resorcinol[37].

X-ray diffraction methods cannot be used to locate directly the position of the proton in a hydrogen bond, but may give some indication of the position of the associated electron. Limitations in experimental and in Fourier technique prevented the location of such electrons till recently, but their positions were often deduced indirectly from known bond lengths and angles, and allowance for hydrogen atoms in structure factor calculations secured improved agreement between observed and calculated structure factors, as in the analysis of the crystal structure of melamine[30].

By measuring the X-ray intensities with a Geiger-counter, and by calculating the electron density as $(\rho_o - \rho_c)$ rather than as ρ_o, where ρ_c is the electron density of a model structure which does not include the hydrogen atoms, several investigators have located hydrogen positions with a standard deviation of about 0.1 Å. In this way electron density maxima corresponding to hydrogen atoms placed unsymmetrically in OH...O and NH...O bonds have been observed[31,32].

In certain crystal structures, e.g. potassium hydrogen bisphenylacetate[33], and other acid salts[34,35] hydrogen bonded oxygen atoms are related by a crystallographic centre of symmetry. This however does not necessitate a symmetrical hydrogen bond, for the hydrogen atom could be distributed randomly throughout the structure at one or other of the two positions available to it at a covalent bond distance from one or other of the oxygen atoms. A determination of the infrared absorption spectrum of potassium hydrogen bisphenylacetate does not support the idea of a symmetrical bond[36].

While neutron diffraction studies can locate hydrogen atoms much more accurately than even the most refined X-ray studies, the latter are still of importance since they allow a determination to be made of the number of electrons associated with the proton, and thus indicate the state of ionisation of a hydrogen atom involved in hydrogen bonding.

2.4. Short Hydrogen Bonds

There is evidence for the existence of a second type of hydrogen bond in which the proton is symmetrically placed.

The one example of this type which has been firmly established is the ion $(FHF)^-$. The fluorine-fluorine distance has been estimated by Helmholz & Rogers[38] to be 2.26 Å, which is much smaller than the comparable

separation of 2.55 Å in $(HF)_n$[39]. The theoretical separation for a symmetrical $(FHF)^-$ ion has been calculated by Donohue[40], using a theory of Pauling[41], to be 2.20 Å.

The residual entropy of potassium hydrogen bifluoride crystals at 0°K is zero[42], indicating a symmetrical bond, and the bond energy of 27 k.cals. found by Ketelaar[43] is very much higher than that of a long, unsymmetrical hydrogen bond (4-6 k.cal./mol.).

The first application of Fourier methods to neutron diffraction data was made by Peterson & Levy[44] in 1952 in the study of potassium hydrogen bifluoride. The nucleus density map prepared confirmed the symmetrical position of the proton in the $(FHF)^-$ ion.

A recent X-ray analysis of the crystal structure of ammonium hydrogen bifluoride by McDonald[45] using three-dimensional Geiger-counter measured intensity data has also confirmed the symmetrical position assigned to the hydrogen atom in the $(FHF)^-$ ion. Although this hydrogen atom is partially ionized it still retains an appreciable part of its electron, which is rather surprising in view of the electronegativity of the fluoride ions associated with it.

Nickel dimethylglyoxime possesses an OH...O bond of 2.44 Å, and it has been suggested by Rundle & Parasol[46] that

Table 1

The variation, calculated by two different methods, of the relative weights w_1, w_2 and w_3 of the three structures contributing to the hydrogen bond in the system O - H ... O.

OH .. O	2.5 Å	2.8 Å
w_1%	60.3	64.9
w_2%	28.4	30.6
w_3%	11.3	4.5
w_1%	50.2	56.8
w_2%	23.6	26.7
w_3%	26.2	16.5

the hydrogen atom is symmetrically placed in this bond. The theoretical length of a symmetrical OH...O bond is 2.30 Å[40]. The nature of this bond is still unsettled.

It appears to be the case that only for hydrogen bonds which are about 0.30 Å shorter than the normal distance is there a possibility of the hydrogen atom being symmetrically situated.

2.5. Theoretical Treatment of the Hydrogen Bond

Although the hydrogen bond can be explained very satisfactorily on the basis of an electrostatic model, attempts have been made to investigate whether there is any significant covalent contribution to the bond. Coulson & Danielsson[47] regard the O-H...O system as a resonance hybrid of the structures (i), (ii) and (iii) below.

(i) $-O-H \quad O=$

(ii) $-\bar{O}\ \overset{+}{H} \quad O=$

(iii) $-\bar{O}\ H---\overset{+}{O}=$

By using empirical relations connecting bond lengths with dipole moments and bond energies they calculate the variation of the relative weights w_1, w_2 and w_3 of these three structures as the oxygen - oxygen distance is varied. Two different methods of calculating the weights lead to the following results shown in Table 1.

Table 2

The weights w_1, w_2 and w_3 of the three contributing structures, and the dissociation energy D for the hydrogen bond at the equilibrium position of the hydrogen atom.

OH .. O	2.50 Å	2.65 Å	2.80 Å
w_1%	83.2	85.0	86.1
w_2%	12.9	12.6	12.3
w_3%	3.9	2.4	1.6
D (k.cal./ mol.)	9.8	6.4	4.4
	p-orbitals		
w_1%	81.7	83.7	85.2
w_2%	12.2	12.2	12.0
w_3%	6.1	4.1	2.8
D (k.cal./ mol.)	14.4	10.0	6.8
	sp^3-orbitals		

These weights confirm the essentially electrostatic nature of the bond, but they do suggest, however, that as the oxygen - oxygen distance becomes smaller the covalent contribution w_3 begins to become appreciable.

In a second paper[48] on this subject the same authors attempt an approximate wave-mechanical treatment of the OH...O system to estimate the weights w_1, w_2 and w_3. Only the four electrons involved in bond formation are considered and oxygen - oxygen interactions are neglected, but both p and sp^3 orbitals for the oxygen bonding orbitals are discussed. The results obtained are summarised in Table 2.

The main conclusion arrived at is that except for the short bond (O...O 2.5 Å) the bonding is essentially electrostatic, though for the short bond the covalent contribution is beginning to become significant. Despite the essentially electrostatic nature of the bond the bond energy varies smoothly with the weight of the covalent contribution (iii). The predictions of equilibrium distances and bond energies agree well with experiment.

For the O...O distance of 2.65 Å found in carboxylic acids (iii) may be neglected to a first approximation and only forms (i) and (ii) considered. Since (ii) makes an

appreciable contribution to the structure of the bond it is to be expected that the hydrogen atom will be partly ionised, and in consequence an electron count should reveal a transfer of electrons from the hydrogen atom to the oxygen. This is in qualitative agreement with the results obtained by Cochran[31] in his analysis of salicylic acid, though his results would indicate a larger transfer than the theory suggests. On this point the weights w_2 given in Table 1 seem more reasonable than the value to be found in Table 2.

CHAPTER III

THE CRYSTAL STRUCTURE OF BENZOIC ACID DERIVED FROM VISUALLY ESTIMATED INTENSITIES

1. PREVIOUS EXAMINATION OF SIMILAR COMPOUNDS

The crystal structures of many simple benzene derivatives have now been examined, but there are very few determinations of accuracy sufficient to reveal reliable bond length variations from the standard values of the order that may be expected to occur in such compounds. Quite large variations in the ring bond lengths have been reported in p-nitroaniline by Abrahams & Robertson[49], and in 1:4-dimethoxybenzene by Goodwin, Przybylska & Robertson[50], but the accuracy is not as great as can now be attained. Cochran[51] in his recent analysis of salicylic acid found the ring bonds to vary in length between 1.369 and 1.414 Å, with a standard deviation of about 0.01 Å in the measurements. Variations in ring bond lengths from 1.38 to 1.45 Å were found by Bertinotti, Giacomello & Liquori[51] in their analysis of p-amino-salicylic acid. These variations in ring bond lengths in salicylic acid and p-amino-salicylic acid can be explained largely in terms of probable resonance structures, but similar variations in other compounds cannot be so readily explained.

Thus a recent analysis of acetanilide by Brown & Corbridge[52] using three-dimensional Fourier syntheses showed the ring bonds to vary between 1.366 and 1.413 Å in length, with a standard

deviation in bond length of 0.0056 Å. It is impossible to postulate any reasonable resonance forms which can explain the large variations in this structure.

Benzoic acid was first studied by Bragg[53], but no structure determination was attempted. The hydrogen bonding present in the crystal structure was studied by means of the deuterium isotope effect by Robertson & Ubbelohde[54]. A small but definite expansion of the spacings of certain planes in the ($h0\ell$) zone was found, indicating the presence of fairly strong hydrogen bonds lying mainly in the (010) plane.

2. EXPERIMENTAL DETAILS

2.1. Preparation of the Crystals

The crystals of benzoic acid were grown from alcohol/water and acetone/petroleum ether mixtures. They were obtained in the form of fine needles with b as needle axis and also as fine plates developed on (001). Small specimens of approximately square cross-section, with sides between 0.1 and 0.2 m.m. perpendicular to the rotation axis, were chosen so that no corrections for absorption would be required.

2.2. Unit Cell Dimensions, Space Group, Density and Axial Ratios

Rotation, oscillation and moving-film photographs

around the a and b axes were taken with copper K_α radiation ($\lambda = 1.542$ Å). The cell dimensions were determined from rotation and equatorial layer line moving-film photographs calibrated with superimposed NaCl powder lines. From these the following values were obtained,

$a = 5.52 \pm 0.02$, $b = 5.14 \pm 0.02$, $c = 21.90 \pm 0.05$ Å; $\beta = 97^\circ\ 0'$.

Earlier values obtained by Bragg[53] were

$a = 5.44$, $b = 5.18$, $c = 21.6$ kX; $\beta = 97^\circ\ 5'$.

The volume of the unit cell was calculated using the expression

$$V = abc \sin\beta \qquad \ldots\ldots\ldots\ldots\ldots\ldots \quad (24)$$

and was found to be 617 $Å^3$.

Inspection of the zero layer Weissenberg photographs showed that the absent spectra are $(h0\ell)$ when ℓ is odd and $(0k0)$ when k is odd. Consequently the space group is uniquely determined to be $P2_1/c - C_{2h}^5$.

The specific gravity as determined by Steinmetz[55] is 1.322 and consequently the number of molecules in the unit cell, given by

$$n = dV/1.66M \qquad \ldots\ldots\ldots\ldots\ldots\ldots \quad (25)$$

is four. This number of molecules leads to a calculated specific gravity of 1.315.

The axial ratios calculated from the above cell dimensions are 1.074:1:1.4260. Bodewig[56] has described the morphology and obtained for the axial ratios the values 1.051:1:4.208, $\beta = 97^{\circ}\ 5'$.

The calculated linear absorption coefficient for copper $K\alpha$ radiation is 9.35 cm.$^{-1}$. The total number of electrons per unit cell, F(000), is 256.

2.3. Recording of X-ray Data, Measurement and Correction of Intensities

The X-ray data used in the present survey were obtained from equatorial layer moving-film photographs around the a and b axes, a pack of five films being placed in the camera for each exposure in order to be able to correlate strong and weak reflexions. The intensities were estimated visually. This multiple-film technique has been described by Robertson[57].

The intensities were corrected for Lorentz and polarisation factors assuming the usual mosaic crystal formula:

$$F^2 = I \sin 2\theta/(1 + \cos^2 2\theta) \quad \ldots\ldots\ldots\ldots\ldots (26)$$

In this way a set of $|F|$ values on a relative scale was obtained.

Two sets of $|F_o|$ values were obtained from different crystals of benzoic acid and these were averaged in order to ensure that the data used in the analysis would be reasonably accurate.

3. STRUCTURE DETERMINATION

3.1. Introductory Remarks

At the outset it seemed probable that the benzoic acid molecules would occur as approximately planar centrosymmetrical dimers in the crystal, with hydrogen bonding between adjacent carboxyl groups. From known bond lengths and interbond angles it would have been possible to set up a trial model and the problem would have been reduced to one of finding the three parameters which define the orientation of the model with respect to the crystal axes. However, as described in Chapter I, the most direct way of determining the crystal structure of a planar molecule, especially one with a centre of symmetry, is to evaluate the Fourier transform[9,10] and compare it with the observed intensities.

3.2. The Fourier Transform of Benzoic Acid

For the purpose of calculating the transform a planar dimer was postulated with carbon-carbon, and carbon-oxygen bonds of 1.36 Å in length, and with oxygen-oxygen hydrogen bonded distances of 2.72 Å. The interbond angles were assumed to be 120°.

Because of the centre of symmetry in the dimer the transform will everywhere be real. The centre of symmetry was chosen as origin and axes X and Y were chosen in the

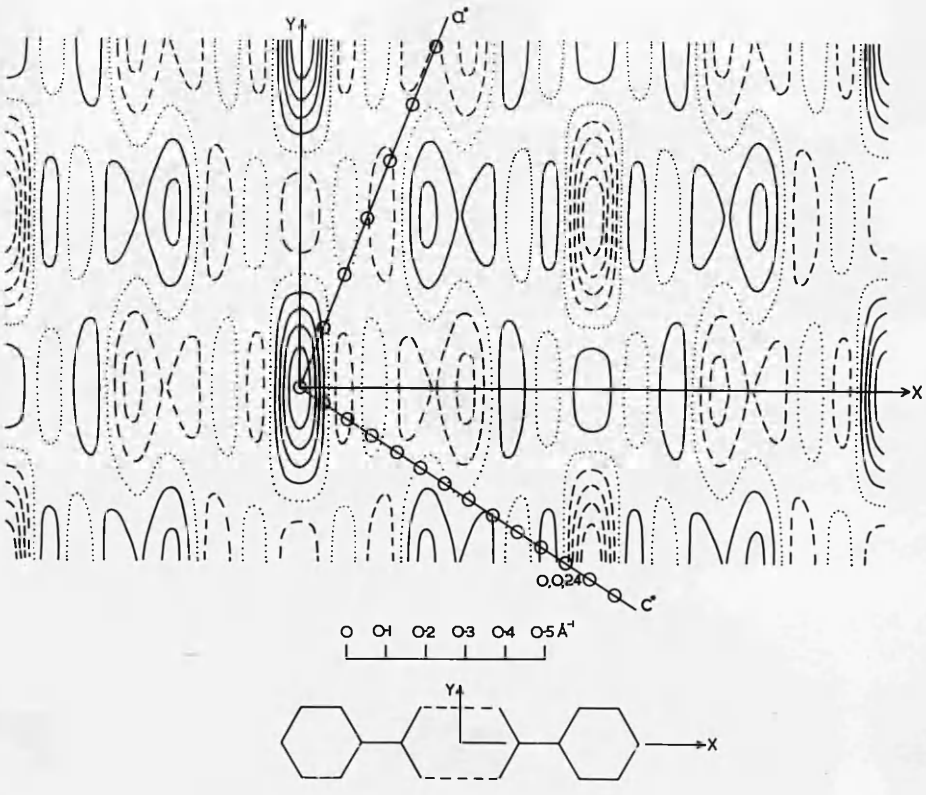

Fig. 2. Fourier transform of benzoic acid dimer, with the projections of the $\underline{a}^*$ and $\underline{c}^*$ axes. Negative contours broken, zero contour dotted.

plane of the molecule as shown in Fig. 2. Denoting the coordinates of the jth atom with respect to these axes by (x_j, y_j) and referring the reciprocal vector $\underline{R}$ also to the same axes X and Y, but with components (X,Y), the transform is then

$$T(XY) = 2 \sum_{j=1}^{N/2} N_j \cos 2\pi(x_j X + y_j Y) \quad \ldots\ldots\ldots \quad (15a)$$

The x coordinates of all the atoms are multiples of 0.68 Å, while the y coordinates are multiples of 1.18 Å. These lengths were used as units of distance along their respective axes, so that the transform of this idealised structure is periodic in the XY plane with repeat distances of 1.47 and 0.85 Å^{-1} in the X and Y directions respectively.

The function evaluated was

$$\begin{aligned} T(XY) = {} & 8\{\cos(2X + Y) + \cos(2X - Y)\} \\ & + 6\{\cos 3X + \cos 5X + \cos 9X + \cos(6X + Y) \\ & + \cos(8X + Y) + \cos(6X - Y) + \cos(8X - Y)\} \end{aligned}$$

The evaluation was made using Beevers-Lipson strips[58] at intervals of 6° in the X direction and 12° in the Y direction.

Since the $\underline{b}$ axis projection contains two dimers similarly oriented and separated by c/2, their centres coinciding with the centres of symmetry of the projection,

$$F(h0\ell) = 2\hat{f}T(XY) \quad \ldots\ldots\ldots\ldots\ldots\ldots \quad (27)$$

where $\hat{f}$ is a scattering factor, and where T(XY) is the value of the transform at the position assigned to the reciprocal lattice point (h0ℓ).

The orientation of the (h0ℓ) section of the reciprocal lattice on the transform was found readily and the signs of the majority of the (h0ℓ) structure factors obtained directly.

The transform, along with the positions assigned to the $\underline{a}^*$ and $\underline{c}^*$ axes of the reciprocal lattice, is shown in Fig. 2.

3.3. Fourier Refinement of the b-axis Projection

The electron density projected along the $\underline{b}$ axis will be given by the formula

$$\rho(xz) = \frac{1}{A} \sum_{-\infty}^{\infty}\sum F(h0\ell) \exp.\{-2\pi i(hx + \ell z)\} \quad \ldots\ldots\ldots\ldots \quad (11a)$$

Since there is a centre of symmetry in the projection the formula reduces to

$$\rho(xz) = \frac{2}{A} \sum_{-\infty}^{\infty}\sum F(h0\ell) \cos 2\pi(hx + \ell z) \quad \ldots\ldots\ldots\ldots\ldots \quad (28)$$

The signs of the majority of the (h0ℓ) structure factors had been determined from the transform and these structure factors were used to compute an electron density projection on (010). This was evaluated with Beevers - Lipson strips at intervals of 12^o along the $\underline{a}$ axis and 3^o along the $\underline{c}$ axis.

This projection was found to resolve the atoms clearly and enabled x and z coordinates to be estimated. From these

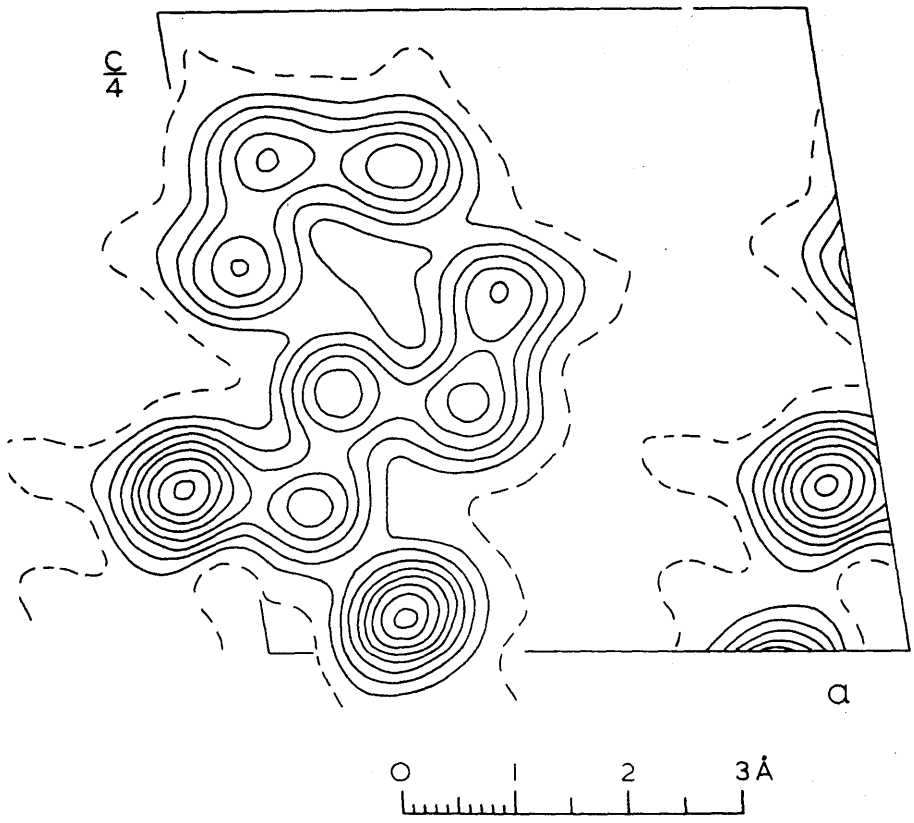

Fig. 3. Electron-density projection on (010). Contours at intervals of 1 e.Å^{-2}, the one-electron line being dotted.

coordinates (h0ℓ) structure factors were calculated, and signs allotted to the remaining F_o values. A new series was evaluated containing these additional F_o values, and provided a better approximation to the true electron density. This electron-density projection is shown in Fig. 3.

The process of successive Fourier summation followed by structure-factor calculation is the normal Fourier method of refining coordinates. The limitation of this process is that once all the signs have been determined the refinement ceases.

In order that the Fourier series should give an exact replica of the electron density structure factors corresponding to all reciprocal lattice points should be included in the series. However, the geometrical conditions for obtaining X-ray reflexions are such that only F_o values corresponding to reciprocal lattice points within the "sphere of reflexion" for the radiation employed, can be observed. This limitation on the F_o values which can be employed causes errors known as "series termination errors" in the electron density projection resulting in the points of maximum electron density being displaced slightly from their true positions. Booth[59] has discussed these errors and suggested a technique for their correction. This consists of evaluating a Fourier synthesis

using calculated structure factors as coefficients. Any deviations between the coordinates obtained from the synthesis and those used in calculating the structure factors must be due to series termination errors. Those deviations, with reversed signs, give the corrections to apply to the coordinates taken from the F_o synthesis.

This technique assumes that the series termination errors will be identical for the F_o and F_c syntheses. This, however, need not necessarily be the case unless the agreement between F_o and F_c values is sufficiently good for corresponding peaks on the F_o and F_c syntheses to have identical shapes. Normally isotropic scattering factors are used in calculating structure factors so that the peaks on an F_c synthesis will be circular, provided that overlapping does not occur. The peaks on an F_o synthesis are not normally circular, due to anisotropic vibration of the atoms and also to random errors in the F_o values. In consequence the errors in estimating the peak maxima may very well differ in the two syntheses, and the corrections taken from the F_c synthesis will not then be wholly applicable to the F_o synthesis.

Once the general outline of a structure has been solved X-ray data can be used in various ways to give accurate atomic

coordinates. Hughes[60] has suggested minimizing $\Sigma w(F_o - F_c)^2$ - method of least squares. Booth[61] has described a method in which parameters are systematically varied in order to minimize $\Sigma w(F_o^2 - F_c^2)^2$ - method of steepest descents. The weighting factors w allow for the fact that the F_o values are not all measured with the same accuracy, and the weight assigned to a particular term should be taken inversely proportional to the square of the probable error of F_o. Cochran[62] has shown that parameters obtained from Fourier syntheses are such as to minimize $\Sigma \frac{1}{f}(F_o - F_c)^2$, and the method is therefore a special case of the method of least squares in which the weighting factors are inversely proportional to the magnitude of the atomic scattering factors employed.

The disadvantages of the Fourier method are that no allowance is made for the varying accuracy of the reflexions, errors are introduced by the termination of the series and excessive weight is given to high order F values. These disadvantages can be overcome to some extent by the following procedures.

Observations suspected of being seriously in error because of extinction may be given zero weight by replacing F_o by F_c. By introducing an artificial temperature factor

for each plane, of the form

$$\alpha = \exp.\{-B(\sin\theta/\lambda)^2\},$$

the function minimized becomes $\Sigma(F_o - F_c)^2\alpha/f$. This process reduces errors due to termination of series, but at the same time the resolution is decreased and errors due to overlapping of adjacent peaks may result. Booth has claimed that this method will reduce the effect of experimental errors, but as it reduces the amount of data used in the analysis its use is not recommended.

A particularly important method of correcting for termination of series is to employ a synthesis whose coefficients are values of $(F_o - F_c)$. This synthesis has a number of properties which make it particularly useful in the final stages of refinement of a crystal structure and the properties of this synthesis and its application to the benzoic acid structure are discussed in sections 3.6 and 3.7 of this chapter.

3.4. Calculation of Structure Factors

In calculating the structure factors for the **b** axis projection of space group $P2_1/c$ the expression to be evaluated is

$$F(h0\ell) = 4\sum_j f_j \cos 2\pi(hx_j + \ell z_j) \quad \ldots\ldots\ldots\ldots \quad (7a)$$

where x_j and z_j are fractional coordinates of the jth atom. The geometrical part was expressed as

$$\cos \{h(2\pi x_j) + \ell(2\pi z_j)\}$$

and $2\pi x_j$ and $2\pi z_j$ were calculated for each atom to the nearest 0.1°. For a constant value of h successive values of $2\pi z_j$ were added to $h2\pi x_j$ on a Facit calculating machine, and the cosine of the angle, correct to 0.01, was obtained from tables.

The atomic scattering factors f_j used were those listed by McWeeny[2], modified by a temperature factor $\exp.(-\gamma \sin^2\theta)$ where γ was initially taken to be 1.9.

In allowing for the contributions of the hydrogen atoms their coordinates were determined initially by placing the benzene hydrogens radially at a distance of 1.0 Å from the carbon atoms. The oxygen hydrogen was placed 1.0 Å from O_2 on the line to the oxygen of the opposite carboxyl group and was given half the weight of the benzene hydrogens.

The F_o values were placed on an absolute scale by summing $\Sigma|F_o|$ and $\Sigma|F_c|$ for all observed planes and then multiplying each F_o value by $\Sigma|F_c| / \Sigma|F_o|$.

3.5. Progress of Refinement

A numerical test of the agreement between F_o and F_c values which is generally adopted is the sum of the differences between

the observed and calculated amplitudes divided by the sum of the observed amplitudes for all measured reflexions:

$$R = \Sigma|F_o - F_c| / \Sigma|F_o| \quad \ldots\ldots\ldots\ldots\ldots\ldots \quad (29)$$

R is known as the agreement index. Expressed as a percentage 100R is the percentage discrepancy.

Although R does not correspond to the function minimized by the Fourier or least squares method of refinement it is easily calculated and is a useful indication of the progress of a refinement. It cannot be used to give a proper quantitative estimate of the accuracy of the analysis, but other expressions are available for this purpose.

Structure factors calculated on the basis of coordinates taken from the electron density projection shown in Fig. 3 led to a value of R of 15.1%.

3.6. The $(F_o - F_c)$ Synthesis in Crystal Structure Analysis

The difference synthesis is a Fourier synthesis with coefficients $(F_o - F_c)$, and the resultant map will show the difference between the observed and calculated electron densities. Finback & Norman[63] first used this synthesis in an attempt to locate hydrogen atoms in a crystal structure and it has been used for this purpose frequently in recent years, e.g. by Cochran in the analysis of adenine hydrochloride[64] and salicylic acid[31], and by Penfold in the analysis of α-pyridone[32].

Its use as a method for refining atomic coordinates was suggested by Booth[65], and in his accurate determination of the electron density in adenine hydrochloride Cochran gave convincing evidence of its value in this respect. Cochran[66] has investigated further properties of this synthesis, and it is now widely accepted as a very convenient method of refining crystal structures.

The $(\rho_o - \rho_c)$ distribution has several advantages over a ρ_o map.

(a) Systematic errors caused by termination of series can be eliminated.

The electron density in a crystal is given by

$$\rho_o = \frac{1}{V}\sum_n F_o \cos\phi$$

where $\phi = 2\pi(hx + ky + \ell z)$, and the summation is over the n observed planes. Coordinates taken from the maxima of ρ_o are subject to termination of series errors, and more accurate coordinates will be obtained by minimizing

$$\varphi = \sum_n w(F_o - F_c)^2 \quad \ldots\ldots\ldots\ldots\ldots\ldots \quad (30)$$

Let us use instead the function

$$\varphi_1 = \sum_n (F_o - F_c)^2/f_j \quad \ldots\ldots\ldots\ldots\ldots\ldots \quad (30a)$$

where f_j is the scattering factor of the jth atom. The condition for φ_1 to be a minimum with respect to the coordinates of the jth atom is

$$\partial\varphi_1/\partial x_j = \partial\varphi_1/\partial y_j = \partial\varphi_1/\partial z_j = 0 \quad \ldots\ldots\ldots (31)$$

For a centrosymmetric structure

$$F_c = 2\sum_{j=1}^{N/2} f_j \cos \textcircled{H}_j$$

and $\partial F_c/\partial x_j = \frac{-4\pi h}{a} f_j \sin \textcircled{H}_j$.

Now, $\partial\varphi_1/\partial F_c = -2\sum_n (F_o - F_c)/f_j$

and since $\partial\varphi_1/\partial x_j = (\partial\varphi_1/\partial F_c).(\partial F_c/\partial x_j)$

we have $\partial\varphi_1/\partial x_j = \frac{8\pi}{a}\sum_n h(F_o - F_c) \sin \textcircled{H}_j \quad \ldots\ldots\ldots (32)$

Now $D_j = (\rho_o - \rho_c)_j$, the difference electron density at the centre of the jth atom, is given by

$$D_j = \frac{1}{V}\sum_n (F_o - F_c) \cos \textcircled{M}_j;$$

and consequently we have

$$(\partial D/\partial x)_j = \frac{-2\pi}{aV}\sum_n h(F_o - F_c) \sin \textcircled{H}_j$$

$$= \frac{1}{4V}(-\partial\varphi_1/\partial x)_j \quad \ldots\ldots\ldots\ldots\ldots\ldots (33)$$

When φ_1 is minimized $\partial\varphi_1/\partial x = 0$, and consequently

$$(\partial D/\partial x)_j = 0 \quad \ldots\ldots\ldots\ldots\ldots\ldots\ldots (34)$$

Similarly it can be shown that

$$(\partial D/\partial y)_j = (\partial D/\partial z_j) = 0 \quad \ldots\ldots\ldots\ldots\ldots\ldots (34a)$$

Thus when D_j has zero slope at atomic centres φ_1 has been minimized. If a map of $(\rho_o - \rho_c)$ is drawn out and the coordinates $(x_j y_j z_j)$ used to calculate F_c values marked upon

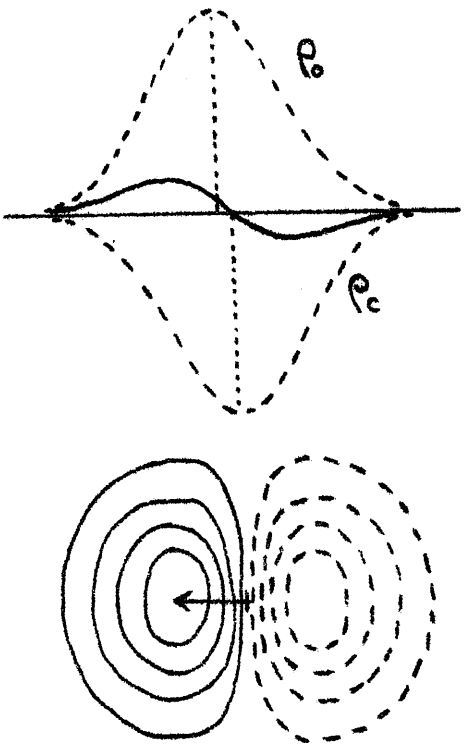

Fig. 4. Difference map feature caused by an atom requiring a coordinate shift, above in profile, and below in contour.

it, then the directions of greatest ascent at these points give the directions in which the atoms must be moved to minimize φ_1. The gradients at these points are proportional to the magnitudes of the required shifts.

The appearance of a difference map corresponding to an atom requiring a coordinate shift is shown in Fig. 4.

(b) The effect of both isotropic and anisotropic thermal vibration of atoms is apparent on the map, and the refinement of thermal parameters (if necessary, different for each atom) can be carried out at the same time as coordinate refinement. When the temperature parameter (B) of an atom has been chosen too small the atom concerned will appear in a hollow, for an electron density which is too concentrated will have been subtracted out. Conversely when B has been chosen too large the atom concerned will appear on a peak in the difference map.

Atoms which possess anisotropic thermal vibration cause characteristic difference-map features, such as shown in Fig. 5, and the appearance of the map enables suitable thermal parameters of the form

$$B = \alpha + \beta \sin^2(\varphi - \psi) \quad \ldots\ldots\ldots\ldots\ldots\ldots\ldots \quad (35)$$

to be chosen[30,64]. In this expression α and β are constants,

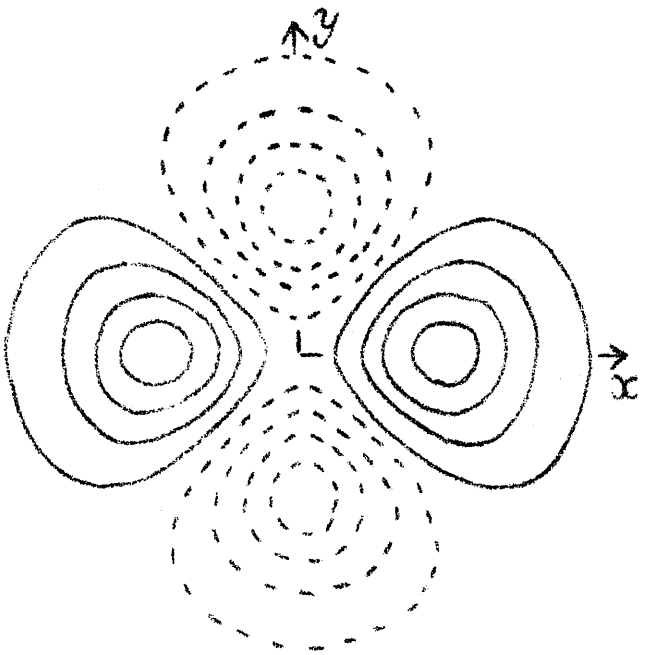

Fig. 5. Difference synthesis feature corresponding to an atom whose thermal vibration is greater in the x than in the y direction.

ψ is the angle between the maximum vibration direction and the c axis, and $(2 \sin\theta, \varphi)$ are the polar coordinates of a point in the $(h0\ell)$ section of the reciprocal lattice.

Fig. 6 shows a graph of $\alpha + \beta \sin^2(\varphi - \psi)$ against φ, the values of the constants used being $\alpha = 1.5$, $\beta = 0.7$, $\psi = 116^\circ$.

(c) When atoms in their correct positions and with correct thermal parameters have been subtracted out details of the structure not allowed for in ρ_c, such as hydrogen atoms or bonding electrons, may become observable.

Although $(\rho_o - \rho_c)$ maps make the greatest possible use of the experimental data it should be realized that values of $(F_o - F_c)$ are comparatively small in the later stages of refinement, and consequently may not be much larger than the experimental errors in F_o, unless intensities have been measured accurately. Because of this it may not be possible to detect hydrogen atoms, or more possibly bonding electrons, against the random background of peaks and hollows due to the experimental errors in the F_o values.

3.7. Application of $(F_o - F_c)$ Syntheses to the Analysis of Benzoic Acid

The b axis projection was refined by evaluating successive $(F_o - F_c)$ syntheses followed by structure factor calculations.

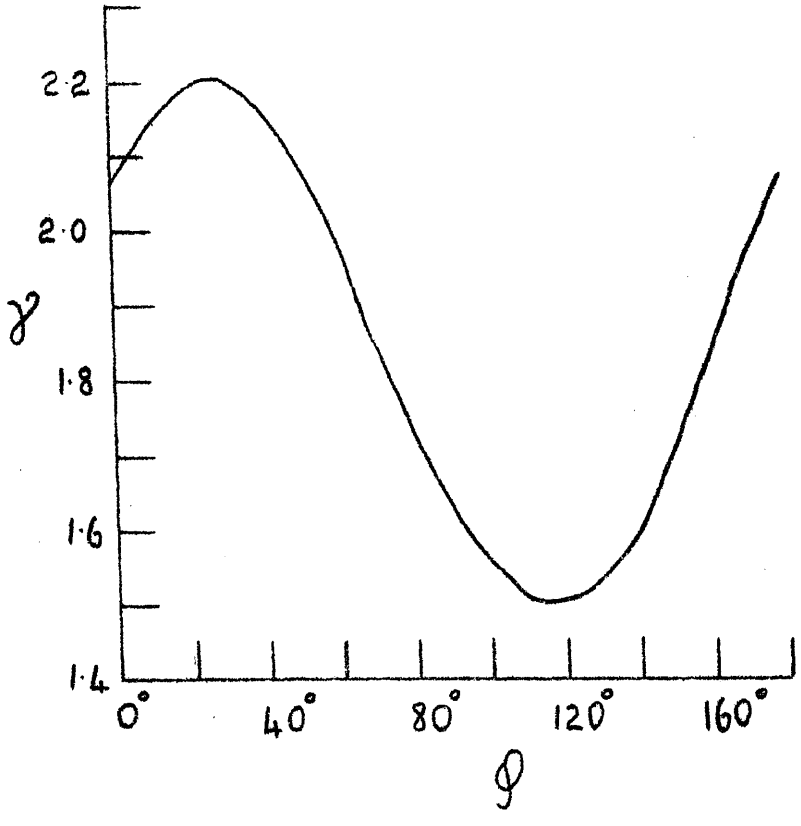

Fig. 6. Variation of the temperature-factor parameter, γ, with polar angle, φ, for an atom showing anisotropic thermal vibration.

A study of these difference maps showed that the structure-factor discrepancies were due to several factors.

(a) The coordinates of several atoms required adjustment.

(b) It was not correct to assume that the constant γ in the temperature factor $\exp.(-\gamma \sin^2\theta)$ was the same for all the atoms.

(c) Atoms O_1 and C_5 showed marked thermal anisotropy.

These factors were dealt with in the following ways.

(a) Adjustments were made to the atomic coordinates till the electron density slope at the atomic centres became zero, i.e. till $(\partial D/\partial r) = 0$. These adjustments were made by moving the atoms in the direction of greatest ascent. The magnitudes of the required shifts are given by the expression

$$\Delta r_j = -\left(\frac{\partial D}{\partial r}\right)_j \Big/ \left(\frac{\partial^2 \rho}{\partial r^2}\right)_j \quad \ldots\ldots\ldots\ldots\ldots\ldots\ldots\ldots (36)$$

If we assume that the projected electron density near the centre of an atom may be represented by

$$\rho(r) = \rho(0) \exp.(-pr^2) \quad \ldots\ldots\ldots\ldots\ldots\ldots\ldots\ldots (37)$$

where p is a constant depending upon the temperature factor associated with the atom, then

$$\frac{\partial^2 \rho}{\partial r^2} = -2p\rho(0) \quad \ldots\ldots\ldots\ldots\ldots\ldots\ldots\ldots\ldots\ldots (38)$$
$$= -2p\rho(0)$$

and equation (36) takes the form

$$\Delta r_j = \left(\frac{\partial D}{\partial r}\right)_j \div 2p\rho(0) \quad \ldots\ldots\ldots\ldots\ldots\ldots\ldots\ldots\ldots\ldots \quad (36a)$$

The constants p and $\rho(0)$ were evaluated by plotting log ρ against r^2, values of $\rho(r)$ for various values of r being measured on well resolved peaks on the electron density projection shown in Fig. 3. Values obtained were

oxygen $\quad \rho(0) = 9.4 \quad p = 4.0$

carbon $\quad \rho(0) = 6.7 \quad p = 4.0.$

In consequence the required shifts on the difference map were given by

$\Delta r \left(\frac{\partial D}{\partial r}\right)/75.2$ for an oxygen atom,

and $\Delta r \left(\frac{\partial D}{\partial r}\right)/53.6$ for a carbon atom.

$(\partial D/\partial r)$ for each atom requiring adjustment was measured from the separation of the contour lines on the $(F_o - F_c)$ synthesis near the atomic centre.

The shifts obtained in this way were not usually completely correct in magnitude due to the overlapping of peaks associated with different atoms, but this was unimportant, for the process was one of successive approximation, and the slope at each atomic centre was reduced on each successive $(F_o - F_c)$ synthesis.

(b) The thermal parameters δ were adjusted till $(\rho_o - \rho_c)$ became zero at each atomic centre. This adjustment was also one of successive approximation.

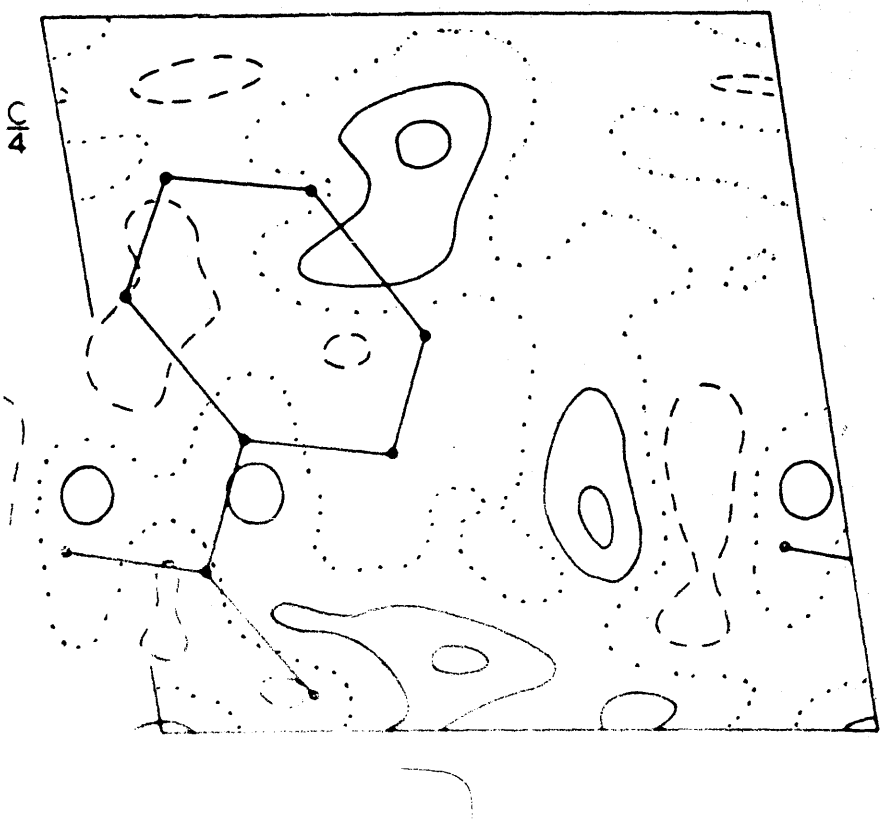

Fig. 7. Final (F_o-F_c) synthesis. All atoms including hydrogen have been subtracted. Contour interval 0.2 e.Å^{-2}, negative contours broken, zero contour dotted.

(c) In the case of the atoms O_1 and C_5 to which anisotropic temperature factors were given, the values of the constants α and β were so chosen that deviations of $(\rho_o - \rho_c)$ from zero around these atoms became as small as possible. The values of α, β and ψ used to calculate the variation of γ with φ shown in Fig. 6 were those assigned to atom O_1 after the first $(F_o - F_c)$ synthesis. This value of β was found after the second $(F_o - F_c)$ synthesis to be too small and a larger value was then used.

For each reflexion the appropriate values of γ for atoms O_1 and C_5 were obtained from graphs of γ against φ, such as that shown in Fig. 6, and were then substituted in

$$f = f^o \exp.(-\gamma \sin^2\theta), \quad \ldots\ldots\ldots\ldots\ldots\ldots \quad (39)$$

where f^o is the appropriate McWeeny scattering factor without temperature correction, to obtain the required anisotropic scattering factors.

The last $(F_o - F_c)$ synthesis in this series used to refine atomic coordinates and temperature parameters is shown in Fig. 7. All atoms, including hydrogen, have been subtracted out and the general flatness of the map, especially at atomic centres, shows that most of the outstanding features of the electron distribution have been accounted for. There are no systematic peaks occurring between bonded atoms such as would

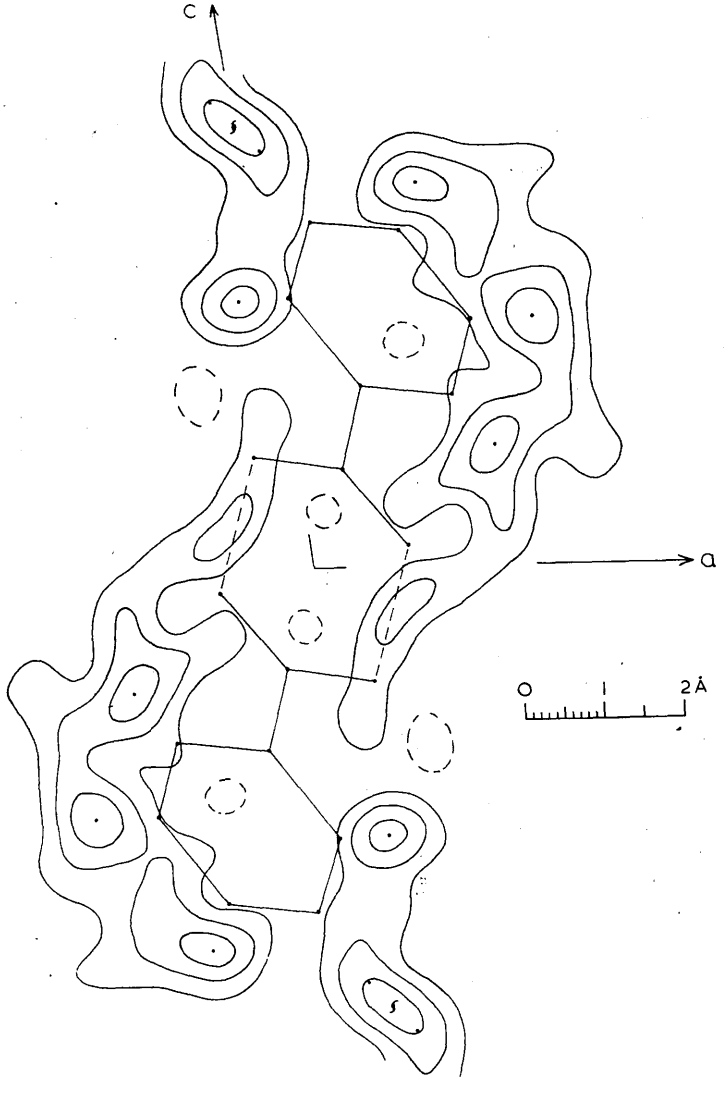

Fig. 8. Difference-synthesis projection on (010) showing the electron distribution due to the hydrogen atoms in two benzoic acid molecules. Contours at intervals of 0.2 e.Å^{-2}, negative contours broken and zero contour omitted.

be expected if any concentration of electrons were present in the bonds due to bonding. There is some evidence, however, that the departure from spherical symmetry to be expected, will be small. Bacon[67] estimates the number of electrons associated with the bonds in graphite as 0.12. March[68] has calculated the electron distribution in benzene using the Thomas-Fermi and molecular-orbital methods, and his results suggest a slight concentration of electrons in the bonds, probably of the order of 0.05 electrons per atom. This is equivalent to an average deviation from circular symmetry of less than 0.1 e.$\mathring{A}^{-2}$.

Later calculations showed that the standard deviation of electron density of this $(F_o - F_c)$ synthesis shown in Fig. 7 was 0.17 e.$\mathring{A}^{-2}$, and with such a value for $\sigma(\rho_o)$ it is not to be expected that peaks of the order of 0.1 e.$\mathring{A}^{-2}$ should be detected.

In his accurate analysis of the electron density in salicylic acid, Cochran[31], using Geiger-counter measured intensities, prepared an $(F_o - F_c)$ synthesis with a standard deviation of electron density of less than 0.1 e. $\mathring{A}^{-2}$, and in this projection peaks are found between bonded atoms representing a departure from spherical symmetry of the order of 0.05 electrons per atom.

Table 3

Coordinates of the carbon, oxygen and hydrogen atoms as determined from the b axis projection expressed as fractions of the unit cell sides.

Atom	x	z
O_1	0.223	0.0129
O_2	-0.089	0.0643
C_1	0.103	0.0567
C_2	0.180	0.1033
C_3	0.383	0.0973
C_4	0.455	0.1393
C_5	0.330	0.1903
C_6	0.133	0.1956
C_7	0.051	0.1533
$H(C_3)$	0.457	0.068
$H(C_4)$	0.593	0.140
$H(C_5)$	0.383	0.217
$H(C_6)$	0.047	0.235
$H(C_7)$	-0.060	0.153

3.8. Location of the Hydrogen Atoms

An $(F_o - F_c)$ synthesis in which the hydrogen contributions were not allowed for in the F_c values was prepared and is shown in Fig. 8. It represents the difference between the electron distribution existing in the crystal and that calculated for oxygen and carbon atoms only, at their appropriate positions in the unit cell and with appropriate thermal parameters. The significant peaks on this map are clearly due to the hydrogen atoms. Four of these atoms, attached to the benzene carbon atoms C_3, C_4, C_5 and C_7 are well resolved, but the fifth attached to C_6 appears as an unresolved doublet on the screw-axis projection.

The most interesting hydrogen atom, that belonging to the carboxyl group and responsible for the hydrogen bonding which exists between the two molecules, is only poorly resolved and cannot be attributed with certainty to either of the oxygen atoms engaged by the hydrogen bond. On the basis of the C-O bond length measurements which are discussed later, it was assigned to O_2.

The hydrogen coordinates which were obtained from the projection shown in Fig. 8 differ a little from those assumed earlier and used in calculating the contributions of the hydrogen atoms to the $(h0\ell)$ structure factors. The new coordinates are given in Table 3.

Table 4

Atomic temperature-factor parameters derived from the b axis projection.

Atom	α	β	γ	ψ
O_1	0.8	2.6	(2.1)	111°
O_2			2.1	
C_1			1.5	
C_2			1.6	
C_3			1.9	
C_4			2.2	
C_5	1.2	1.2	(1.8)	50°
C_6			2.1	
C_7			2.0	

The final percentage discrepancy for the (h0ℓ) structure factors taking account of the hydrogen atoms is 8.8. If the hydrogen atoms are not taken into account the percentage discrepancy rises to 11.8.

3.9. Final Coordinates and Temperature Factors for (h0ℓ) Zone

Atomic coordinates (x,z) for carbon and oxygen atoms are listed in Table 3. The final temperature factors for the various atoms are listed in Table 4.

The coordinates are referred to the monoclinic crystal axes and are expressed as fractions of the axial lengths, with origin at the centre of symmetry.

Final values of F_o and F_c are listed in Appendix 1.

3.10. Calculation of Approximate y-Coordinates

The coordinates of the atoms, x and z, obtained from the (010) projection were converted to orthogonal coordinates X' and Z'. The orthogonal coordinates are referred to orthogonal axes a, b and c', c' being taken perpendicular to the a and b crystal axes, so that

$$X' = X + Z \cos\beta , \quad Z' = Z \sin\beta \quad \ldots\ldots\ldots\ldots\ldots\ldots (40)$$

The coordinates were expressed in Angstrom units.

These coordinates were then converted to new coordinates X", Z", where X", Y" and Z" are coordinates referred to axes

parallel to $\underline{a}$, $\underline{b}$ and $\underline{c}'$ with origin at the centre of the benzene ring. Since the benzene ring centre is at

$$X' = 0.965, \quad Y' = q, \quad Z' = 3.176,$$

where q was to be determined later, the following relations were obtained

$$X'' = X' - 0.965,$$

$$Z'' = Z' - 3.176,$$

$$Y'' = Y' - q,$$

allowing X" and Z" for the ring atoms to be calculated.

To a first approximation all the atoms in the benzene ring were regarded as being 1.39 Å from the centre of the ring, so that Y" coordinates could be calculated from

$$(Y'')^2 = 1.39^2 - (X'')^2 - (Z'')^2 \quad \ldots\ldots\ldots\ldots\ldots\ldots \quad (41)$$

Using this equation a complete set of coordinates, X", Y" and Z" were obtained for the six carbon atoms of the benzene ring.

Since these atoms should be coplanar their coordinates should satisfy an equation of the type

$$Y'' = AX'' + BZ'', \quad \ldots\ldots\ldots\ldots\ldots\ldots\ldots\ldots\ldots\ldots \quad (42)$$

there being no constant term C since the plane passes through the origin at the centre of the ring. Substituting the known values of X", Y" and Z" for each atom in equation (42), six equations in A and B were obtained. A least-squares reduction

of these equations led to values of A and B being determined. The values calculated were $A = 0.7552$, $B = 0.8478$.

Assuming that the whole molecule was planar Y" coordinates for all the atoms were calculated from the equation

$$Y'' = 0.7552X'' + 0.8478Z'' \quad \ldots\ldots\ldots\ldots\ldots\ldots \quad (42a)$$

The oxygen - oxygen hydrogen bonded distance between normal carbonyl groups is known to be about 2.64 Å in length, and it was assumed that this value would apply to the oxygen-oxygen separation in benzoic acid in order to estimate q, the Y' coordinate of the centre of the benzene ring. If O_2' is the oxygen atom related to O_2 by the centre of symmetry at the origin we can form the equation

$$\left[Y'(O_1) - Y'(O_2')\right]^2 = 2.64^2 - \left[X'(O_1) - X'(O_2')\right]^2 - \left[Z'(O_1) - Z'(O_2')\right]^2$$

in which all the quantities on the right-hand side are known. Solving this equation led to the values

$$Y'(O_1) - Y'(O_2') = \pm 1.964.$$

However,

$$Y'(O_1) = q + Y''(O_1), \quad Y'(O_2') = -\left[q + Y''(O_2)\right],$$

and values of $Y''(O_1)$ and $Y''(O_2)$ had been calculated by the use of equation (42a) so that

$$\pm 1.964 = Y'(O_1) - Y'(O_2') = 2q - 5.041,$$

and consequently $q = 3.503$ or 1.539.

It was found that q = 3.503 was the correct choice, and Y' coordinates were calculated from

$$Y' = 3.503 + Y'',$$

for all the atoms. These were converted to fractional coordinates, y, by dividing the Y' coordinates by 5.14 Å, the length of the b axis.

In this way a set of approximate y values was obtained and was used, along with the Z coordinates derived from the (010) projection, to calculate a set of (0kℓ) structure factors. The hydrogen atoms were positioned as described in section 3.4, and were allowed for in all structure factor calculations.

3.11. Calculation of (0kℓ) Structure Factors

The (100) projection belongs to the plane group pgg, with equivalent positions:

$$(y, z); \quad (\bar{y}, \bar{z}); \quad (\tfrac{1}{2} + y, \tfrac{1}{2} - z); \quad (\tfrac{1}{2} - y, \tfrac{1}{2} + z).$$

The structure factor equations corresponding to this plane group are

(a) $F(0k\ell) = 4 \cos 2\pi ky \cos 2\pi \ell z$ when $(k + \ell)$ is even,

(b) $F(0k\ell) = -4 \sin 2\pi ky \sin 2\pi \ell z$ when $(k + \ell)$ is odd. ...(43)

Using equations (43) structure factors were calculated from the y and z coordinates derived as described in section 3.10.

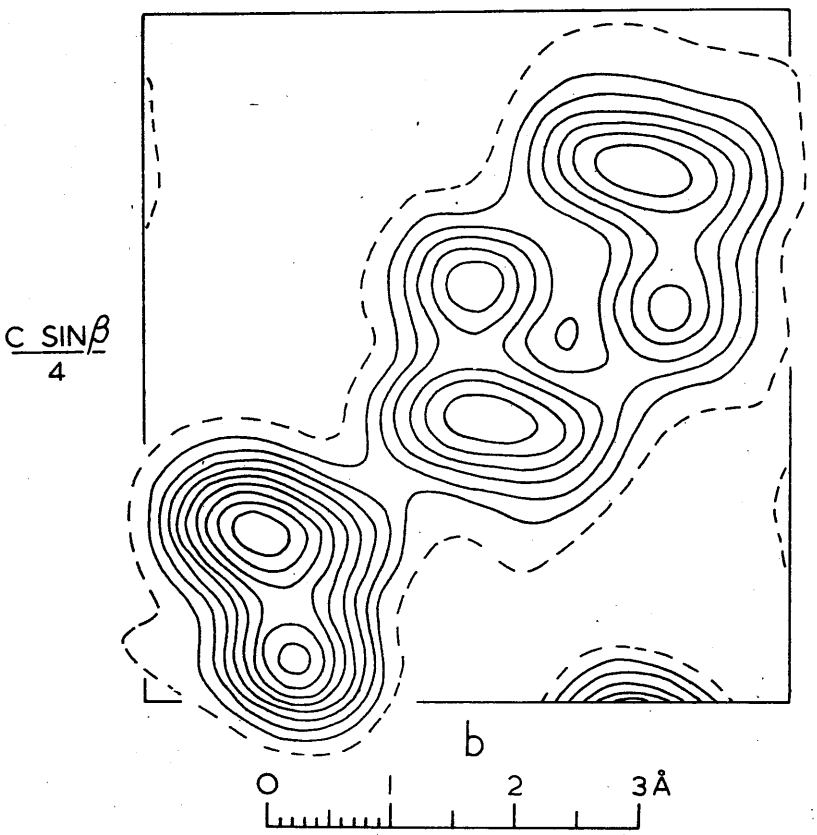

Fig. 9. Electron-density projection on (100). Contours at intervals of 1 e. $Å^{-2}$, the one-electron line being broken.

The percentage discrepancy between these calculated structure factors and the (0kℓ) observed structure factors was 16.6.

3.12. Refinement of (100) Projection

This projection was further refined by evaluating Fourier and difference Fourier projections. The formula used in computing electron-density projections on (100) is

$$\rho(yz) = \frac{1}{A}\Big[F_{oo} + 2\Big\{\sum_{2}^{\infty} F(k0)\cos 2\pi ky + \sum_{2}^{\infty} F(0\ell)\cos 2\pi \ell z\Big\}$$

$$+ 4\Big\{\sum_{1}^{\infty}\sum_{1}^{\infty}{}^{k+\ell=2n} F(k\ell)\cos 2\pi ky \cos 2\pi \ell z - \sum_{1}^{\infty}\sum_{1}^{\infty}{}^{k+\ell=2n+1} F(k\ell)\sin 2\pi ky \sin 2\pi \ell z\Big\}\Big] \ldots \quad (44)$$

The electron density projection for this zone is shown in Fig. 9. Because of the greater tilt of the molecule in this projection only atoms O_1, C_4 and C_7 are clearly resolved in this map and it was not possible to use this map to obtain more accurate coordinates. This lack of resolution, however, did not hinder refinement by difference Fourier projections, though the magnitude of the atomic shifts required became largely a matter of trial and error. The coordinates of the atoms and the temperature parameters ($\mathring{B}$) were adjusted as in the (010) projection, but no corrections for anisotropic thermal vibration were made though atom O_2 showed evidence of this.

Table 5

Carbon and oxygen atomic coordinates, expressed as fractions of the unit cell sides, and final temperature-factor parameters as determined from the a axis projection.

Atom	y	z	γ
O_1	0.237	0.0133	2.1
O_2	0.140	0.0640	2.1
C_1	0.278	0.0571	1.5
C_2	0.481	0.1051	1.55
C_3	0.631	0.0961	2.05
C_4	0.823	0.1406	2.15
C_5	0.875	0.1893	2.25
C_6	0.720	0.1963	1.8
C_7	0.516	0.1537	1.95

Because of the presence of molecules with different orientations in this projection the structure factor formulae given in equation (43) would require considerable modification if allowance for anisotropic thermal vibration was made. It would be necessary to use

$$F(0k\ell) = 2\{f_A \cos 2\pi(ky + \ell z) + f_B \cos 2\pi(ky - \ell z)\}$$

when $(k + \ell)$ is even, and

$$F(0k\ell) = 2\{f_A \cos 2\pi(ky + \ell z) - f_B \cos 2\pi(ky - \ell z)\} \quad \ldots.(45)$$

when $(k + \ell)$ is odd. f_A and f_B are anisotropic scattering factors for corresponding points in adjacent quadrants of the reciprocal lattice section, that is if f_A is the scattering factor for the reciprocal lattice point $(0k\ell)$, then f_B is the scattering factor for the point $(0k\bar{\ell})$.

As the greater lack of resolution in this projection and the smaller number of observed F_o values prevented the same accuracy being attained as in the (010) projection, it was not felt worthwhile to allow for anisotropic vibration.

The final percentage discrepancy for the observed $(0k\ell)$ reflexions is 10.3. The observed and calculated structure factors are listed in Appendix 1, while the atomic coordinates (y, z) for the carbon and oxygen atoms derived from this zone are given in Table 5, along with the values of the temperature parameter γ.

Table 6

Final atomic coordinates.

Atom	x	y	z	x'	Y	Z'
O_1	0.223	0.237	0.013	1.192	1.216	0.290
O_2	-0.089	0.143	0.064	-0.663	0.737	1.398
C_1	0.103	0.278	0.057	0.413	1.430	1.236
C_2	0.180	0.481	0.104	0.713	2.470	2.255
C_3	0.383	0.631	0.097	1.849	3.241	2.103
C_4	0.455	0.823	0.140	2.129	4.231	3.048
C_5	0.330	0.875	0.190	1.310	4.497	4.121
C_6	0.133	0.720	0.196	0.210	3.700	4.251
C_7	0.051	0.516	0.154	-0.128	2.653	3.338

3.13. Coordinates and Molecular Dimensions

The final coordinates of the oxygen and carbon atoms are listed in Table 6, the z coordinates being a weighted mean of the values listed in Table 3 and 5. The coordinates x, y and z are referred to the monoclinic axes, and are expressed as fractions of the axial lengths. The coordinates X', Y and Z' are referred to orthogonal axes and were obtained as described in section 3.10. These coordinates are expressed in Angstrom units.

It was found that the coordinates of the ring atoms C_2, C_3, ... C_7 could be fitted to an equation of the form

$$Y = AX' + BZ' + C \quad \ldots\ldots\ldots\ldots\ldots\ldots\ldots\ldots \quad (46)$$

A, B and C were determined by the method of least squares to be 0.8057, 0.8284 and 0.0090 respectively. Using this equation Y coordinates were calculated for all the atoms and compared with those derived from the final difference map for the (100) projection. The deviations, Δ , between these estimates are listed in Table 7, along with the corresponding displacements of the atoms from the molecular plane given by

$$\text{Displacement} = \Delta / \{1 + A^2 + B^2\}^{\frac{1}{2}} \quad \ldots\ldots\ldots\ldots \quad (47)$$

The average deviation between the two values of Y for the ring atoms is 0.012 $\mathring{A}$, equivalent to a perpendicular displacement

Table 7

Deviations from the plane

$Y = 0.8057X' + 0.8284Z' + 0.0090.$

Atom	$Y_{calc.}$	$Y_{obs.}$	Δ	Displacement
O_1	1.210	1.216	-0.006	-0.004
O_2	0.633	0.737	-0.104	-0.068
C_1	1.366	1.430	-0.064	-0.042
C_2	2.452	2.470	- 0.018	-0.012
C_3	3.241	3.241	0.000	0.000
C_4	4.249	4.231	0.018	0.012
C_5	4.478	4.497	-0.019	-0.012
C_6	3.700	3.700	0.000	0.000
C_7	2.671	2.653	0.018	0.012

from the plane of 0.008 Å. Atoms C_1 and O_2, however, appear to depart significantly from the mean plane, their displacements being 0.042 and 0.068 Å respectively. By evaluating

$$2C/\{1 + A^2 + B^2\}^{\frac{1}{2}}$$

the perpendicular separation of the two benzene rings in the dimer was found to be 0.012 Å. If this is assumed not to be significant then the constant C in equation (46) should be zero. The two new constants A' and B' were calculated by least squares and values of 0.8069 and 0.8306 were obtained. Using the equation

$$Y = 0.8069X' + 0.8306Z'$$

a new set of $Y_{calc.}$ coordinates was calculated and compared with the values of Y obtained by use of equation (46) and those obtained from the final difference map for the (100) projection. The results are shown in Table 8. The average displacement of the ring atoms from this plane is 0.008 Å, exactly the same result as that obtained for the plane

$$Y = 0.8057X' + 0.8284Z' + 0.0090.$$

The displacements of atoms C_1 and O_2 (0.046 and 0.072 Å) are, however, slightly larger.

The bond lengths and valency angles in the benzoic acid molecule are shown in Fig. 10. These were calculated from the coordinates in Table 6 except for the Y coordinates of the

Table 8

Deviations from the plane
$Y = 0.8069X' + 0.8306Z'$.

Atom	previous $Y_{calc.}$	$Y_{calc.}$	$Y_{obs.}$	Displacement
O_1	1.210	1.203	1.216	-0.008
O_2	0.633	0.627	0.737	-0.072
C_1	1.366	1.360	1.430	-0.046
C_2	2.452	2.449	2.470	-0.014
C_3	3.241	3.240	3.241	-0.001
C_4	4.249	4.250	4.231	0.012
C_5	4.478	4.481	4.497	-0.010
C_6	3.700	3.701	3.700	0.001
C_7	2.671	2.669	2.653	0.010

ring atoms, where the $Y_{calc.}$ values shown in Table 7 were employed. These do not differ significantly from the observed values, and are probably more reliable.

X' and Z' coordinates for four hydrogen atoms which are well resolved had been obtained from the difference-synthesis projection shown in Fig. 8, and by substituting these values in equation (46) Y coordinates were calculated. These are listed in Table 9, along with the C-H bond lengths calculated from them.

4. ESTIMATION OF ACCURACY

4.1. Introduction

In the past the accuracy of an X-ray structure analysis was judged by the consistency of the results, or by the effect of variation of the coordinates on the percentage discrepancy. If a planar molecule was being examined then the apparent deviations of the atoms from the mean molecular plane gave an indication of the order of magnitude of the errors to be expected. If the molecule under examination possessed some molecular symmetry which was not utilized by the crystal, then a comparison of chemically identical but crystallographically distinct bonds gave a measure of the errors present.

An example of the latter case is the analysis by Robertson & White[16] of the highly symmetrical condensed ring hydrocarbon

Table 9

Hydrogen coordinates and bond lengths.

Atom	X'(Å)	Y(Å)	Z'(Å)
$H(C_3)$	2.32	1.49	3.11
$H(C_4)$	2.88	3.03	4.85
$H(C_5)$	1.53	4.71	5.14
$H(C_7)$	-0.74	3.32	2.16

$H\text{-}C_3 = 0.79$, $H\text{-}C_4 = 0.96$, $H\text{-}C_5 = 0.91$,
$H\text{-}C_7 = 0.79$ Å.

coronene, $C_{24}H_{12}$. This molecule possesses hexagonal symmetry but this symmetry is not displayed in the crystal. There are two molecules in the monoclinic cell, the asymmetric unit being half a molecule. By averageing the lengths of chemically equivalent bonds the authors consider their results to be accurate to 0.02 Å, or better.

There are several disadvantages to this method of estimating errors, the main one being that it assumes what may not be true. Thus, in the structure analysis of ethylene thiourea[69] it was found that the sulphur atom was displaced 0.03 Å from the plane of the heterocyclic ring. An estimate of accuracy on this basis would take this displacement as being of the order of magnitude of the error involved, whereas an application of the quantitative method discussed later showed this displacement to be highly significant.

Estimates made by comparison of chemically identical bonds are based on only a few determinations of a given bond, so that the reliability of the estimate must be small even when the assumption that the bonds are identical is justified.

4.2. Quantitative Accuracy Theory

If the electron density is written as

$$\rho_o(xy) = \frac{1}{A}\Sigma\Sigma F_o \cos 2\pi(hx + ky),$$

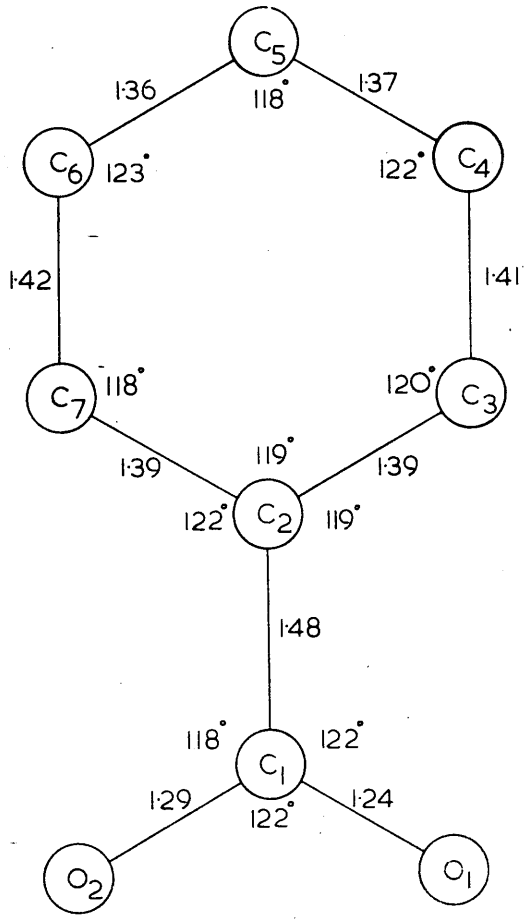

Fig. 10. Bond lengths and valency angles in benzoic acid.

then the standard deviation of electron density is given by[70]

$$\sigma(\rho_o) = \frac{1}{A}\{\sum\sum \sigma^2(F)\}^{\frac{1}{2}}, \quad \ldots\ldots\ldots\ldots\ldots\ldots \quad (48)$$

for any general position in the unit cell. For special positions a more general formula due to Cruickshank & Rollet[71] must be used.

The coordinate standard deviation depends on the peak curvature and on the errors in the slope of the electron density. Cruickshank[70, 72] has derived the equation

$$\sigma(x) = \frac{\sigma(\partial\rho/\partial x)}{\partial^2\rho/\partial x^2} \quad \ldots\ldots\ldots\ldots\ldots\ldots \quad (49)$$

For a general position,

$$\sigma(\partial\rho/\partial x) = \frac{2\pi}{aA}\{\sum\sum h^2\sigma^2(F)\}^{\frac{1}{2}}, \quad \ldots\ldots\ldots\ldots \quad (50)$$

where A is the area of the cell projection, $\partial^2\rho/\partial x^2$ is the curvature at the centre of the atom, and

$$\partial^2\rho/\partial x^2 = -2p\rho_o \quad \ldots\ldots\ldots\ldots\ldots\ldots\ldots \quad (37)$$

In section 3.7 values of p and ρ_o were determined for the oxygen and carbon atoms.

In order to use this formula an estimate of $\sigma(F)$ must be made. The most frequently used method of estimating $\sigma(F)$ is to take it as being equal to $|F_o - F_c|$. This includes random errors and any residual finite-series errors, though in the case of benzoic acid such errors should have been eliminated by the difference-synthesis method employed in the refinement.

If independent measurements of F_o values are available then it is possible to estimate $\sigma(F)$ from these, but such measurements are not generally available unless, perhaps, when the measurements have been made on a Geiger-counter spectrometer.

4.3. Application of Cruickshank's Formula to Benzoic Acid

The coordinate standard deviations obtained by use of equation (49) were

$\sigma(x) = \sigma(z) = 0.010$ Å, $\sigma(y) = 0.014$ Å for carbon

$\sigma(x) = \sigma(z) = 0.008$ Å, $\sigma(y) = 0.010$ Å for oxygen.

The standard deviation of position of atom A, $\sigma(A)$, is given by

$$\sigma^2(A) = \{ \sigma^2(x_A) + \sigma^2(y_A) + \sigma^2(z_A) \} \quad \ldots\ldots\ldots\ldots (51)$$

The standard deviation $\sigma(\ell)$ of the distance between two atoms whose positions have been determined independently with standard deviations in position of $\sigma(A)$ and $\sigma(B)$, is given by

$$\sigma(\ell) = \{ \sigma^2(A) + \sigma^2(B) \}^{\frac{1}{2}} \quad \ldots\ldots\ldots\ldots\ldots\ldots (52)$$

Application of equations (51) and (52) to the benzoic acid results led to

$\sigma(\ell) = 0.016$ Å for a carbon-carbon bond

and $\sigma(\ell) = 0.014$ Å for a carbon-oxygen bond.

The standard deviation $\sigma(\theta)$ of the interbond angle between three atoms computed by the equation given by Ahmed & Cruickshank[73] was found to be 0.9^o.

The standard deviation of electron density, computed by equation (48), was found to be 0.17 e.Å^{-2} for the (h0ℓ) zone, and 0.31 e.Å^{-2} for the (0kℓ) zone.

4.4. Significance Tests

From a knowledge of the standard deviation of a bond length it is desirable to be able to set an upper limit to the magnitude of the possible error in that bond length. The errors to be expected are random and may be expected to show a normal Gaussian distribution. The probability, P, that an observed difference in bond length, Δ , is due to chance only is given in terms of the standard deviation, σ , in the following table.

P = 5%	$\Delta = 1.645\,\sigma$
P = 1%	$\Delta = 2.327\,\sigma$
P = 0.1%	$\Delta = 3.090\,\sigma$

A difference of more than three times the standard deviation may be taken as significant.

5. DISCUSSION OF RESULTS

5.1. Planarity of the Molecule

The displacements of the carbon atoms of the benzene ring from a plane (Tables 7 and 8) vary from zero to 0.012 Å, and are not significant. The ring may therefore be assumed strictly planar. The displacements of the atoms C_1 and O_2 from the molecular plane are 0.042 and 0.068 Å (taking the

figures from Table 7). These displacements, though small, appear to be significant, because they are several times greater than the standard deviation of position of a carbon or oxygen atom.

The two benzene rings in the dimer are separated by a distance of only 0.012 Å, which is not significant, so that the two benzene rings may be regarded as coplanar.

5.2. Bond Variations in the Ring

The ring bonds vary from 1.36 to 1.42 Å in length. There appears to be a plane of symmetry at right angles to the plane of the ring, passing through atoms C_2 and C_5, for the lengths of corresponding bonds on either side of this plane are very nearly equal, with differences of only 0.01 Å being observed.

Bonds $C_3 - C_4$ and $C_6 - C_7$ differ from $C_4 - C_5$ and $C_5 - C_6$ by an average value of 0.051 Å. The total estimated standard deviation, calculated by the equation given by Parry[74],

$$\sigma^2(t) = \tfrac{1}{4}\{\sigma^2(C_3C_4) + \sigma^2(C_6C_7) + \sigma^2(C_4C_5) + \sigma^2(C_5C_6) - 2\sigma^2(C_4)\cos\theta_1 - 2\sigma^2(C_5)\cos\theta_2 - 2\sigma^2(C_6)\cos\theta_3\} \quad \ldots\ldots\ldots\ldots (53)$$

was found to be 0.017 Å. In consequence we have

$$\Delta/\sigma(t) = 0.051/0.017 = 3.0$$

and the difference appears to be significant.

These differences are difficult to explain in terms of any reasonable resonance structures that may be written for the benzoic acid molecule. Moreover, molecular-orbital calculations by Dr. T.H. Goodwin do not suggest that these bonds should be longer than the others. Similar variations, however, were found in the analysis of acetanilide[52] in which, after a careful three-dimensional Fourier analysis, the standard deviation of bond length is only 0.0056 Å. The observed differences in ring bond lengths in the acetanilide structure exceed the standard deviation of bond length by up to nine times, and must be significant.

5.3. Dimensions of the Carboxyl Group

The two C-O bonds in the carboxyl group differ in length by 0.046 Å. The total estimated standard deviation of the difference, given by

$$\sigma^2(t) = \sigma^2(C_1O_1) + \sigma^2(C_1O_2) - 2\sigma^2(C_1) \cos\theta, \quad \ldots\ldots\ldots(54)$$

where θ is the angle between the bonds C_1-O_1 and C_1-O_2, was calculated to be 0.021 Å. Consequently, we have

$$\Delta/\sigma(t) = 0.046/0.021 = 2.2,$$

and the difference may perhaps be significant. It is smaller than the C-O bond differences found in some carboxyl groups, e.g. salicylic acid[31], where the difference is 0.092 Å, and

Table 10

Values of the C-C bonds and the sum of the two C-O bonds in some carboxyl groups.

Compound	C-C (Å)	Sum of C-O (Å)
dipotassium nitroacetate	1.38	2.60
p-amino-salicylic acid	1.41	2.56
salicylic acid	1.46	2.57
benzoic acid	1.48	2.53
nicotinic acid	1.48	2.52
L-glutamine	1.52	2.49
oxalic acid dihydrate	1.53	2.47
α-oxalic acid	1.56	2.48

p-amino-salicylic acid[51], where the difference is 0.11 Å, and is closer to the differences reported for some of the 'zwitterion' amino acids, e.g. DL-alanine[75], hydroxy-L-proline[76], and glutamine[77], which have differences of 0.06, 0.02 and 0.05 Å respectively. It is difficult to advance any reason for the small difference found in benzoic acid. On the basis of the C-O bond length measurements the hydrogen atom of the carboxyl group was assigned to O_2, though the resolution of this atom in Fig. 8 is not good enough to confirm this assignment.

The bond C_2-C_1, leading to the carboxyl group is 1.48 Å and therefore appears to be significantly shortened from the standard single-bond value of 1.54 Å, and is even less than twice the radius, 0.75 Å, suggested by Coulson[78] as appropriate to a carbon atom hybridized in the sp^2 state. The value found agrees with that found for salicylic acid (1.46 Å), and nicotinic acid[80] (1.48 Å), but is distinctly less than that found in other carboxylic acids, e.g. oxalic acid dihydrate[73] (1.53 Å), L-glutamine[77] (1.52 Å) and several other of the amino acids which have received detailed study. Even shorter bonds leading to a carboxyl group have been reported. Sutor, Llewellyn & Maslen[79] from a three dimensional Fourier analysis of dipotassium nitroacetate report a bond of this type to have a length of 1.38 Å, with standard deviation of 0.02 Å.

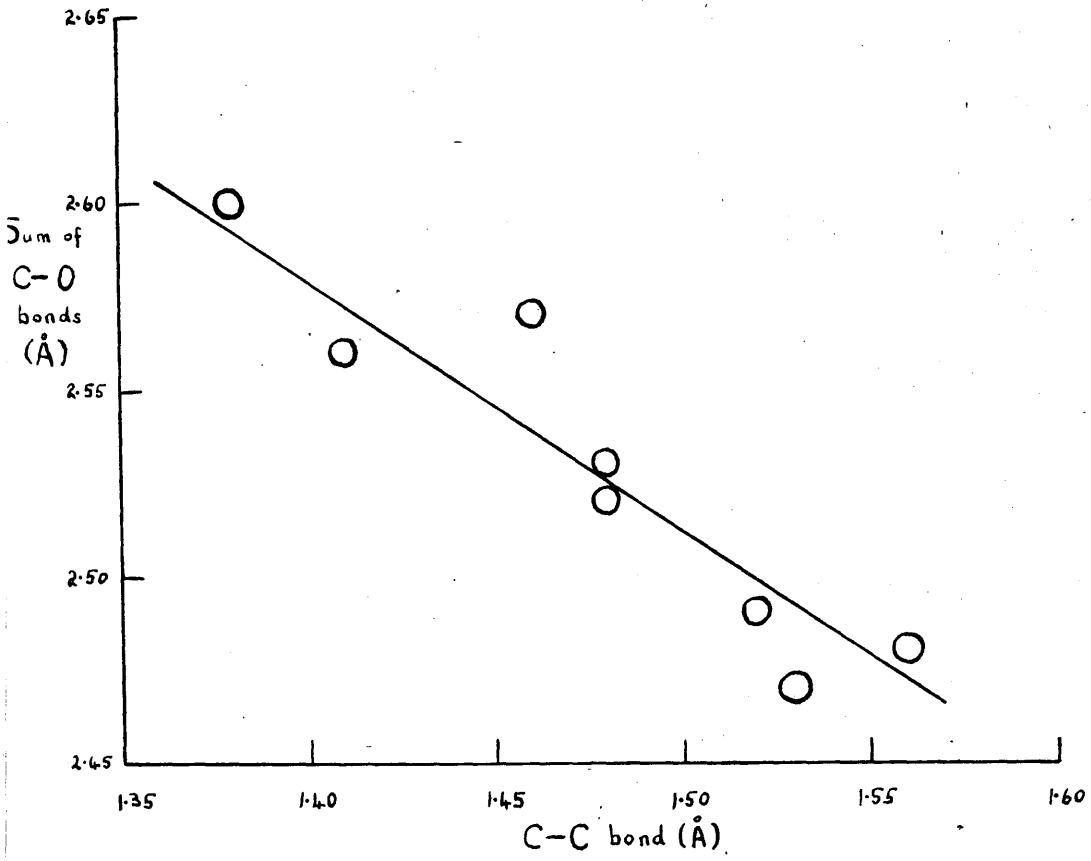

Fig. 11. Graph of the sum of the two C-O bond lengths plotted against the C-C bond length for some carboxyl groups. Values are taken from Table 10.

In p-amino-salicylic acid[51] a value of 1.41 Å has been found.

Robertson[81] has pointed out that the shortening of this C-C bond from the single-bond value of 1.54 Å may be correlated with the observed increase in the sum of the lengths of the two C-O bonds in the carboxyl groups. In Table 10 values of the C-C bond lengths and the sum of the two C-O bond lengths are listed for some carboxylic acids. In Fig. 11 these values are plotted in the form of a graph of C-C bond length against the value of the sum of the two C-O bond lengths. A "best" straight line through the experimental values was calculated by least squares and it will be seen that there is quite a striking correlation.

These results suggest that in the benzene carboxylic acids and in the nitroacetate anion, the structure

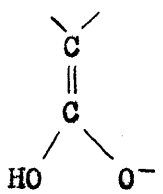

makes a considerable contribution, in addition to the structures

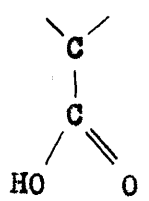

and

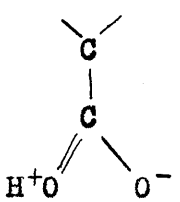

which normally contribute to the structure of the carboxyl group.

5.4. Hydrogen Atom Results

With regard to the positions of the hydrogen atoms that are resolved in Fig. 8, the average value of the C-H bond lengths (Table 9) is 0.86 Å. This value is considerably less than the accepted value of 1.07 Å derived spectroscopically, but agrees well with the value of 0.89 Å found in salicylic acid. These results suggest strongly that the point of estimated maximum electron density does not coincide with the proton.

For an isolated hydrogen atom 95% of the electron is contained in a circle of radius 1 Å drawn about the centre of the atom. Electron counts for the benzene hydrogens varied from 0.7 to 1.3 electrons, so that there is a considerable error associated with these values. The content of the oxygen hydrogen is even less conclusive, for the shape of the elongated peak is such that it was very difficult to decide where to draw a boundary. In order to include all the elongated peak it was necessary to include areas which were more distant from the hydrogen centre than 1 Å. When this was done a content of 0.9 electrons was found, but as the area of the count included areas which could properly be assigned to the oxygen atoms this gives no information about the possible transfer of part of the electron to the oxygen atom. The smaller peak height of the oxygen

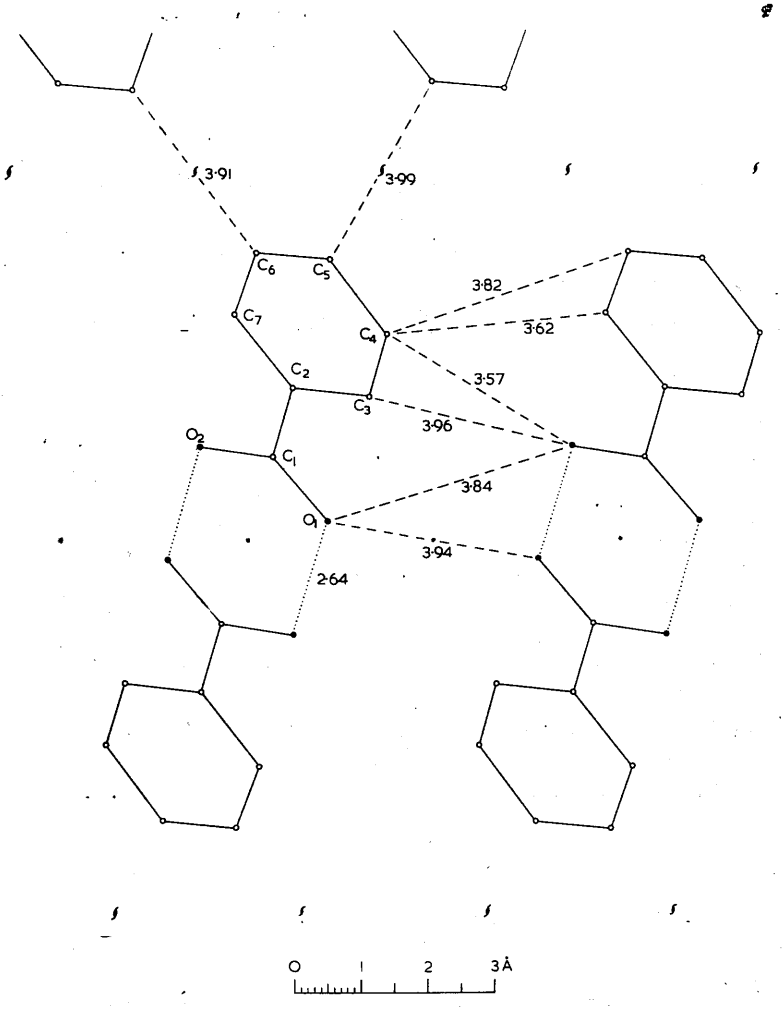

Fig. 12. Arrangement of the molecules in the (010) projection.

hydrogen compared with the benzene hydrogens does suggest that a possible transfer has taken place.

In salicylic acid the two hydrogen atoms involved in hydrogen bonding were found to contain 0.3 and 0.5 electrons, so that there is a considerable transfer from hydrogen to oxygen in the case of this compound. This is in qualitative agreement with the theoretical results of Coulson & Danielsson[47, 48].

5.5. Intermolecular Approach Distances

The arrangements of the molecules in the (010) and (100) projections are indicated in Figs. 12 and 13. Some of the smaller of the intermolecular approach distances are indicated in these diagrams. The closest approach distance occurs between the oxygen atoms of neighbouring carboxyl groups. The O-H...O distance is 2.64 Å, which is normal for this type of hydrogen bonding.

The other intermolecular approach distances are over 3 Å, and correspond to normal van der Waals interactions. The closest contact, 3.34 Å, occurs between C_1 of one dimer and O_1 of a dimer related to the first by a translation **b**.

5.6. Completeness of Refinement

The F_o values used in this analysis were obtained by averaging two independent sets, the percentage discrepancy

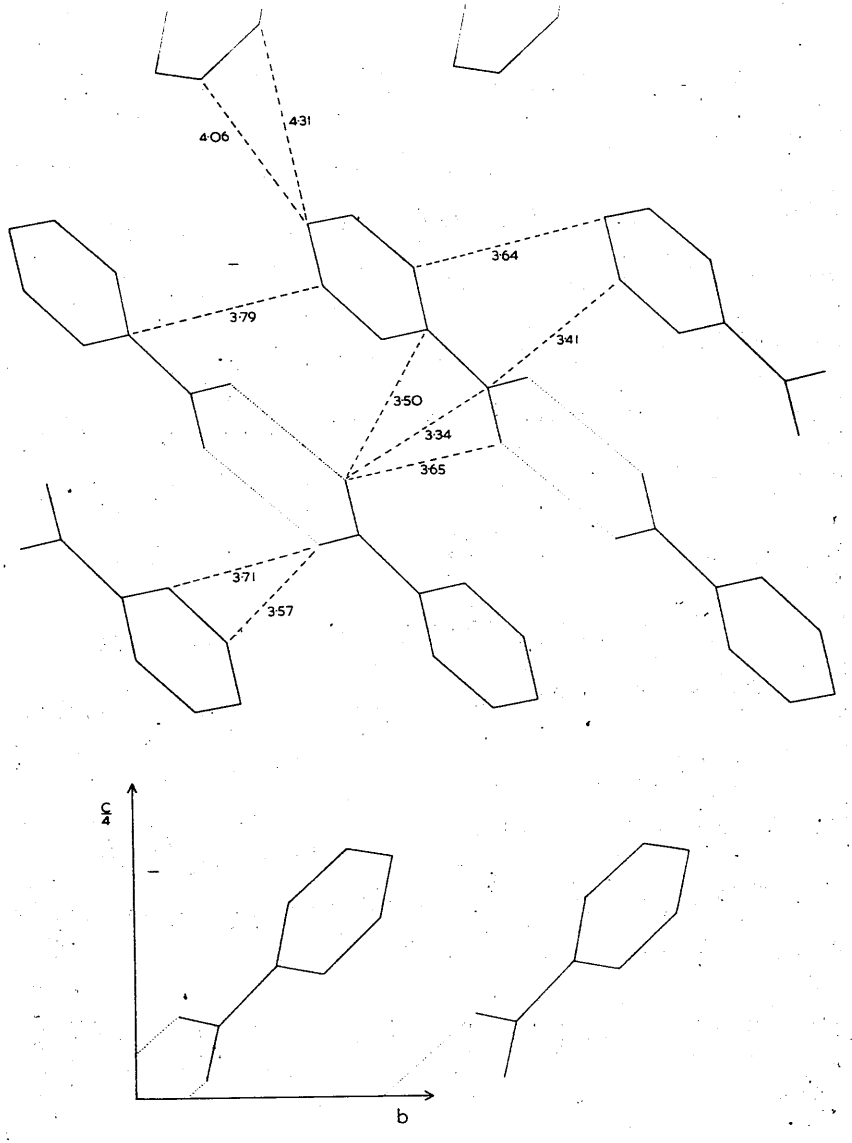

Fig. 13. Arrangement of the molecules in the (100) projection.

between the two sets of F_o values for the (h0ℓ) zone being 8.0. It is to be expected that the averaged F_o values will be rather more accurate than this.

As the final percentage discrepancy between observed and calculated structure factors for the same reflexions is 8.8% it seems clear that the refinement has been carried through to about the maximum accuracy which the experimental data will allow. Consequently, the electron density has been represented accurately by a set of discrete atoms with McWeeny scattering factors and appropriate temperature factors. Other factors, such as the concentration of bonding electrons between atoms seem relatively unimportant, though it must be admitted that the method of choosing temperature factors would tend to obscure such details.

The completeness of the refinement suggests that the McWeeny scattering factors are reasonably accurate and that there is little justification for improving the agreement between F_o and F_c values, in the structure analysis of an organic compound, by deducing empirical scattering curves for the light atoms. Such a process may still be necessary when dealing with heavy atoms for which the theoretical scattering factors are only known approximately, but would seem both unnecessary and rather questionable where light atoms are concerned.

CHAPTER IV

THE CRYSTAL STRUCTURE OF BENZOIC ACID DERIVED FROM GEIGER-COUNTER MEASURED INTENSITIES

1. INTENSITY MEASUREMENTS ON THE GEIGER-COUNTER SPECTROMETER

1.1. Introduction

Because of the relationship between the accuracy of an electron-density projection and the accuracy of the F_o values used in the synthesis it is necessary to possess accurate X-ray data in attempting to determine fine details of the electron density in a crystal.

As there are considerable random personal errors involved in the visual estimation of photographically recorded intensities, F_o values derived in this way may be considerably in error. Cochran[82] has estimated the standard deviation of eye-estimated intensities of average strength to be about 12% in a typical case; while the discrepancy between two independent sets of visually-estimated F_o values for benzoic acid was 8%. Integrating photometers give more accurate results, but their use is rather tedious.

Counters can be made very accurate and sensitive instruments for the measurement of X-ray intensities, and they have the great advantage that such errors as are inherent in their operation may be corrected readily. Integrated intensities from single crystals can be measured with a standard deviation of about 2%.

Both argon filled end-window Geiger counters and xenon filled side-window proportional counters are excellent detectors for copper Kα radiation having a quantum efficiency of about 60% at this wavelength[85]. For molybdenum K radiation, with λ = 0.71 Å, a krypton filled side-window proportional counter is preferable because of its higher quantum efficiency at this shorter wavelength.

At short wavelengths the efficiency of an argon filled Geiger counter drops considerably, being 17% at 0.77 Å and 6% at 0.51 Å. This is advantageous for single crystal diffraction with copper Kα radiation, for it means that scattered radiation from the continuous X-ray spectrum, such as $\lambda/2$ being reflected from the second order of the plane under examination, is relatively poorly detected and in consequence is less important than in the case of a photographic film.

A sodium-thallium crystal scintillation counter has a higher efficiency (about 95%) for all wavelengths. This can be a disadvantage, for it causes this counter to have a greater background than the Geiger or proportional counter. The background, however, can be reduced to considerably below that of a Geiger counter by means of a pulse-height discriminator circuit.

The Geiger counter has a resolving time of about 200 μsecs., so that its response is non-linear and for even moderate counting rates quite large "lost-counts" corrections are required. Apart from the difficulty of making these corrections highly accurate, it is necessary to reduce really strong reflected beams by means of absorbing foils placed in the path of the beam so that the counting rate does not become too high. The reduction factor of the foils must be known accurately and they must be uniform. These constitute definite disadvantages to the use of the Geiger counter.

The resolving time of a proportional or scintillation counter is about 1 μsec., so that both these counters have linear responses up to very high counting rates. No corrections for lost counts are required, and as it is not necessary to reduce strong reflexions by means of absorbing foils all reflexions are automatically on the same scale.

The main drawback to the use of counter techniques is the time required for intensity measurements. With the Geiger counter apparatus which was used in this work about twenty minutes were required for each reflexion and it was necessary to measure a standard reflexion about every hour or so in order to put all the intensity measurements on the same

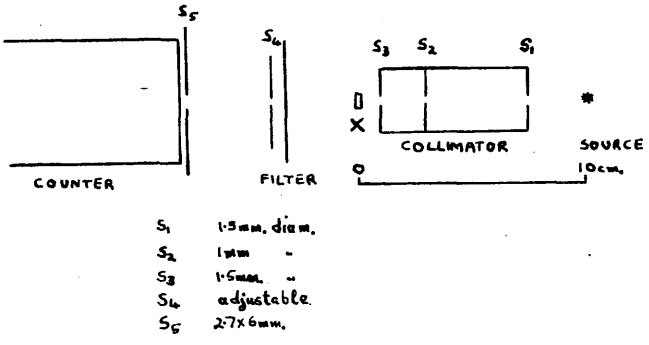

Fig. 14. Diagram of the experimental arrangement for recording X-ray intensities on the Geiger-counter spectrometer. The vertical scale of the diagram has been exaggerated. The position of the crystal is marked by a cross.

scale. As measurements were repeated on crystals of different sizes and the results averaged, several weeks were required to obtain a complete set of structure factors for one zone of reflexions.

The procedures followed in this analysis were those used by Cochran in his analysis of adenine hydrochloride[64], and described by him elsewhere[82].

1.2. Description of the Apparatus

The Geiger-counter spectrometer used in this analysis was designed in the Cavendish Laboratory by Dr. W. Cochran. It consists of a standard 'Unicam' single-crystal goniometer to which is attached a circular scale with an arm to carry the counter. The counter is detachable and can be replaced by the usual telescope, and a cylindrical film holder can then be mounted in the usual way about the axis of rotation of the goniometer arcs. In this way the crystal can be centred optically about the axis of rotation and setting photographs taken.

An argon-alcohol filled counter about six inches long was used for intensity measurements made with copper $K\alpha$ radiation. A diagram showing the relative positions of the collimator, crystal specimen and counter is given in Fig. 14. A brass collimator containing three coaxial holes, the smallest

being not less than 1 mm. in diameter, was used so that crystals of normal size would be completely bathed in a uniform X-ray beam. Of the two vertical slits through which the reflected beam passes S_4 is adjustable to conform with the crystal size, and S_5 is fixed, being sufficiently large to admit any reflected beam of a size likely to be met.

The central wire of the counter is connected to a unit supplying a stabilised high voltage. The number of counts made in a selected time is recorded on a standard scaling unit. A counting-rate meter is also used to give an indication of the intensity of the reflected beam. This is designed so that the magnitude of the deflection of a micro-ammeter is proportional to the number of counts recorded per second, the average being formed over a time varying from one second to four minutes depending on choice. A quenching unit, whose effect is to render the counter insensitive to further counts for a period of time of about 200 μsecs. after each count, is also provided. This period is the resolving time of the instrument.

1.3. Adjustment of Crystal and Apparatus

The goniometer legs were adjusted so that the crystal was completely bathed in the central part of the X-ray beam of

uniform intensity. The width of S_4 was adjusted so that it was about 0.5 mm. greater than that of the reflected beam, the width of which was measured by inserting a piece of film behind S_4. The slit S_4 has to be closed as much as possible to reduce the X-ray background and to prevent more than one reflexion passing through but it is necessary to leave a small safety margin so that no part of the reflected beam is cut off due to any slight mis-setting.

The crystal was centred optically and the desired axis adjusted to the vertical by taking composite Laue photographs according to the method of Weisz & Cole[83], the film-holder being rotated horizontally by about 1 mm. between each photograph. In this way the crystal could be set very accurately.

1.4. Calculation of Crystal Settings

There are two settings which must be calculated for any one reflexion, one being the setting of the counter and the other of the crystal.

The counter setting is 2θ, where θ is the Bragg angle of the reflexion concerned. For a reflexion in the $(h0\ell)$ zone the angle θ is calculated from the equation

$$\sin^2\theta_{h0\ell} = h^2\sin^2\theta_{100} + \ell^2 \sin^2\theta_{001} + 2h\ell \sin\theta_{100} \sin\theta_{001} \cos\beta^* \quad \ldots\ldots\ldots\ldots (55)$$

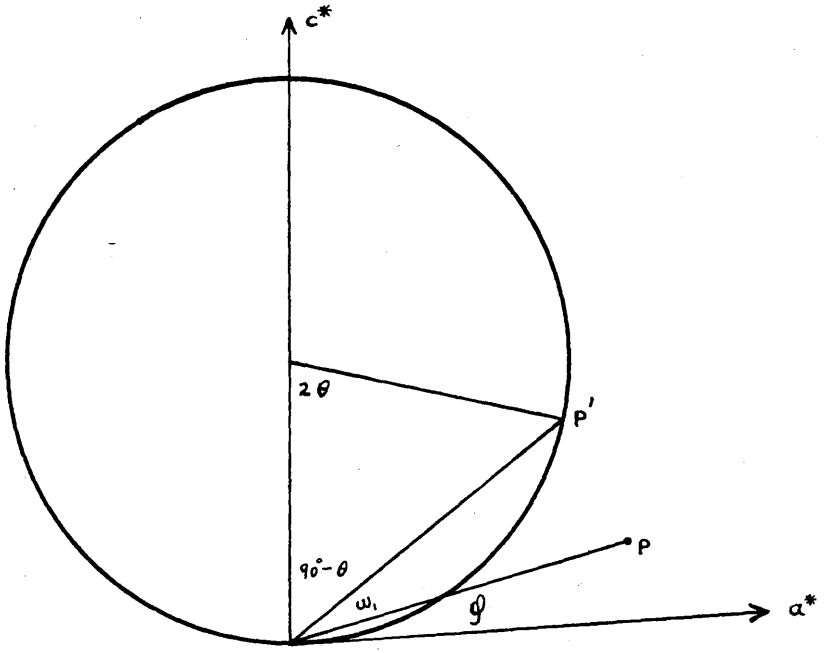

$$\beta^* = (90^\circ - \theta) + \omega_1 + \varphi$$

Fig. 15. Diagram illustrating how the crystal setting for a given (h0ℓ) or (0kℓ) reflexion depends on θ and φ, where (2 sinθ, φ) are the polar co-ordinates of an (h0ℓ) or (0kℓ) point in the reciprocal lattice.

For a reflexion in the (0kℓ) zone the third term in the right-hand side of this equation is zero.

Fig. 15 illustrates how the setting of the crystal is obtained for a given reflexion.

Let the incident beam be travelling initially along the $\underline{c}^*$ axis. For a point P, with polar coordinates (2 sin θ , φ) in the reciprocal-lattice net, to reach a reflecting position the reciprocal latiice must be rotated through an angle ω_1, so that point P touches the sphere of reflexion at P^1.

Since β^* is then equal to the sum of $(90^\circ - \theta)$, φ and ω_1, the angle ω_1 is given by

$$\omega_1 = \beta^* - 90^\circ + \theta - \varphi \quad \ldots\ldots\ldots\ldots\ldots\ldots\ldots \quad (56)$$

Normally, however, when the crystal setting is 0° the incident beam makes some angle with the $\underline{c}^*$ axis, so that ω, the crystal setting with reference to the scale on the apparatus, will be given by

$$\omega = \theta - \varphi + K \quad \ldots\ldots\ldots\ldots\ldots\ldots\ldots\ldots \quad (56a)$$

where K is a constant, which is determined in practice by locating some prominent low-order reflexion such as the (002) for benzoic acid.

For the (h0ℓ) zone φ was calculated from the expression

$$\sin\varphi = \frac{ha^* \sin\beta}{\sin\theta} \quad \ldots\ldots\ldots\ldots\ldots\ldots\ldots \quad (57)$$

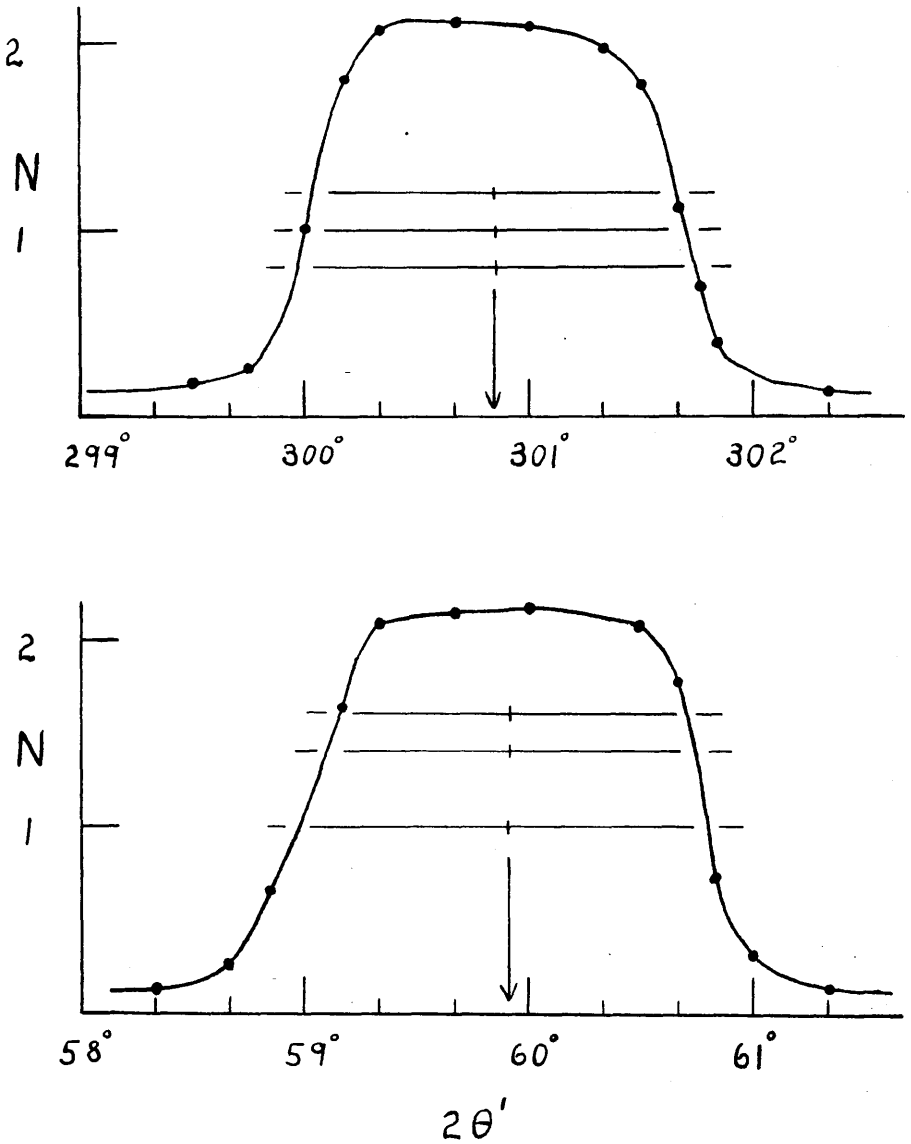

Fig. 16. Variation with 2θ of the counting rate for a given reflexion. The median position gives the Bragg angle of the reflexion.

and for the (0kℓ) zone from the expression

$$\tan \varphi = \frac{\ell c^*}{k b^*} \qquad \ldots\ldots\ldots\ldots\ldots\ldots\ldots\ldots\ldots\ldots\ldots\ldots (58)$$

Values of θ and φ for reflexions in the (h0ℓ) and (0kℓ) zones of benzoic acid are listed in Appendix 2.

1.5. Measurement of Accurate Cell Dimensions

Using the previously determined unit cell dimensions (Chapter III, section 2.2), crystal settings were calculated for reflexions of a crystal of benzoic acid set (1) with the b axis vertical, (2) with the a axis vertical. For a given reflexion the crystal was set to give maximum reflection, and the counting rate measured as the counter was set at successive 2θ positions in the reflected beam. The type of graph obtained is shown in Fig. 16. The median position was found by drawing horizontal lines across the figure and bisecting these. In this way the Bragg angle of the reflexion concerned could be obtained, accurate to about one or two minutes of arc.

This procedure was repeated with the counter set at $(360^\circ - 2\theta)$ in order to eliminate any error in the zero of the circular scale.

By measuring the 2θ values of several axial planes, accurate values for a, b and c were obtained. In order to determine β the 2θ values of some (h0ℓ) reflexions were measured and β calculated by the use of equation (55). The results obtained

are as follows:

$$\underline{a} = 5.507 \pm 0.005 \text{ Å}$$

$$\underline{b} = 5.125 \pm 0.005$$

$$\underline{c} = 21.88 \pm 0.02$$

$$\beta = 97^{\circ}\ 8' \pm 6'.$$

These agree well with the previously determined values.

Using these values crystal and counter settings for the (h0ℓ) and (0kℓ) zones of benzoic acid were recalculated.

1.6. Measurement of Integrated Intensities by the Oscillating Crystal Method

The crystal was set in one of its maximum reflecting positions and was oscillated through a range of 2° by means of a cam and lever system, one complete oscillation being made in one minute. By keeping the averaging time of the circuit associated with the microammeter of the counting-rate meter constant at about one second, so that the meter recorded the X-ray intensity with very little time lag, it was possible to verify that the intensity was at its maximum at the centre of the range of oscillation, and fell to zero at either end.

The intensity of any reflexion was recorded as a number of counts on the scaling unit, the intensity being reduced if necessary by inserting nickel foils of known absorption factor in front of S_4, so that not more than 3000 counts per oscillation

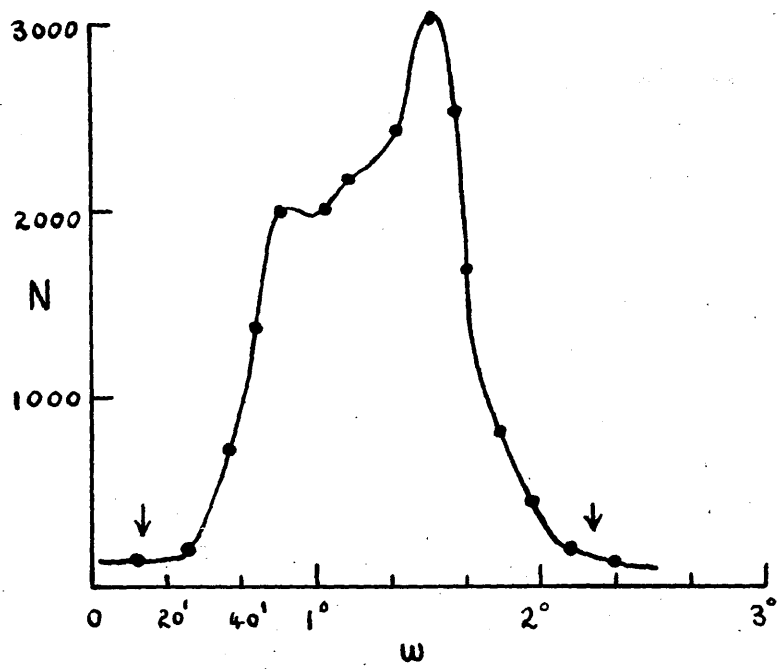

Fig. 17. Variation with crystal setting of the counting rate for a given reflexion.

were recorded. Readings of two minutes were made for each reflexion for each of the equivalent settings. Fluctuations in the mains voltage were corrected by manual control of the input voltage and tube current, for the X-ray tube which was used was not stabilized.

A standard reflexion was measured at intervals of about an hour, the counts from other reflexions being later corrected in the ratio of the decrease of the standard. This decrease was fairly regular and was due to the volatility of the benzoic acid crystals.

By measuring the counting rate for a given reflexion at different positions in the 2° oscillation range and plotting the counting rate against crystal setting, it was possible to derive the shape of that reflexion. The type of graph obtained for an $(h0\ell)$ reflexion is shown in Fig. 17. The very sharp maximum at one point of the irregular graph suggests that it would be rather difficult to obtain an accurate estimate of intensity by a stationary crystal method with the apparatus used in this analysis. The vertical arrows at either end of the graph indicate the normal oscillation range.

1.7. Corrections for Background

The integrated intensity which has to be measured is that

of the copper K doublet which has been reflected from the plane concerned. What is actually measured is this intensity plus a certain background count due to cosmic radiation, incoherent scattering from the air near the crystal and, possibly, reflected white radiation. This background could be considerably reduced if the radiation emitted by the X-ray tube were to be monochromatized by reflection from another crystal, but this would raise further difficulties.

With the X-ray tube which was used the intensity of the resultant beam would have been too low to enable a sufficient number of counts to be recorded in a reasonable time. Because of the statistical uncertainty of $\sqrt{N}$ in an observation of N counts it is necessary to record as many counts as possible. To obtain a standard deviation of 1% it is necessary to record 10,000 counts.

Moreover an X-ray beam monochromatized by reflection from a crystal is small in cross-section, so that the crystal would not be completely bathed in a uniform beam, and in different settings different volumes of the crystal would be irradiated by the beam, so causing errors in the measured intensities. One way of overcoming this difficulty would be to use a crystal considerably larger than the monochromatic X-ray beam so that the beam passes completely into the crystal

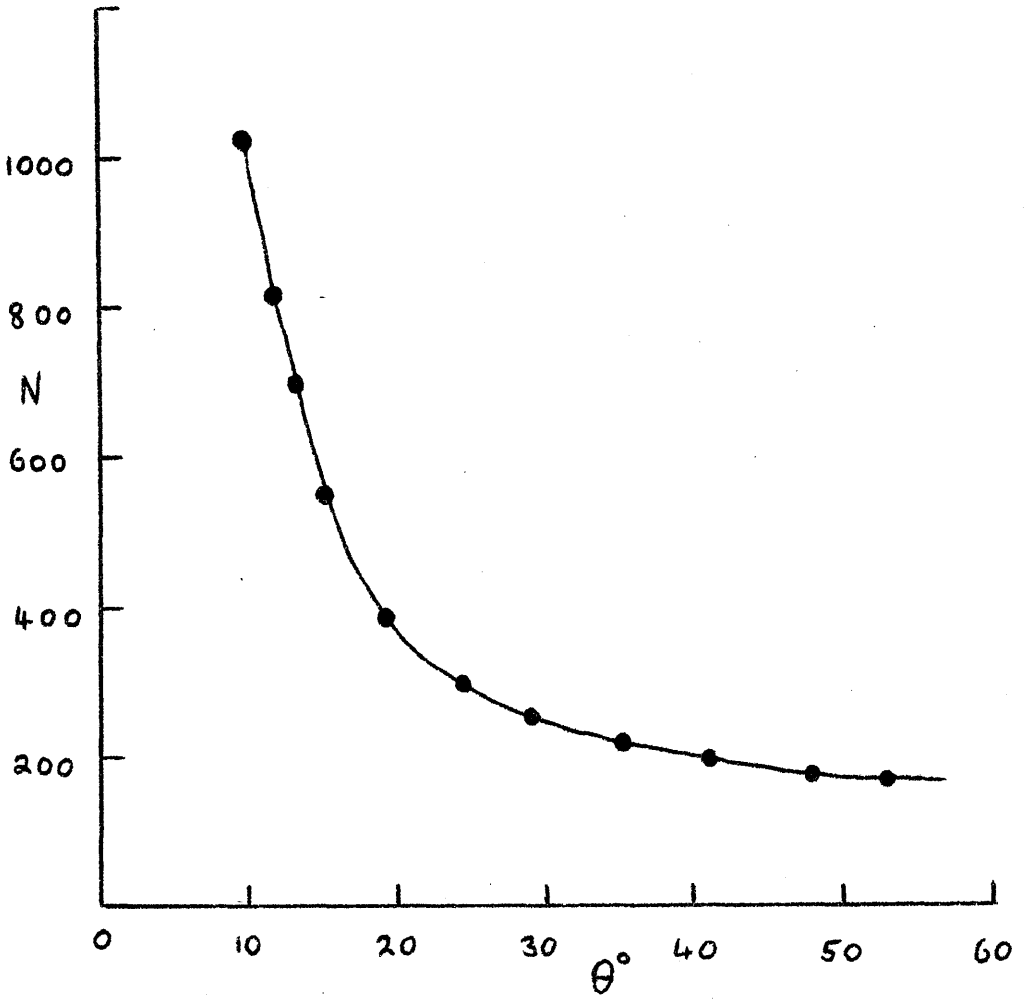

Fig. 18. Variation with θ of the X-ray background for a particular crystal.

at all crystal settings. With a large crystal, however, extinction effects are liable to be serious. For these reasons no attempt was made to use monochromatic radiation.

The background of the counter caused by cosmic radiation was measured by recording the number of counts made in ten minutes when the X-ray tube window was closed. This background was usually about 60 counts per minute for the argon filled counter which was used.

The X-ray background due to incoherent scattering from the crystal and to air scattering was measured for each reflexion with the crystal turned so that no $K\alpha$ reflected radiation was recorded. This background count varied smoothly with 2θ in the manner shown in Fig. 18 which shows the variation of X-ray background with 2θ for one of the crystals used.

No attempt was made to correct for white radiation with wavelengths of between 1.48 and 1.77 Å. These are the wavelengths of the Ni K and Fe K absorption edges. Although such radiation comes only from the plane whose intensity is being measured, its greater dispersion at high angles results in a lower proportion passing through the counter slits at these angles, so that at first sight it would appear necessary to allow for it. However, Cochran observed with a similar

tube voltage that from being 6% of the recorded intensity at $2\theta = 10^{\circ}$, it fell off rapidly to 2% at 30°, so that it is only for a few of the lowest angle reflexions that it is not quite negligible.

The presence of at least one nickel filter at the slit S_4 eliminates completely the copper Kβ reflected radiation.

White radiation outside the range 1.48 - 1.77 Å consists mainly of $\frac{1}{2}\lambda(K\alpha)$ reflected from the second order of the plane being measured. Where Weissenberg photographs showed reflexions to be overlapped by such second order reflexions two readings were taken, one with the normal Ni filter, and another with an Fe filter of such a thickness that its absorption for $\frac{1}{2}\lambda(K\alpha)$ was the same as that of the Ni filter. Because of its absorption edge the Fe filter will pass practically no Kα radiation, so that the difference between the readings with each filter is the corrected reading. This is the 'balanced filter' method of Ross[84].

It was found that the corrections for $\frac{1}{2}\lambda(K\alpha)$ radiation were insignificant for all the reflexions in the $(h0\ell)$ and $(0k\ell)$ zones of benzoic acid. This, presumably, is because the counter is much less sensitive to such radiation than is a photographic film.

1.8. Correction for 'Lost Counts'

All the counts occurring within the resolving time of the counter are recorded as one. This causes a serious loss of counts at high counting rates.

It has been shown by Cochran[82] that the corrected counting rate N may be simply expressed as

$$N = N_0/(1 - N_0 K\tau) \quad \ldots\ldots\ldots\ldots\ldots\ldots\ldots\ldots \quad (59)$$

where N_0 is the number of counts recorded in one second, τ is the resolving time in seconds, and K is a constant depending upon the variation of intensity with time, i.e. upon the form factor of the X-ray source and the angular velocity of oscillation of the crystal.

In order to determine $K\tau$ the same reflexion was measured at different counting rates. If the recorded counting rate for a reflexion with its intensity reduced by a certain number of nickel foils is N_1 then from equation (59), after rearrangement, we obtain

$$\frac{1}{N} = \frac{1}{N_1} - K\tau \quad \ldots\ldots\ldots\ldots\ldots\ldots\ldots\ldots \quad (60)$$

If some of the nickel foils are removed so that the effective intensity is increased r times, and the new recorded rate is N_2, then

$$\frac{1}{rN} = \frac{1}{N_2} - K\tau \quad \ldots\ldots\ldots\ldots\ldots\ldots\ldots \quad (60a)$$

and we obtain finally

$$K\tau = \frac{r/N_2 - 1/N_1}{r - 1} \quad \ldots\ldots\ldots\ldots\ldots\ldots \quad (61)$$

A reflexion was selected for which the counting rate was about 2000/min. with several reducing foils in place. Readings were made at this rate and at each of two other rates obtained by removing one foil and adding one respectively. The reducing factor of the nickel foils was 2.0. By combining the three different counting rates three independent values for $K\tau$ were obtained. Their mean was used in all calculations. An evaluation was made for each crystal used since the precise value depends both on the range of oscillation and the mosaic structure of the crystal, and the latter may be expected to vary slightly from crystal to crystal. The values found varied between 2.6×10^{-3} and 4.3×10^{-3} seconds. The true counting rate for each reflexion was obtained from the recorded rate by application of equation (59).

The following percentage corrections had to be applied to the recorded counting rates for a value of $K\tau = 3.5 \times 10^{-3}$ seconds.

500	counts/min.	2%	correction
1500	" "	10%	"
2500	" "	18%	"

1.9. Absorption Corrections

For the measurements of the (h0ℓ) reflexions crystals of almost square cross section were used so that absorption factors for different reflexions would not differ.

For the measurements of the (0kℓ) reflexions the smaller crystals used had cross-sections which were almost square so that absorption corrections were not required, but for the largest crystal, which had minimum and maximum dimensions at right angles to the rotation axis of 0.17 x 0.40 mm., absorption corrections were felt to be required.

The method used to correct for absorption was based on that due to Albrecht[86]. The absorption factor for a crystal is given ideally by

$$A = \int_S \text{exp.} \{-\mu(r+t)\} dS, \quad \ldots\ldots\ldots\ldots\ldots\ldots \quad (62)$$

where S is the area of cross-section of the crystal, and r and t are the lengths of the incident and reflected rays within the fractional area dS. This integral can be represented approximately by a summation, the degree of approximation depending on the number of terms in the summation. The crystal cross-section is divided into n equal fractional areas ΔS (so that $n\Delta S = 1$), and exp. $\{-\mu(r+t)\}$ evaluated at the centre of each area. We then obtain

$$A = \sum_n \text{exp.} \{-\mu(r+t)\} \Delta S \quad \ldots\ldots\ldots\ldots\ldots\ldots \quad (63)$$

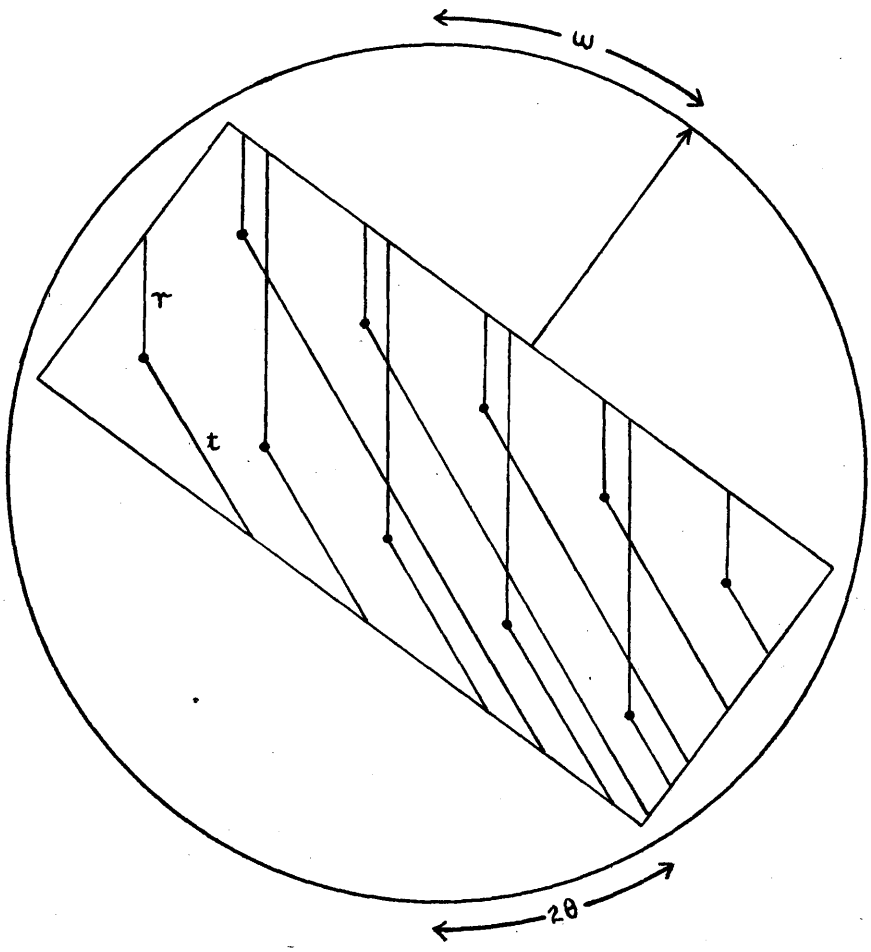

Fig. 19. Illustration of the procedure used to calculate absorption factors.

and since the areas ΔS are equal,

$$A = \overline{\exp.\{-\mu(r+t)\}} \quad \ldots\ldots\ldots\ldots\ldots\ldots\ldots\ldots \quad (64)$$

The crystal cross-section was drawn out to scale (50 cm. = 1 mm.), and divided into ten equal areas. For each reflexion the crystal and counter settings derived in section 1.4 were used to draw lines representing the incident and reflected rays at the centres of the areas into which the cross-section had been divided. A scale, marked out with values of exp.(-9.35x) on the same scale as the crystal cross-section, was used to derive values of $\exp.\{-\mu(r+t)\}$ for the path-lengths in the crystal, and the ten values for each reflexion were then averaged.

This procedure is illustrated in Fig. 19.

The values of $\overline{\exp.\{-\mu(r+t)\}}$ ranged from 0.759 to 0.849.

1.10. Calculation of Integrated Intensities

By applying the above corrections to the recorded counting rates in the following way the integrated intensities were obtained.

1. The natural background count was subtracted.
2. The readings from different crystal settings were averaged.
3. The lost counts correction was applied.
4. The corrected value from (3) was multiplied by the total reducing factor of all the Ni foils used.

Table 11

Comparison of some $(h0\ell)$ F_o values measured on different crystals. Crystal 1 was the smallest crystal used, crystal 3 the largest.

	F_o values		
h0	Crystal 1	Crystal 2	Crystal 3
002	32.2	32.2	
004	30.0	31.3	
006		8.6	8.2
008	20.5	20.4	20.2
0,0,10		9.9	9.5
0,0,12		5.5	5.5
100	38.5	40.0	
102	34.2	34.6	
104	26.3	26.9	
106	16.9	17.4	
108		19.4	19.2
1,0,10		22.4	22.1
1,0,12		23.2	23.2
$10\bar{2}$	72.6	71.6	
$10\bar{4}$		2.6	2.9
$10\bar{6}$		6.3	6.6
$10\bar{8}$	35.6	34.9	34.4
$1,0,\bar{10}$		4.3	4.5
$1,0,\bar{12}$		35.2	34.9
$1,0,\bar{14}$		15.4	15.6

5. The average X-ray background was subtracted.

6. The value from (5) was scaled to the appropriate value of the standard reflexion.

7. The Lorentz and polarisation factors were applied.

8. Where necessary, values from (7) were divided by absorption factors.

F_o values were obtained by taking the square-roots of the integrated intensities from (8).

1.11. Discussion of Results

The (h0ℓ) F_o values were measured for three crystals of varying sizes, and for common reflexions the percentage discrepancy between independent measurements is 1.7.

In Table 11 independent measurements for some reflexions are compared.

The close agreement between the independent determinations shows clearly the superiority of Geiger-counter measured intensities over visual estimates.

The percentage discrepancy between the final averaged Geiger-counter measured (h0ℓ) structure factors and the visually estimated structure factors is 7.4. The percentage discrepancy between the Geiger-counter measured structure factors and the final calculated (h0ℓ) structure factors of the earlier analysis (Chapter III) is 9.7, slightly higher than the value of 8.8

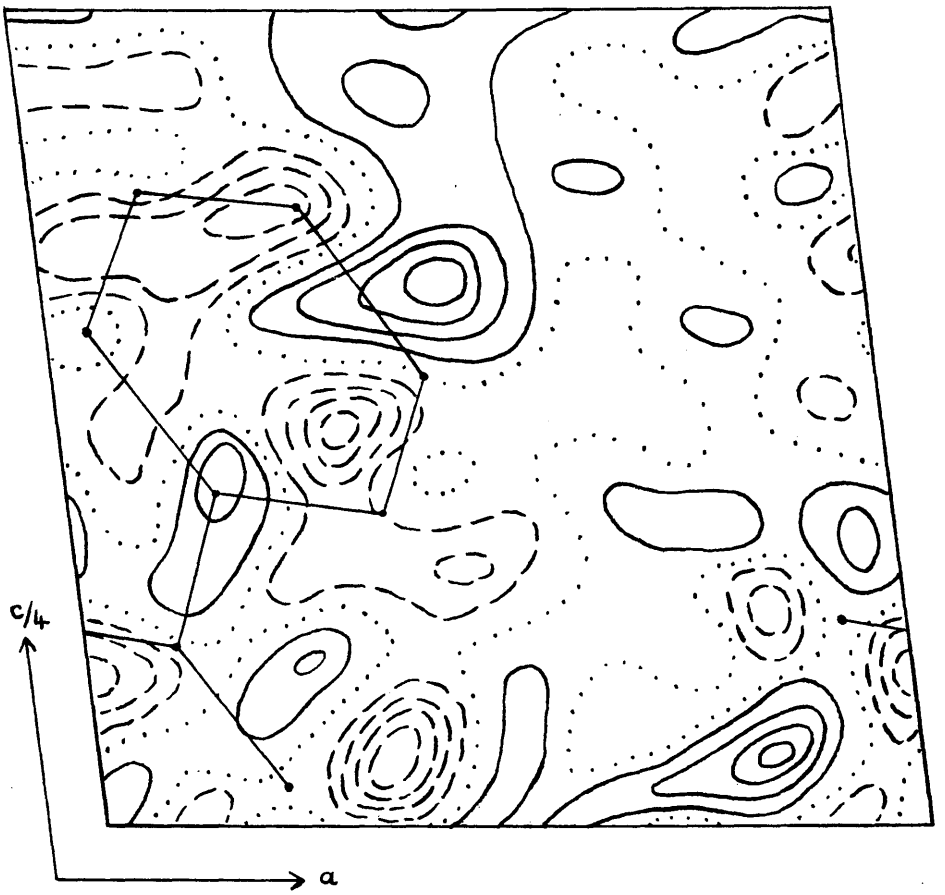

Fig. 20. First difference-synthesis projection on (010). Contours at intervals of 0.1 e. A^{-2}, negative contours broken and zero contour dotted.

obtained with the visually estimated structure factors.

Up to the present only one set of Geiger-counter measured structure factors for the (0kℓ) zone has been evaluated. This is the set associated with the crystal of dimensions 0.17 x 0.40 mm. perpendicular to the rotation axis. Although this cross-section is very far from being square, it was found that because of the low absorption factor for copper Kα radiation ($\mu = 9.35$ cm.$^{-1}$), absorption corrections are not very large. Values of $A = \overline{\exp.\{-\mu(r+t)\}}$ vary from 0.759 to 0.849 only, and the percentage discrepancy between the structure factors, with and without absorption corrections, is 1.5.

The percentage discrepancy between the visually estimated (0kℓ) structure factors and the present set of Geiger-counter measured structure factors is 8.1, and the percentage discrepancy between the final calculated values and the Geiger-counter measured structure factors is 10.9.

2. STRUCTURE REFINEMENT

2.1. Introduction

From a study of other crystal structure analyses made with Geiger-counter measured structure factors, it was realized that the main cause of the percentage discrepancy of 9.7 for

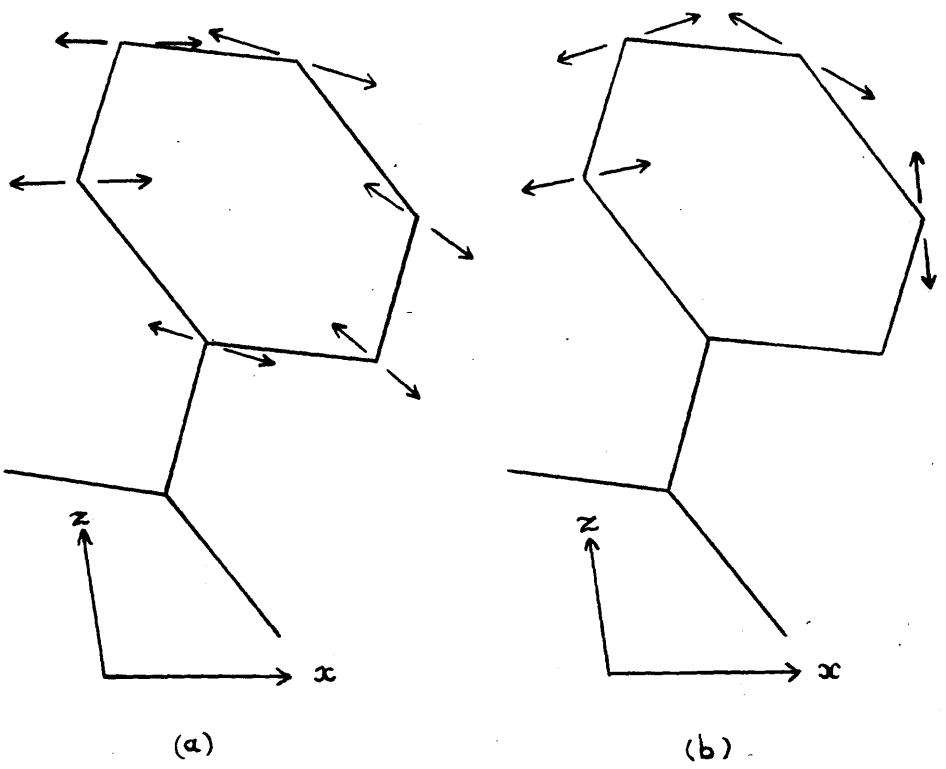

Fig. 21. Comparison of calculated (a) and observed (b) directions of maximum vibration of the carbon atoms of the benzene ring.

the (h0ℓ) data was probably the anisotropic vibration of the atoms. In the previous analysis of benzoic acid only the anisotropic vibration of atoms O_1 and C_5 had been allowed for, as they had been most pronounced.

It was decided that the refinement could best proceed by means of a study of difference Fourier projections which would allow atomic coordinates and thermal parameters to be adjusted by a process of successive approximation.

2.2. Difference Electron-Density Projections on (010)

The first difference map prepared was one in which the Fourier coefficients were differences between the Geiger-counter measured (h0ℓ) structure factors and the final calculated structure factors of the analysis using visually estimated structure factors. This synthesis was computed (as were all the others mentioned in this chapter) on the Hollerith machine in the Cambridge University Mathematical Laboratory. Fig. 20 shows this difference map.

A study of this map revealed that while atom O_1 showed anisotropic thermal vibration, the effect of this had been overestimated in the previous analysis. In addition, atom O_2 was seen to be vibrating preferentially in a direction roughly at right angles to the C_1-O_2 bond, the magnitude of

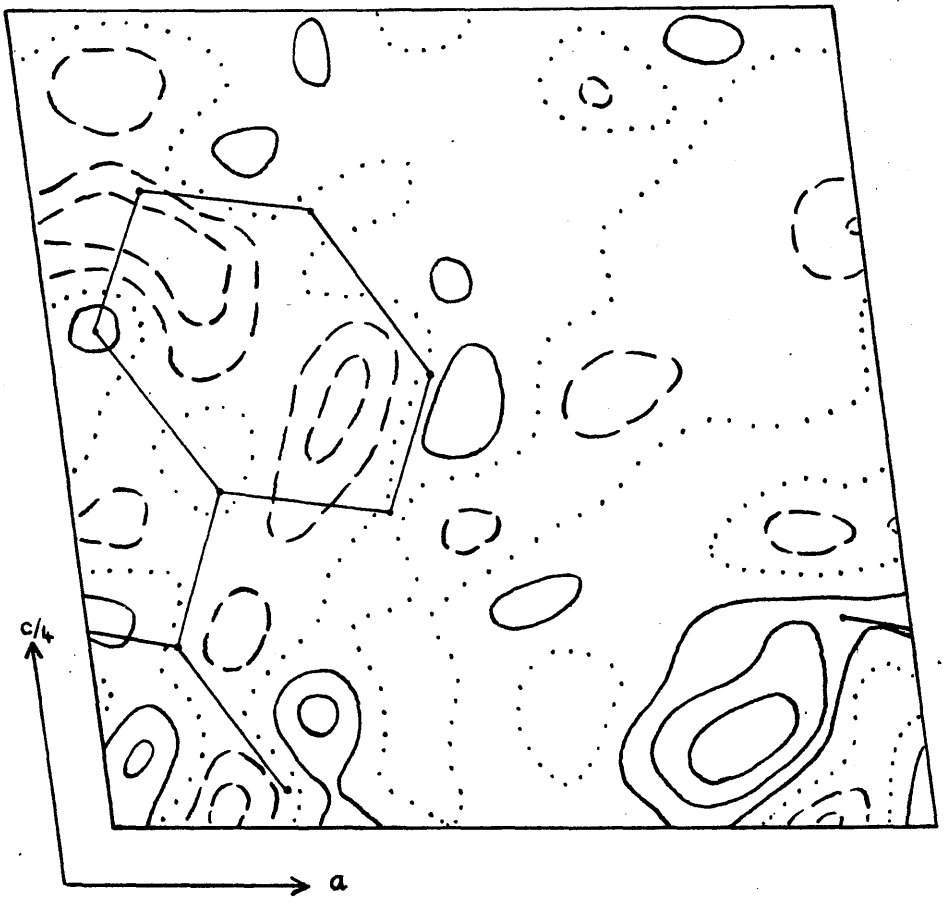

Fig. 22. Fourth difference-synthesis projection on (010). Contours at intervals of 0.1 e.Å^{-2}, negative contours broken and zero contour dotted.

the temperature factor, δ, of atom C_5 had been underestimated, and various small atomic adjustments were required.

It was felt that the structure factors would have to be calculated rather more accurately than in the previous analysis, in order to make full use of the accuracy of the observed values. The coordinates of the atoms were expressed as fractions of the cell edge to three decimal places and the cosines evaluated from the table of cos $2\pi x$ in the International Tables, (1935),[87] correct to three significant places. The atomic scattering factors for each reflexion were evaluated to two significant decimal places and on multiplying by the appropriate cosine values, atomic structure factors correct to two decimal places were obtained. After summing the atomic structure factors for each reflexion, the structure factor values were rounded off to one decimal place. By performing the calculations in this way it was felt that there was very little possibility of rounding-off errors in the F_c values introducing errors into the analysis.

Later difference Fourier projections showed the necessity for introducing anisotropic scattering factors for most of the atoms in the benzene ring. The directions of maximum vibration of the benzene carbon atoms as deduced from the difference maps agree roughly with the directions to be expected if the dimer

Table 12

Temperature-factor parameters for the oxygen and carbon atoms, deduced from the difference-synthesis projections on (010).

Atom	α	β	$\gamma = \alpha + \frac{1}{2}\beta$	ψ
O_1	1.6	1.0	2.1	111°
O_2	2.0	0.4	2.2	140°
C_1			1.55	
C_2			1.45	
C_3			1.9	
C_4	1.8	0.7	2.15	2°
C_5	1.8	0.6	2.1	52°
C_6	1.8	0.8	2.2	100°
C_7	1.55	0.5	1.8	94°

is regarded as a rigid body oscillating in its own plane about the centre of the dimer. These directions are compared in Fig. 21. A similar phenomenon was observed in the analysis of salicylic acid[31].

The final temperature-factor parameters for the oxygen and carbon atoms are listed in Table 12.

So far four cycles of refinement have been carried out with the (h0ℓ) structure factors and the fourth difference synthesis is shown in Fig. 22. This still reveals the necessity for further adjustments to the structure but these have not yet been made. In this projection all the atoms apart from the carboxyl hydrogen atom have been subtracted out.

2.3. Progress of Refinement

After four cycles of refinement the percentage discrepancy for the (h0ℓ) structure factors dropped from 9.7 to 6.9. The actual average discrepancy for each plane, expressed in absolute units, is 0.7 and the largest, apart from that of the $(10\bar{2})$ plane, is 2.8 for the (102) plane. For the $(10\bar{2})$ plane, however, the F_o value is considerably smaller than F_c, the discrepancy being 12.2. This suggests that the plane is affected by extinction and if this individual discrepancy is ignored, the overall percentage discrepancy drops from 6.9 to 5.7 for the (h0ℓ) structure factors.

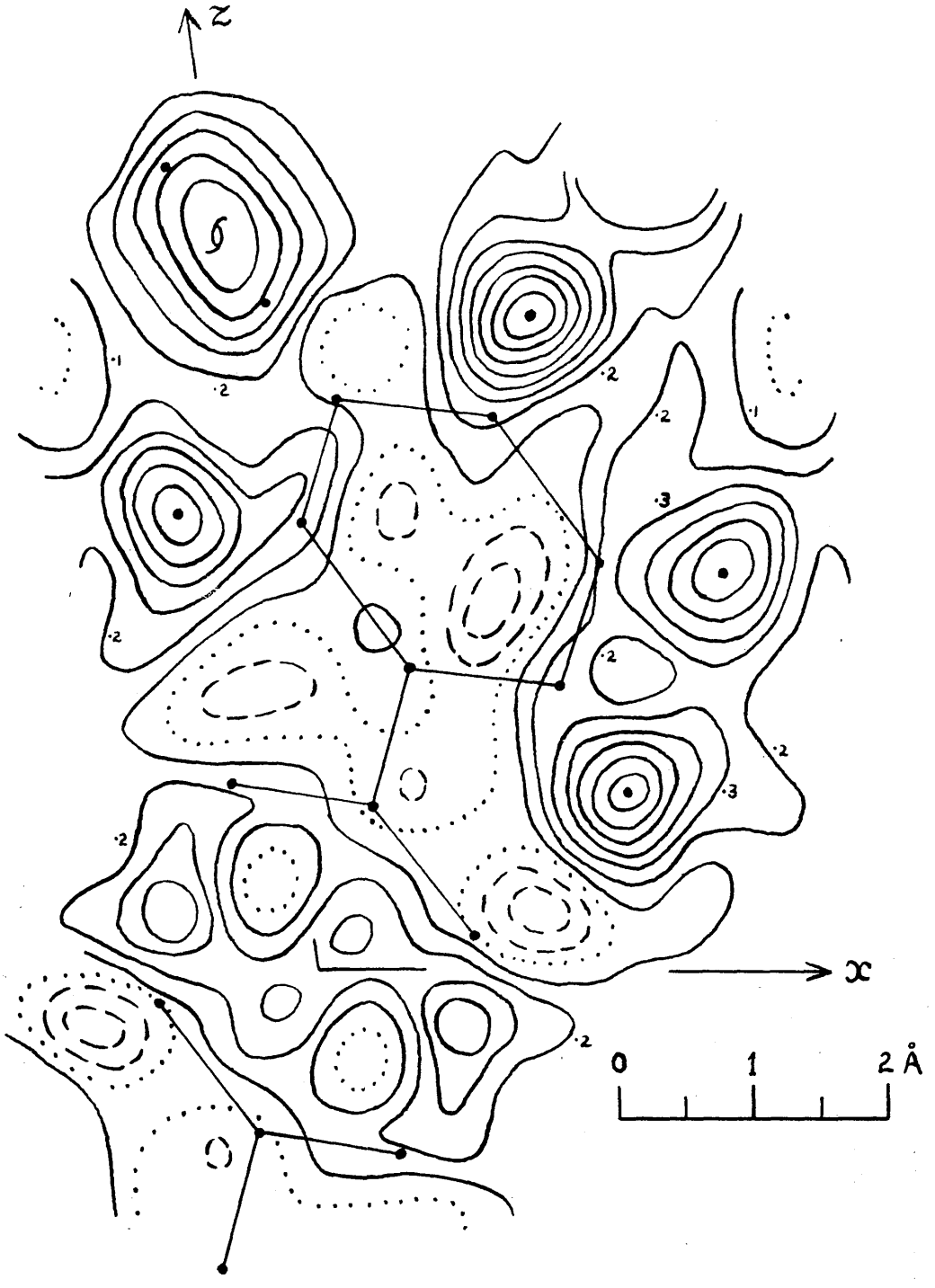

Fig. 23. Difference-synthesis projection on (010) showing the electron distribution due to the hydrogen atoms in the benzoic acid molecule. Contours at intervals of 0.1 e. $Å^{-2}$, negative contours broken and zero contour dotted.

Because of the probability of extinction affecting the $(10\bar{2})$ plane, it was omitted from all the difference Fourier projections.

Observed and calculated structure factors are listed in Appendix 2.

2.4. Location of the Hydrogen Atoms

An $(F_o - F_c)$ synthesis in which the hydrogen contributions were not allowed for in the F_c values was prepared when the percentage discrepancy for the $(h0\ell)$ zone had dropped to 7.5. This is shown in Fig. 23 and reveals clearly the hydrogen atoms bonded to the carbon atoms of the benzene ring. Four of these hydrogen atoms are very well resolved, but the fifth, attached to C_6, appears as an unresolved doublet on the screw-axis projection.

The hydrogen atom of the carboxyl group is only poorly resolved, as in the previous analysis, and cannot be attributed with certainty to either of the oxygen atoms involved in the hydrogen bond. In Fig. 22 this peak appears again, though with a slightly different shape, as the atomic positions and thermal parameters for the oxygen atoms were changed slightly after preparing the projection shown in Fig. 23. The poor resolution of this hydrogen atom is discussed more fully in a later section.

Table 13

Coordinates of the oxygen and carbon atoms.

Atom	x	y	z	X'	Y	Z'
O_1	0.220	0.237	0.0125	1.178	1.215	0.272
O_2	-0.089	0.140	0.0642	-0.667	0.718	1.395
C_1	0.102	0.275	0.0575	0.404	1.409	1.248
C_2	0.180	0.478	0.1033	0.710	2.451	2.243
C_3	0.383	0.627	0.0975	1.846	3.212	2.118
C_4	0.460	0.822	0.1406	2.151	4.214	3.052
C_5	0.334	0.867	0.1897	1.325	4.442	4.123
C_6	0.133	0.717	0.1960	0.201	3.674	4.255
C_7	0.051	0.517	0.1535	-0.134	2.648	3.336

The x and z coordinates of the four well resolved hydrogen atoms are given in Table 17.

2.5. Refinement of the Projection on (100)

Using the F_c values of the earlier analysis and the (0kℓ) Geiger-counter measured F_o values, an (F_o-F_c) synthesis for the (100) projection was prepared. This difference synthesis is shown in Fig. 24. It suggested changes in atomic coordinates for most of the atoms, the largest being a shift of 0.05 Å parallel to the b axis for C_5. Owing to the poorer resolution in this projection, however, the magnitudes of the atomic shifts were rather uncertain.

Because of lack of time it has not yet been possible to carry out any cycles of refinement on this projection, so that the y coordinates of the atoms derived in this analysis must be of a lower degree of accuracy than the x and z coordinates.

The (0kℓ) structure factors are listed in Appendix 2.

2.6. Atomic Coordinates and Molecular Dimensions

The final coordinates of the oxygen and carbon atoms are listed in Table 13. The coordinates x, y and z are referred to the monoclinic axes and are expressed as fractions of the axial lengths. The coordinates X', Y and Z' are referred to

Table 14

Bond lengths in the benzoic acid molecule calculated from the coordinates listed in Table 13.

Bond	Length (Å)
C_1-O_1	1.261
C_1-O_2	1.283
C_1-C_2	1.473
C_2-C_3	1.373
C_2-C_7	1.395
C_3-C_4	1.403
C_7-C_6	1.418
C_4-C_5	1.371
C_5-C_6	1.367

orthogonal axes and were obtained as described earlier. These coordinates are expressed in Ångstrom units.

From these coordinates the bond lengths in the benzoic acid molecule were calculated and the values found are shown in Table 14.

3. DISCUSSION

3.1. Random Arrangement of the Hydrogen Atoms

The main point of interest in the bond lengths listed in Table 14 is the very small difference in length between the C-O bonds of the carboxyl group. The difference is 0.022 Å, rather smaller than the figure of 0.046 Å derived in the earlier analysis.

The only plausible explanation of the near identity of bonds C_1-O_1 and C_1-O_2 is that there is a random arrangement in the crystal of the two types of molecule shown in Fig. 25. The only effective difference between molecules of type (a) and those of type (b), if we ignore differences in bond type, consists of the position of the carboxyl hydrogen. This atom will have only a small effect on the long-range forces governing the packing of the molecules in the crystal, so that it is not surprising that a random arrangement of the two types of molecule exists.

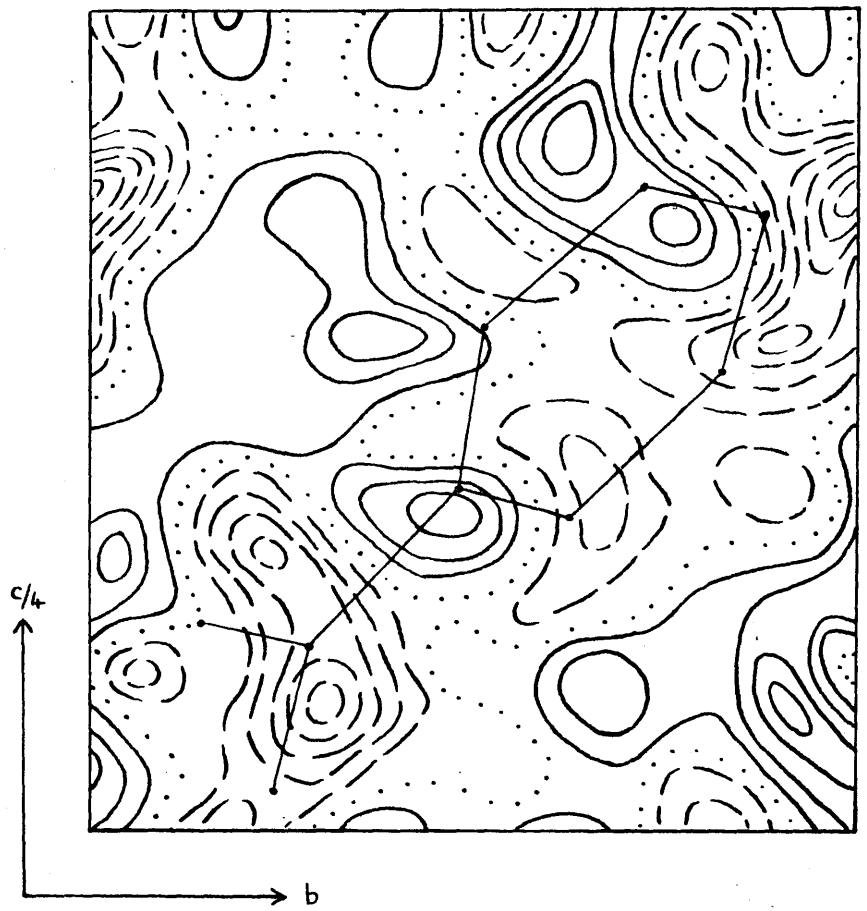

Fig. 24. First difference-synthesis projection on (100). Contours at intervals of 0.1 e.Å^{-2}, negative contours broken and zero contour dotted.

A rather similar phenomenon has been reported by Clews & Cochran[88] in their analysis of the crystal structure of 2-amino-4-methyl-5-chlorpyrimidine. Fourier projections show that the chlorine atoms and methyl groups are distributed randomly through the structure in either the 4- or 6- position.

Other structures are known in which the space group symmetry demands a statistical arrangement. p-Bromochlorobenzene has been reported by Hendricks[89] to have the space group $P2_1/a$ with two molecules in the unit cell, so that a centrosymmetrical molecule is required. Certain acid salts[33,34,35] are required by the crystallographic symmetry to have a symmetrical O-H...O bond. In view of the O...O distances, however, it is certain that the bond symmetry is merely statistical and that the crystals have a random structure.

A random alternation of the two types of benzoic acid molecule would cause an effective plane of symmetry, from C_1 to C_5, through the molecule, with bonds related by this plane being equal in length. The bond lengths listed in Table 14 satisfy this requirement (within the limits of experimental error), as also do the bond lengths reported in the earlier analysis.

Table 15

Displacements of the atoms from the molecular plane

$Y = 0.7709X' + 0.8043Z' + 0.0942.$

Atom	$Y_{calc.}$	$Y_{obs.}$	Δ	Displacement
O_1	1.221	1.215	0.006	0.004
O_2	0.702	0.718	-0.016	-0.011
C_1	1.409	1.409	0.000	0.000
C_2	2.445	2.451	-0.006	-0.004
C_3	3.221	3.212	0.009	0.006
C_4	4.207	4.214	-0.007	-0.005
C_5	4.431	4.442	-0.011	-0.007
C_6	3.671	3.674	-0.003	-0.002
C_7	2.674	2.648	0.026	0.017

3.2. Planarity of the Benzoic Acid Molecule

Another requirement of this random alternation is that the molecule must be effectively planar, that is, the coordinates of all the atoms should satisfy an equation of the type

$$Y = AX' + BZ' + C.$$

A, B and C were determined by the method of least squares to be 0.7709, 0.8043 and 0.0942 respectively. Using this equation Y coordinates were calculated for all the atoms and compared with those derived from the difference synthesis for the (100) projection. The deviations, Δ, between these estimates are listed in Table 15, along with the corresponding displacements of the atoms from the molecular plane. The average deviation between the two values of Y is 0.009 Å, equivalent to a perpendicular displacement of 0.006 Å. The largest deviation (for C_7) is 0.026 Å, equivalent to a perpendicular displacement from the plane of 0.017 Å. All the atoms in the benzoic acid molecule may, therefore, be regarded as coplanar.

A rather different conclusion had been reached in the earlier analysis of benzoic acid, but it was thought that this discrepancy might have been caused by the method which was used to calculate the molecular plane. In that analysis a molecular plane had been calculated by least squares to fit the

Table 16

Displacements of the atomic coordinates derived in Chapter III from the molecular plane

$$Y = 0.7814X' + 0.8156Z' + 0.0787.$$

Atom	$Y_{calc.}$	$Y_{obs.}$	Δ	Displacement
O_1	1.247	1.216	0.031	0.020
O_2	0.701	0.737	-0.036	-0.023
C_1	1.410	1.430	-0.020	-0.013
C_2	2.475	2.470	0.005	0.003
C_3	3.239	3.241	-0.002	-0.001
C_4	4.229	4.231	-0.002	-0.001
C_5	4.464	4.497	-0.033	-0.022
C_6	3.710	3.700	0.010	0.007
C_7	2.701	2.653	0.048	0.032

ring atoms only, i.e. atoms C_2, ... C_7, and it was then found that atoms C_1 and O_2 were displaced significantly from that plane.

It was now realized that a more strictly logical method of establishing the planarity of the whole molecule was to calculate a "best" plane through all the atoms and then to investigate the displacements of the atoms from that plane. Consequently, the calculation of the molecular plane derived from the earlier coordinates was repeated, incorporating the coordinates of all the atoms. A, B and C were found to be 0.7814, 0.8156 and 0.0787 respectively. Using these values, Y coordinates for all the atoms were calculated and compared with those obtained from the final difference synthesis of the earlier analysis. The results are listed in Table 16. The average deviation between the two estimates of Y is 0.021 Å, equivalent to a perpendicular displacement from the molecular plane of 0.014 Å, and the largest deviation (C_7) is 0.048 Å, equivalent to a perpendicular displacement of 0.032 Å. Atoms O_2 and C_1, which were thought previously to have displacements from the plane of the benzene ring of 0.068 and 0.042 Å, have displacements from the recalculated molecular plane of 0.023 and 0.013 Å respectively. These are not significant, so that using the coordinates of the

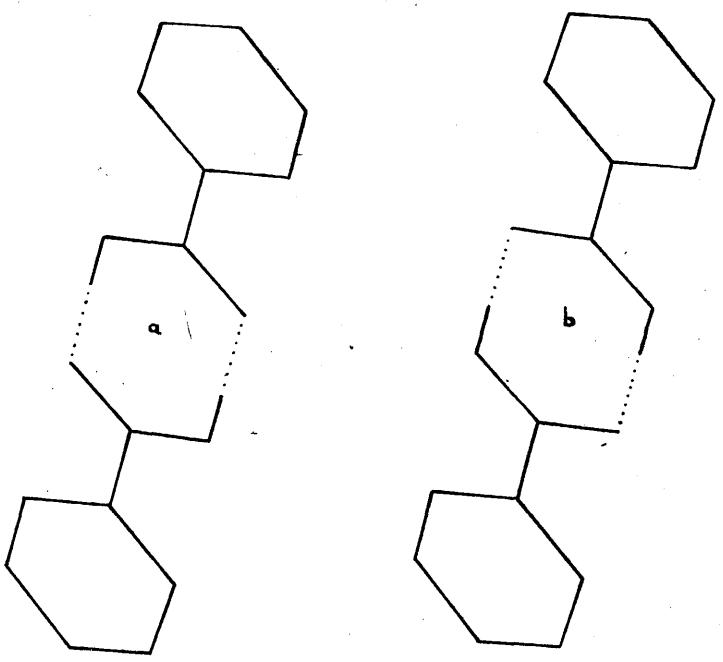

Fig. 25. Illustration of the two types of molecule in the benzoic acid lattice. Molecules of type (b) are obtained by rotating molecules of type (a) through 180° about an axis running from C_5 to C_2. The only hydrogen atom shown is that belonging to the carboxyl group.

earlier analysis the molecule is found to be planar.

As the y coordinates found from the difference synthesis shown in Fig. 24 were thought to be less accurate than the x or z coordinates, bond lengths for the benzoic acid molecule were recalculated using Y coordinates obtained from the equation

$$Y = 0.7709X' + 0.8043Z' + 0.0942.$$

The bond lengths so calculated are shown in Fig. 26.

3.3. Bond Length Variations in the Benzene Ring

The values shown in Fig. 26 differ only slightly from the lengths given in Table 14, the main difference being in the lengths of the bonds C_3-C_4 and C_6-C_7 which are smaller by 0.011 and 0.022 Å respectively.

These bonds differ from C_4-C_5 and C_5-C_6 by an average value of 0.027_5 Å (using the values from Fig. 26) but it is difficult to decide whether this is significant, for, because of the incomplete refinement of the (100) projection, it is not possible to calculate an accurate standard deviation. Using the bond lengths listed in Table 14 this average difference is 0.041_5 Å.

This aspect of the variation of the bond lengths in the ring will have to await the completion of the refinement of the (100) projection for bonds C_3-C_4 and C_6-C_7 are very dependent

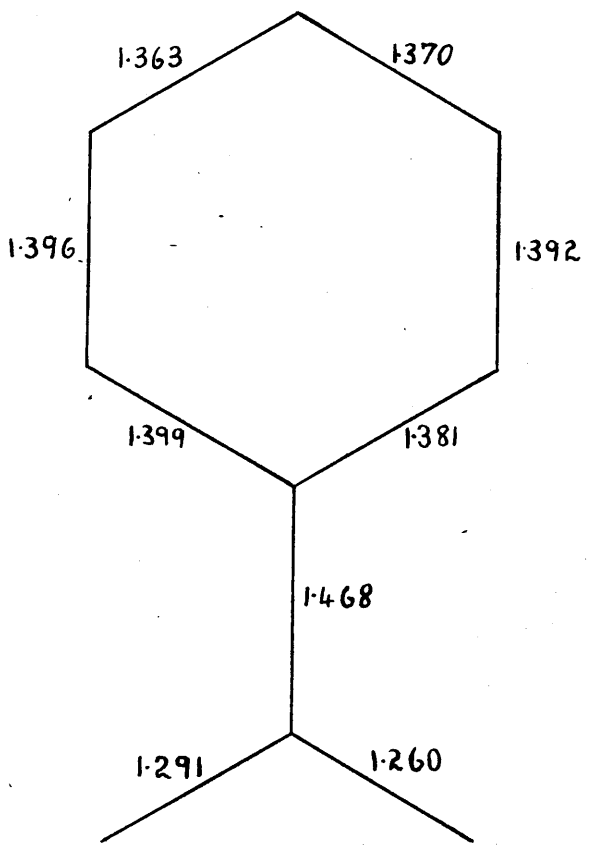

Fig. 26. Bond lengths in the benzoic acid molecule.

on the Y coordinates. Bonds C_2-C_3, C_2-C_7, C_5-C_4 and C_5-C_6 are not so dependent on the Y coordinates and here the bonds C_2-C_3 and C_2-C_7 seem to be slightly longer than the bonds C_5-C_4 and C_5-C_6. The difference is not very great, but as it was found in the previous analysis using visually estimated intensities it may perhaps be real.

The bond C_1-C_2 leading to the carboxyl group is about 1.47 Å in length (1.468 Å in Fig. 26 and 1.473 Å in Table 14) so that it must have an appreciable amount of double bond character. In terms of valence-bond theory this requires the structures I, II and III of Fig. 27 to contribute to the molecular state of benzoic acid. Such a contribution, as well as shortening bond C_1-C_2, would require bonds C_2-C_3 and C_2-C_7 to be longer than the other bonds of the benzene ring. This is in agreement with the observed bond lengths only to the extent that bonds C_2-C_3 and C_2-C_7 are found to be longer than bonds C_5-C_4 and C_5-C_6. Bonds C_3-C_4 and C_6-C_7, however, are found to be the longest bonds in the ring, whereas, if structures I, II and III contribute to the molecular state, they ought to be the shortest. Although the lengths of these bonds are still rather uncertain, it is difficult to believe that they will change sufficiently to make them shorter even than C_5-C_4 and C_5-C_6.

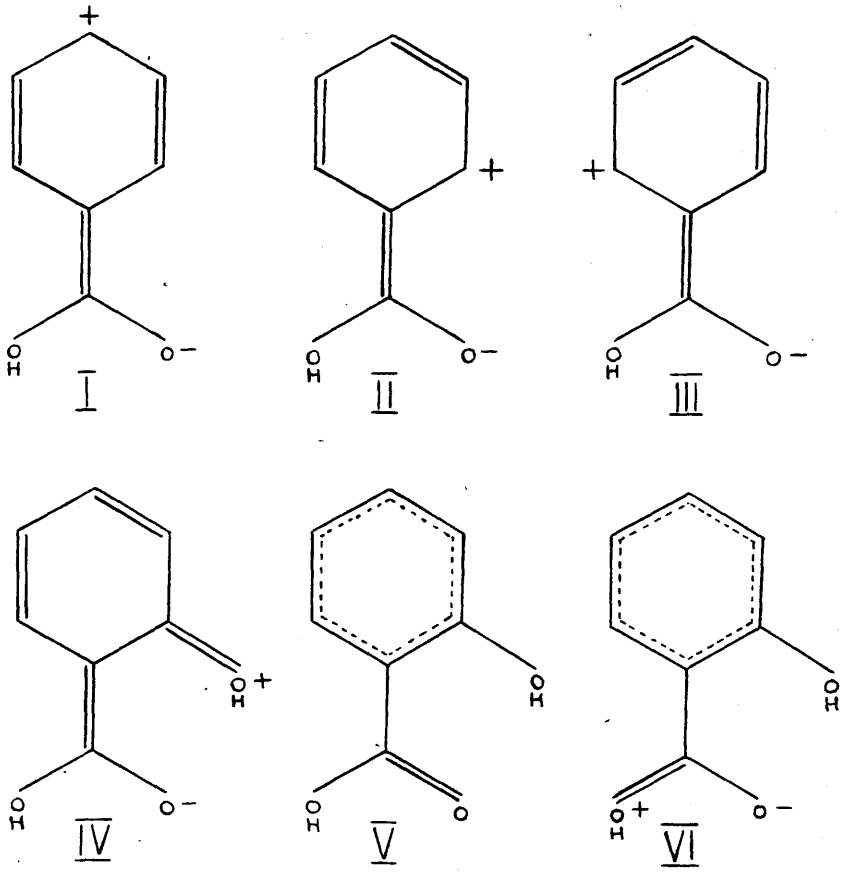

Fig. 27. Resonance "structures" mentioned in the text.

3.4. Correlation of X-Ray Results and Chemical Reactivity

The contribution of structures I, II and III should cause atoms C_3, C_5 and C_7 to have less than six electrons associated with them. Whether this effect is of sufficient magnitude to be detected by an electron count is uncertain. Owing to the incomplete state of the refinement no such counts have yet been made.

Normal aromatic substitution reactions are brought about by electrophilic reagents and consequently are impeded by electron-attracting groups and accelerated by electron-releasing groups. The carboxyl group belongs to the former category and is meta directing. The contribution of structures I, II and III to the molecular state of benzoic acid, which was postulated to explain the short length of bond C_1-C_2, provides a ready explanation of the meta directing effect of the carboxyl group, for it requires the atoms in the ortho and para positions (C_3, C_5 and C_7) to be electron deficient. This electron deficiency will prevent electrophilic reagents attacking the benzene ring in these positions. In agreement with this the nitration of benzoic acid at -30° results in the formation of the ortho, meta and para substituted nitrobenzoic acids in the ratio o:m:p 14:85:0.6[90].

Ri & Eyring[91] showed that it is possible to calculate the

rate of nitration of monosubstituted benzene derivatives by combining the electronic theory of chemical reactions with transition state theory. They assume that the change in the activation free energy ΔF of nitration, caused by the substituent, is due only to coulombic factors and that the value of ΔF of nitration of benzene itself is considered as being essentially nonclassical. They then deduce the equation

$$\frac{k_y}{k_B} = \exp.\left[\left(-\epsilon_y \epsilon_n / rD\right) / kT\right] \quad \ldots\ldots\ldots\ldots\ldots\ldots \quad (65)$$

where k_y is the rate constant of nitration at C_y in the substituted benzene ring, k_B is the rate constant at a carbon atom of benzene, ϵ_y and ϵ_n are the charges on the reacting carbon atom and the attacking reagent, respectively, r is the distance between the carbon atom and NO_2^+ in the transition state and D is the dielectric constant.

The charge on the NO_2^+ ion is assumed to be one electron, that is, 4.8×10^{-10} esu. In order to calculate the charges on the carbon atoms at the various positions in the benzene ring they made use of dipole moment data.

In this way the authors were able to calculate the fraction of nitration at each nuclear position with a fair amount of success.

It would be interesting, when the refinement of the structure of benzoic acid has been completed, to evaluate ϵ_y

at each position in the ring by direct electron counts on the final difference syntheses and then to use these values to calculate the fractions of the various nitrobenzoic acids which are formed on nitration. The main source of error in these counts, however, will be the possible wrong choice of anisotropic temperature factors, for the subtraction of an atom vibrating in one direction results in a transfer of electrons in the difference synthesis from points on either side of the atom in that direction, to points on either side of the atom at right angles to that direction. It seems likely that the correlation of X-ray crystal structure analyses and chemical reactivity, in the way suggested above, will be most successfully accomplished when the temperature factors of the atoms are chosen in some more objective manner, such as by the analysis of neutron diffraction data where, since the scattering is caused by the nuclei alone and the scattering factor of a particular atom is a constant which does not vary with $\sin\theta$, no trouble is caused by possible errors in scattering curves and by the possible existence of peaks in the difference synthesis caused by bonding electrons.

3.5. The Use of Resonance Structures in Calculating Theoretical Bond Lengths

The bond leading to the carboxyl group in salicylic acid is 1.458 Å in length and so agrees well with the corresponding

bond in benzoic acid (1.47 A). On the basis of the standard deviations of length of these two measurements it is not possible to say that the difference is real. One would expect this bond in salicylic acid to be rather shorter than the bond in benzoic acid, for the resonance structure IV shown in Fig. 27 will contribute to the molecular state of salicylic acid in addition to structures similar to I, II and III. As the difference is small either IV must make only a small contribution, or the contributions of I, II and III must be suppressed to some extent when IV contributes to the molecular state of salicylic acid. It is difficult to believe, however, that the contributions of structures similar to I, II and III will be suppressed very much, for the two acids are so similar that it would seem that the explanation of the nearly equal shortening of the C_1-C_2 bond in both should be similar for both compounds.

Cochran found that good agreement with the measured bond lengths could be obtained by describing the molecular state of salicylic acid in terms of resonance between the structures IV, V and VI of Fig. 27, these structures being given weights of 0.14, 0.66 and 0.20 respectively. There is justification, however, for claiming that structures corresponding to I, II and III must make an appreciable contribution, so that the

selection of contributing structures seems to be rather arbitrary. Having chosen the resonance structures in some arbitrary manner their weights are then chosen to give the best possible agreement between the calculated and measured bond lengths. As the contributing structures which were chosen may not include all those which should have been chosen the process seems rather questionable.

What is required is a sounder basis on which to select the contributing resonance forms and the weights to be assigned to them.

3.6. Dimensions of the Carboxyl Group

The two C-O bonds differ by 0.031 Å (Fig. 26) or by 0.022 Å (Table 14). It is difficult to decide whether this small difference may be significant. On the basis of any reasonable estimation of the present standard deviation it is probably not significant, but the fact that the difference in bond lengths is in the same sense as that found in the earlier analysis makes it seem that it may perhaps be real. Further discussion of this should probably await the completion of the refinement.

Two arguments about the completeness of the random arrangement of molecules can be put forward.

(a) If weak long range forces exerted by the carboxyl

hydrogen atom of a molecule of type (a) (Fig. 25) cause a slight preponderance of molecules of the same type around it then, similarly, a molecule of type (b) must have a like preponderance of molecules of type (b) around it. On averaging over the whole unit cell the effect will be to have just as many molecules of one type as of the other. The two bonds should then be identical in length, and the apparent small difference is not significant.

(b) If the crystal is pictured as being formed by the packing of molecules around one primary molecule of type (a) then the weak directive forces exerted by the carboxyl hydrogen atom should cause a slight preponderance of molecules of the same type (a) in the layer immediately surrounding the primary molecule. Each of the molecules in this layer can then be pictured as causing a slight preponderance of molecules of type (a) in the next layer and so on. This would cause the complete crystal to have a small preponderance of molecules of type (a) and the difference in bond lengths would then be real.

This argument seems rather artificial, however, for if the primary molecule were of type (b) we might expect to find some crystals with a preponderance of type (b) and the difference in bond lengths would then be reversed.

Table 17

Hydrogen coordinates and bond lengths.

Atom	x	z	X'	Y	Z'
$H(C_3)$	0.457	0.0608	2.35	2.97	1.32
$H(C_4)$	0.620	0.1350	3.05	4.80	2.93
$H(C_5)$	0.403	0.2233	1.61	5.24	4.85
$H(C_7)$	-0.107	0.1567	-1.02	2.05	3.41

Bond Lengths (Å)	
$H-C_3$	0.98
$H-C_4$	1.08
$H-C_5$	1.13
$H-C_7$	1.08

It is probable, of course, that this argument can only be applied to the small mosaic blocks which make up the benzoic acid crystals, and as each crystal contains very many of these blocks the average effect over the whole crystal will be to have equal numbers of the two types of molecule.

It can probably be safely concluded that there is very little probability of a preponderance of one type of molecule occurring and consequently the two C-O bond lengths in the carboxyl group should be found to be identical in length.

3.7. Discussion of the Hydrogen Positions

From the x and z coordinates of the four well resolved hydrogen atoms X' and Z' coordinates were calculated, and Y coordinates obtained by substituting the X' and Z' coordinates in the equation of the molecular plane. These coordinates are listed in Table 17 along with the C-H bond lengths calculated from them.

The average value of these C-H bond lengths is 1.07 Å, agreeing with the accepted spectroscopic value. Such agreement is rather surprising, for a value of 0.89 Å was found in salicylic acid and a value of 0.86 Å was deduced in the earlier analysis of benzoic acid.

As the difference synthesis from which the hydrogen coordinates were estimated, was prepared before the refinement

of the (010) projection of benzoic acid has been completed, it may be that these coordinates are still only approximate. Further discussion of these bond lengths must await the completion of the structure refinement.

The recognition of the presence of the two randomly occurrring types of molecule explains the difficulty which was experienced in locating the carboxyl hydrogen atom. There will, statistically speaking, be half a hydrogen atom in each of the two possible positions between the oxygen atoms.

It is generally accepted that a carboxyl hydrogen atom only contains about 0.5 electrons, because of a partial transfer of electrons to the oxygen atom to which it is bonded. If it is assumed, to a first approximation, that the O-H bond is about 1.0 Å in length, then the two alternative sites for the carboxyl hydrogen atom will be about 0.6 Å apart and an elongated peak enclosing these two positions will be found in a difference synthesis. As this peak only contains about 0.5 electrons the peak height should be small - about 0.3 or 0.4 $e.Å^{-2}$.

The rather elongated peaks which were found in both Fig. 22 and Fig. 23 agree qualitatively with the existence of two equally likely sites for the carboxyl hydrogen atom.

3.8. Discussion of the Existence of Bonding Electrons

In his analysis of the structure of salicylic acid Cochran

detected evidence of the departure from circular symmetry of the projected carbon and oxygen atoms. The value of $(\rho_o - \rho_c)$ at the centre of every bond in the (001) projection is positive, varying from 0.10 to 0.31 e.Å^{-2}. No such feature is detectable in the difference synthesis projection shown in Fig. 22.

Possible reasons for this discrepancy are

(a) The projection shown in Fig. 22 does not represent the final refinement of the benzoic acid structure. Small adjustments to both the atomic coordinates and the anisotropic temperature factors are still required. The detection of peaks, such as those Cochran found, representing the concentration of electrons in bonds depends to a great extent on the correct choice of temperature factor parameters.

(b) The appearance of a difference synthesis depends to a great extent on the scattering factors which are used. The scattering factors used by Cochran are semi-empirical ones derived from Hartree scattering curves, and differ from the scattering factors calculated by McWeeny which were used in this analysis. In his analysis of the electron density in α-pyridone Penfold, using McWeeny f curves, likewise found no systematic concentration of

Table 18

Comparison of the coordinates X_1', Y_1 and Z_1' obtained in the present analysis with those, X_2', Y_2 and Z_2' obtained previously.

Atom	X_1'	X_2'	$\lvert\Delta\rvert$	Y_1	Y_2	$\lvert\Delta\rvert$
O_1	1.178	1.192	0.014	1.215	1.216	0.001
O_2	-0.667	-0.663	0.004	0.718	0.737	0.019
C_1	0.404	0.413	0.009	1.409	1.430	0.021
C_2	0.710	0.713	0.003	2.451	2.470	0.019
C_3	1.846	1.849	0.003	3.212	3.241	0.029
C_4	2.151	2.129	0.022	4.214	4.231	0.017
C_5	1.325	1.310	0.015	4.442	4.497	0.055
C_6	0.201	0.210	0.009	3.674	3.700	0.026
C_7	-0.134	-0.128	0.006	2.648	2.653	0.005

Atom	Z_1'	Z_2'	$\lvert\Delta\rvert$
O_1	0.272	0.290	0.018
O_2	1.395	1.398	0.003
C_1	1.248	1.236	0.012
C_2	2.243	2.255	0.012
C_3	2.118	2.103	0.015
C_4	3.052	3.048	0.004
C_5	4.123	4.121	0.002
C_6	4.255	4.251	0.004
C_7	3.336	3.338	0.002

electron density between bonded atoms. The greater inclination, however, of α-pyridone in both the (001) and (010) projections might tend to obscure fine details of the electron density in space when projected on to these planes.

If the peaks found by Cochran in salicylic acid are caused by the use of incorrect scattering curves then the number of electrons associated with a bond between two atoms must be very small, even less than the value of 0.05 electrons per bond found by Cochran.

The difficulty of assigning correct temperature factor parameters to atoms could be overcome if a neutron diffraction study of the crystal structure were made. The correct anisotropic motions could be deduced from this and used to prepare a difference synthesis with X-ray data. Such a process would allow a fairer estimate to be made of the possible existence of a small concentration of electrons in bonds.

4. COMPARISON OF THE TWO STRUCTURE DETERMINATIONS OF BENZOIC ACID

The coordinates X_1', Y_1 and Z_1' obtained in the present analysis and those, X_2', Y_2 and Z_2' obtained in the previous analysis are compared in Table 18. The average differences

Table 19

Comparison of bond lengths obtained in the two analyses of benzoic acid.

Bond	Old value	New value	Difference
C_1-O_1	1.244	1.260	0.016
C_1-O_2	1.290	1.291	0.001
C_1-C_2	1.475	1.468	0.007
C_2-C_3	1.392	1.381	0.011
C_2-C_7	1.389	1.399	0.010
C_3-C_4	1.410	1.392	0.018
C_7-C_6	1.416	1.396	0.020
C_4-C_5	1.369	1.370	0.001
C_6-C_5	1.355	1.363	0.008

in these coordinates are 0.010, 0.021 and 0.008 Å respectively. Although the Y coordinates show the largest changes the bond lengths have not been affected to any considerable extent, for the atomic shifts involved are all in the same direction and represent only a small change in the orientation of the molecule.

The bond lengths obtained in the two independent analyses are compared in Table 19. The mean difference is only 0.010 Å and the largest (for C_6-C_7) is 0.020 Å, so that the overall agreement is excellent.

In the earlier analysis bonds C_4-C_5 and C_5-C_6 were found to be the shortest bonds in the benzene ring and this effect still occurs in the present analysis, though bonds C_3-C_4 and C_6-C_7 are no longer quite so long. Since this shortening of the bonds C_4-C_5 and C_5-C_6 occurs in both the estimations of bond lengths it strengthens the view that it may be real.

In the earlier analysis the two C-O bonds of the carboxyl group differed in length by 0.046 Å, and as the total estimated standard deviation of the difference is 0.021 Å it was thought that the difference might be real. This difference is now found to be smaller and because of the random arrangement of molecules in the crystal it does not seem that the difference can be real.

One point on which the two analyses appeared to differ is the question of the planarity of the molecule. The cause of this discrepancy, however, which is only apparent, was the method used to calculate the molecular plane. When, therefore, a plane was calculated to pass through all the atoms (instead of only the carbon atoms of the benzene ring), it was found that none of the atoms were displaced significantly from the plane of the rest.

The random arrangement of carboxyl hydrogen atoms which exists in the benzoic acid crystal is now seen to explain satisfactorily the appearance of the elongated peak representing the carboxyl hydrogen atom which was found in the hydrogen electron-density projection of the earlier analysis (Fig. 8). The centre of this elongated peak is situated about midway between the two oxygen atoms involved in the hydrogen bond. At an earlier stage it had not been realized that the appearance of this map is significant and it was thought that the poor resolution of the expected hydrogen atom was due to random errors in the visually estimated F_o values causing errors in the electron density.

It can be concluded that the two analyses agree very closely and that while the analysis using Geiger-counter measured intensities is bound to give more accurate bond lengths

and electron counts, nevertheless the previous analysis using visually estimated intensities has given atomic coordinates and details about the hydrogen atoms to a fairly high degree of accuracy.

CHAPTER V

THE CRYSTAL STRUCTURE OF 11-AMINO-UNDECANOIC ACID HYDROBROMIDE HEMIHYDRATE

1. PREVIOUS EXAMINATION OF SIMILAR COMPOUNDS

Largely because of the difficulty of obtaining good single crystals the number of complete structure determinations of long chain compounds is very limited.

A few N-mono-n-alkyl substituted ammonium halides have been examined. The lower members of the series possess interesting high-temperature tetragonal forms which exhibit chain rotation[92]. Of the higher members of the series, the structures of n-dodecylammonium chloride and bromide have been studied by Gordon, Stenhagen & Vand[93]. These compounds are not isomorphous in their choice of unit cells and space groups but, nevertheless, their structures are very similar.

A number of long chain acids have been studied. A complete analysis of lauric acid has been made in two projections by Vand, Morley & Lomer[94]; and some others, such as isopalmitic acid[95] and n-pentadecanoic acid[96] have been studied in rather less detail. These compounds crystallize as dimers with hydrogen bonding between adjacent carboxyl groups. Their chain axes are parallel and the hydrocarbon chains exhibit either orthorhombic or triclinic packing. In orthorhomic packing the plane of every second chain is perpendicular to the plane of the others, while in triclinic packing all the planes are parallel.

The salts of long chain acids have also received attention. Form A of potassium caprate has been studied in some detail by Vand, Lomer & Lang[97]. This compound has an interesting crossed chain structure with alternate chains inclined in opposite directions.

Polymorphism occurs frequently with long chain compounds and twinning also is often observed. A detailed review of the physical properties of long chain compounds has been given by Daniel[98].

2. EXPERIMENTAL DETAILS

2.1. Preparation of the Crystals

Tabular crystals were obtained by crystallizing 11-amino-undecanoic acid from aqueous hydrobromic acid. The most prominent face of these crystals is (001).

It was found that small crystals, suitable for recording intensity data, could be obtained by cutting the tabular crystals.

2.2. Crystal Data

Rotation, oscillation and moving-film photographic methods were used with copper Kα radiation ($\lambda = 1.542$ Å). The cell dimensions were determined from rotation and equatorial layer line moving-film photographs calibrated with superimposed NaCl powder lines and the following values were obtained:

$\underline{a} = 11.08 \pm 0.03$, $\underline{b} = 5.27 \pm 0.02$, $\underline{c} = 50.60 \pm 0.20$ Å;

$\beta = 90^{\circ}\ 42' \pm 10'$.

The volume of the unit cell is 2954 $Å^3$ and the total number of electrons per unit cell, F(000), is 1224. The calculated linear absorption coefficient for copper $K\alpha$ radiation is $\mu = 38.6$ cm.$^{-1}$

Inspection of the equatorial layer Weissenberg photographs showed that the absent spectra are $(h0\ell)$ when h is odd and when ℓ is odd, and $(0k\ell)$ when $k+\ell$ is odd. Consequently the space group is either $Aa(C_S^4)$ or $A2/a(C_{2h}^6)$. It was initially assumed that the centrosymmetric space group would be the correct one and the structure refinement confirmed this.

The measured specific gravity is 1.29, so that there are eight molecules in the unit cell. The calculated specific gravity is 1.309.

2.3. Evaluation of the F_o values

The intensity data used in this analysis consisted of a survey of the $(h0\ell)$ and $(0k\ell)$ reflexions and were obtained from equatorial layer moving-film photographs. The multiple-film technique was used, the intensities being estimated visually.

The intensities were corrected for Lorentz and polarisation factors in the usual way.

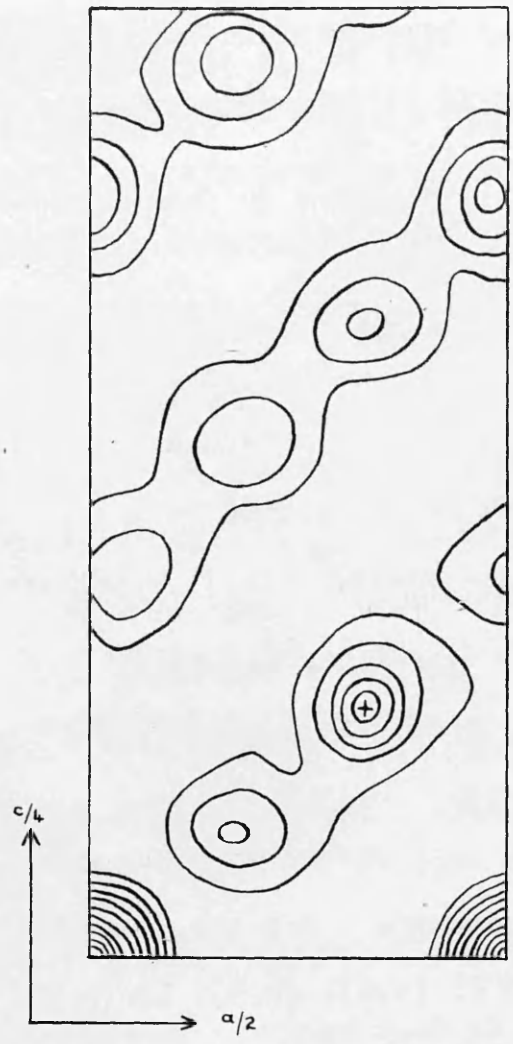

Fig. 28. Patterson projection on (010). Contours at equal, arbitrary intervals. The peak due to the Br - Br vector is marked by a cross.

3. STRUCTURE DETERMINATION

3.1. Patterson Analysis of the (100) Projection

The presence of the heavy bromine atom simplifies the structure determination since if it is located and its contribution to each structure factor evaluated, a first approximation to the true electron density will be obtained by computing a Fourier synthesis with the observed structure factors and the signs of the bromine atom contributions.

As there is only one bromine atom in the asymmetric unit of the structure the Patterson method seemed to present the quickest way of determining its coordinates. Using the squares of the observed structure amplitudes as Fourier coefficients a Patterson projection on (010) was prepared. This is shown in Fig. 28.

The largest peak on this map, marked by a cross, is due to the vector between bromine atoms. For the projection on (010) there are bromine atoms at (x,z); $(\bar{x},\bar{z})$; $(x+\frac{1}{2},z)$; $(\frac{1}{2}-x,z)$; $(x,z+\frac{1}{2})$; etc. producing vector peaks at $(2x,2z)$; $(\frac{1}{2}+2x,2z)$; $(2x,\frac{1}{2}+2z)$; etc. As the coordinates of the peak shown in Fig. 28 are $x = 0.330$, $z = 0.1312$, the bromine atom must have coordinates $x = 0.165$, $z = 0.065$, or values differing from these by 0.25.

The ambiguity arises because of the halving of the cell

in both the a and c directions in this projection, causing the presence of centres of symmetry in projection which are not true centres of symmetry in space. Only by the consideration of the other projections can this ambiguity be resolved.

Later work in fact showed that the correct choice of coordinates is x = -0.085, z = 0.0656.

3.2. Structure-Factor Calculations

Using the coordinates x = 0.330, z = 0.0656, deduced from the Patterson projection bromine contributions to the (h0ℓ) structure factors were calculated. The scattering-factor curve used was the Thomas-Fermi bromine scattering factor without temperature correction. The scattering factors were then multiplied by a temperature factor exp.$(-\gamma \sin^2\theta)$, the constant γ being determined from a graph of log F_o/F_c against $\sin^2\theta$ to be 1.9.

When later carbon, nitrogen and oxygen atoms were allowed for in structure-factor calculations the appropriate McWeeny scattering factors modified by a temperature factor exp.$(-1.9\sin^2\theta$ were used.

3.3. Fourier Refinement of the Projection on (010)

The signs of the bromine contributions were allotted to the observed structure amplitudes and an electron-density

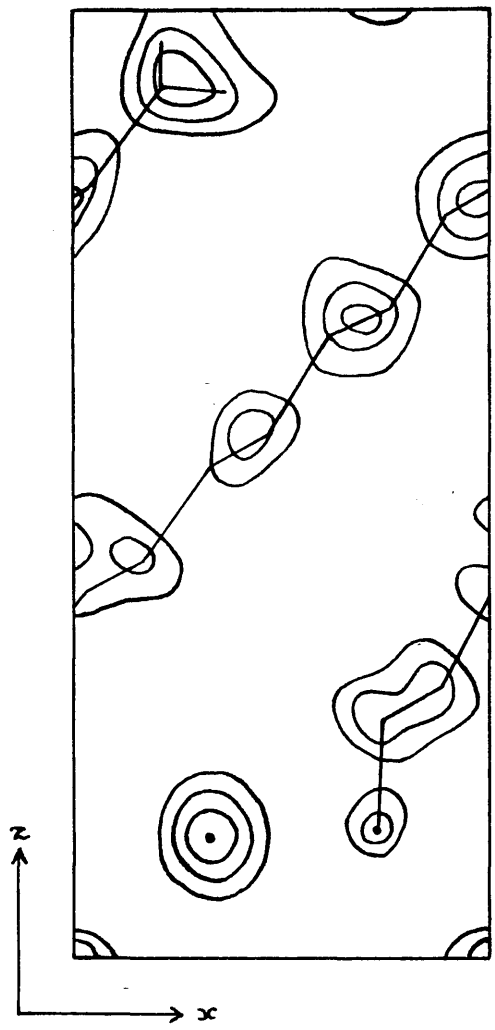

Fig. 29. First electron-density projection on (010). Contours at equal arbitrary intervals, except for those around the bromine atom which are on a different scale.

projection on (010) was calculated. This projection, shown in Fig. 29, enabled approximate coordinates for the atoms of the 11-amino-undecanoic acid molecule to be deduced. The contributions of these atoms were then included in the structure factors.

This process reduced the percentage discrepancy ($100 \sum|F_o-F_c| \div \sum|F_o|$), from a value of 39.0 when only bromine contributions were allowed for in the F_c values, to 28.0 when bromine contributions and the carbon, nitrogen and oxygen contributions were allowed for.

3.4. Further Refinement by (F_o-F_c) Syntheses

The further refinement of this projection was carried out by evaluating successive Fourier difference syntheses with (F_o-F_c) as coefficients. These syntheses showed that the structure-factor discrepancies which remained were due to the following factors.

(a) The light atom coordinates required adjustment.

(b) A large peak at the origin remained in spite of the adjustments made to the other atoms and obviously was due to the presence of a water molecule in the structure. At the outset of the analysis it had not been known that the crystals are hydrated.

(c) The bromine atom showed evidence of anisotropic thermal vibration and in consequence its atomic scattering factor should be of the form

$$f = f_{Br} \exp.\left[-\{\alpha + \beta \sin^2(\varphi - \psi)\} \sin^2\theta\right]$$

In this expression ψ is the angle between the direction of maximum vibration and the c axis, α and β are constants and $(2 \sin\theta, \varphi)$ are the polar coordinates of a point in the $(h0\ell)$ section of the reciprocal lattice.

In order to allow for the anisotropic vibration of the bromine atom the variation of the temperature-factor parameter γ with polar angle φ was determined graphically. The contributions of the carbon, nitrogen and oxygen atoms were subtracted from the observed structure factors to give a set of F_o values dependent only on the bromine contributions. These F_o values were divided into groups with $\varphi = 0^\circ$-15°, 15°-30°, etc. and in each group γ was obtained from a plot of $\log\left(\sum|F_o| \div \sum|Gf_{Br}|\right)$ against $\sin^2\theta$. In this expression G is the geometric part of the structure factor and f_{Br} is the Thomas-Fermi scattering factor without temperature correction.

It was found that the calculated values of γ could be fitted quite closely by a curve of the form

$$\gamma = 1.65 + 0.80 \sin^2(\varphi - 154^\circ).$$

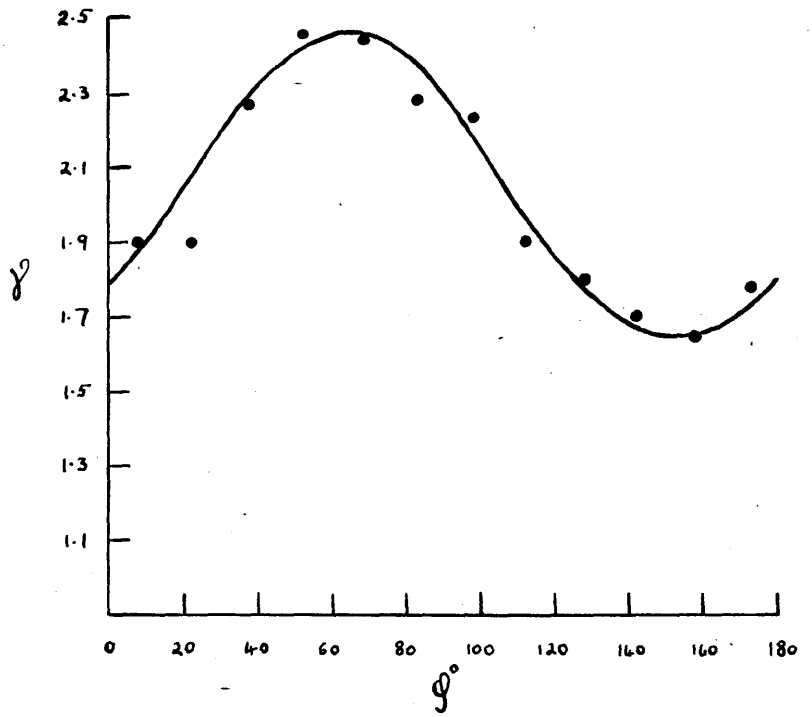

Fig. 30. Calculated values of γ plotted against φ_2. The curve $\gamma = 1.65 + 0.80 \sin^2(\varphi - 154^\circ)$ is superimposed.

This curve and the calculated values of γ plotted against ϕ are compared in Fig. 30. The appropriate value of γ for each reflexion was obtained from the curve and substituted in $f = f_{Br} \exp.(-\gamma \sin^2\theta)$ to determine the bromine anisotropic scattering factor.

The light atom coordinates were improved by moving the atoms in the direction of steepest ascent on the difference maps until the electron density slope at the atomic centres became zero.

3.5. Examination of the Scaling Factor

While these factors were being allowed for an investigation was also made of the scaling factor which had been used to place the F_o values on an absolute scale. The process used had been to sum all the $|F_c|$ and the corresponding $|F_o|$ values after each stage of refinement and then to multiply each $|F_o|$ value by the factor $\Sigma|F_c| / \Sigma|F_o|$. This, however, to be correct requires that what should have been measured, when collecting intensity data, are integrated intensities.

Visually estimated intensities, except in favourable circumstances such as for a small crystal of circular cross-section having a small value of μa, where μ is the linear absorption coefficient of the substance under examination and a is the diameter, are not necessarily identical with integrated

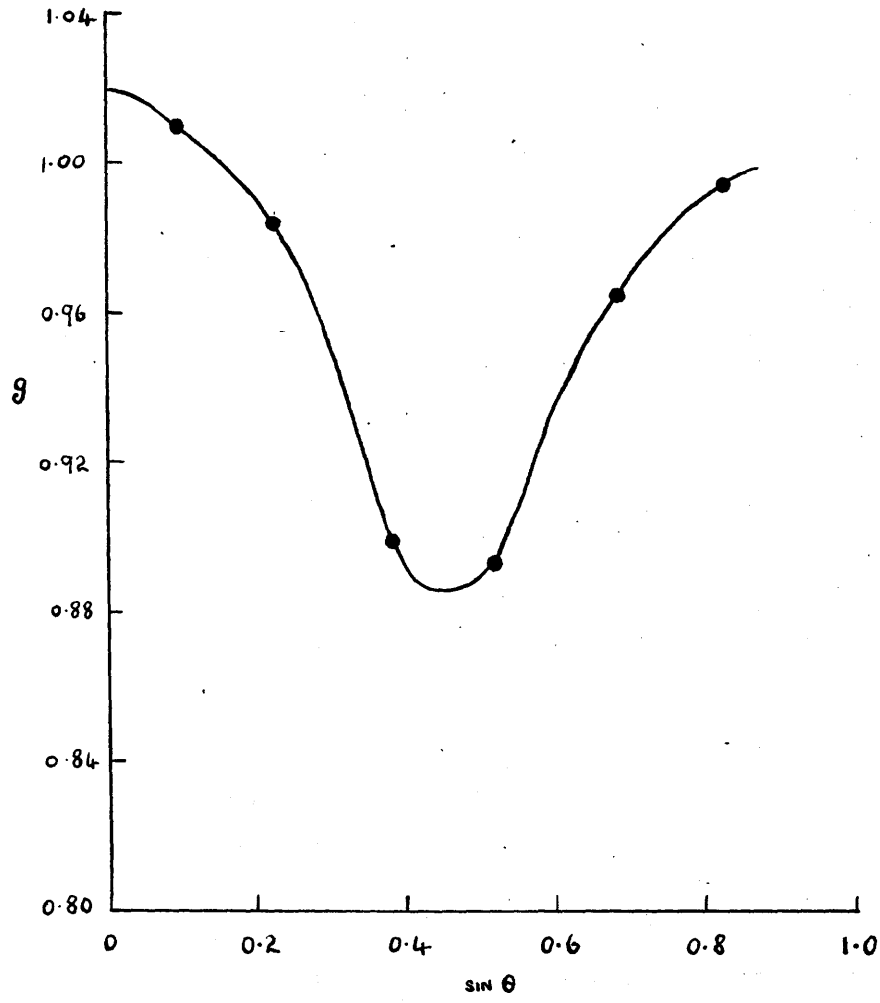

Fig. 31. Scaling curve for the (h0ℓ) structure factors.

intensities. Clews & Cochran[99] point out that for a crystal having a moderate or large value of μa several factors besides absorption are involved in the correlation of visually estimated intensities with integrated intensities.

(a) The divergence of the incident X-ray beam, and the resulting back focussing of the reflected beam, causes the intensities of high-order reflexions to be over-estimated by visual methods.

(b) The gradual separation with increasing Bragg angle of the two components of the $K\alpha$ doublet causes a systematic under-estimation of high-order reflexions.

(c) The variation, for a cylindrical crystal, of the absorption factor with increasing Bragg angle causes high-order reflexions to be underestimated.

(d) The white radiation left in the beam after filtration through nickel foils contributes more to the intensities of low-order reflexions because of its increased dispersion at high angles.

Provided that the specimen is spherical or cylindrical these factors depend only on 2θ, so that visually estimated intensities are proportional to the true integrated intensities but the proportionality "constant" is a function of 2θ. Consequently we can put

$$I = I' g^2(\sin\theta) \quad \ldots\ldots\ldots\ldots\ldots\ldots\ldots\ldots \quad (66)$$

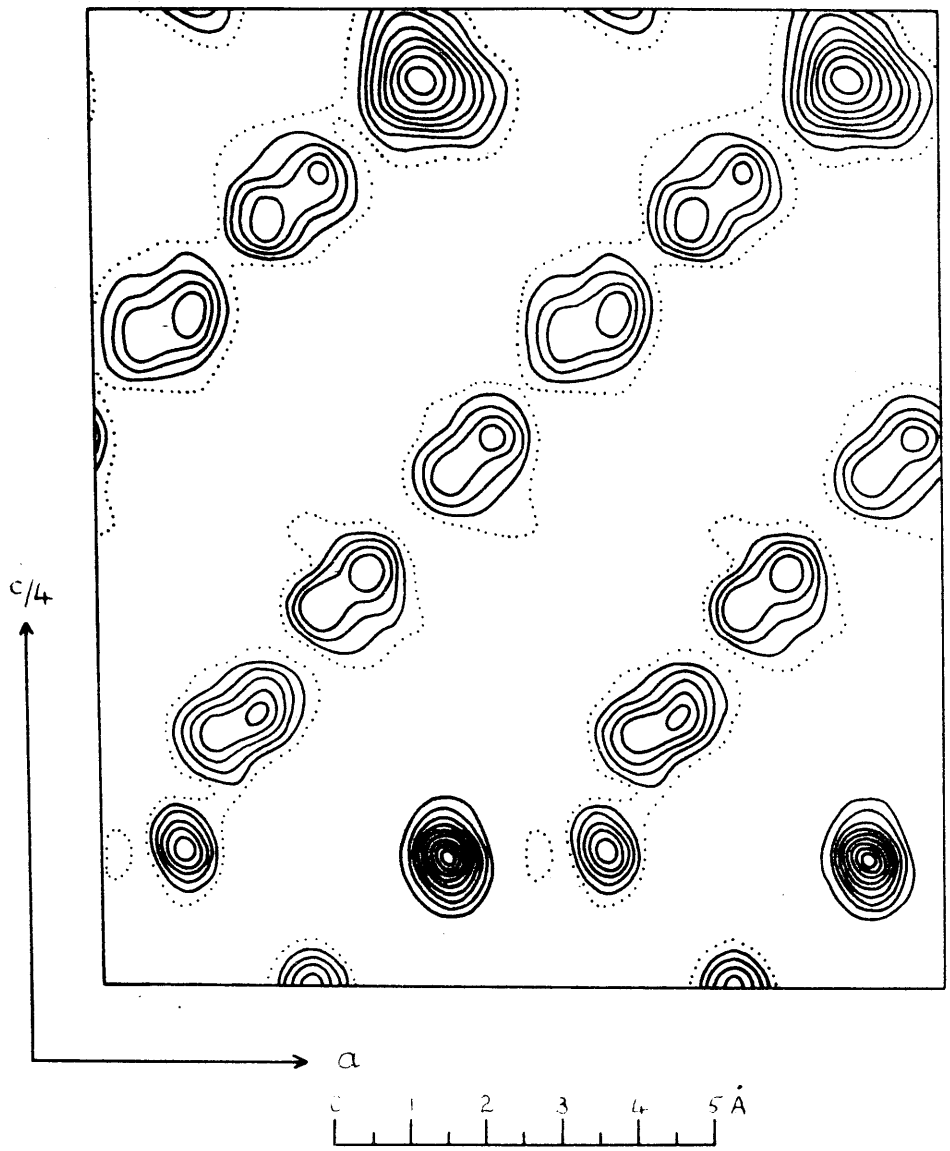

Fig. 32. Final electron-density projection on (010). Contours around the carbon, nitrogen and oxygen atoms at intervals of 1 e.Å^{-2}, starting at the two-electron line which is dotted. Contours around the bromine atom at intervals of 5 e.Å^{-2}.

where I is the integrated intensity, I' is the visually estimated intensity and $g(\sin\theta)$ is a function of 2θ. Since $F_o/F_o' = \sqrt{I}/\sqrt{I'}$ we have

$$F_o = F_o' g(\sin\theta) \quad \ldots\ldots\ldots\ldots\ldots\ldots\ldots\ldots \quad (67)$$

where F_o is the true observed structure factor and F_o' is the structure factor derived from the visually estimated intensity.

The main disadvantage of this method of deriving absolute structure factors from a set of visually estimated F_o values by multiplying by a scaling factor which varies with $\sin\theta$, is that it tends to hide any faults in a heavy atom scattering curve, for deviations between the curve used and the true scattering curve are necessarily a function of $\sin\theta$. In a case like the present, however, where there are different types of atoms present with scattering curves known with varying degrees of accuracy, a systematic discrepancy in one of the curves could not be entirely hidden.

In a given range of $\sin\theta$ g can be treated as a constant and so, for this range,

$$g(\sin\theta) = \Sigma|F_o|/\Sigma|F_o'| = \Sigma|F_c|/\Sigma|F_o'| \quad \ldots\ldots\ldots\ldots\ldots \quad (68)$$

The $(h0\ell)$ structure factors were divided into groups centred about $\sin\theta = 0.08$, 0.23, 0.38, etc. and in each group $\Sigma|F_c|/\Sigma|F_o'|$ was evaluated. As expected the values of g varied

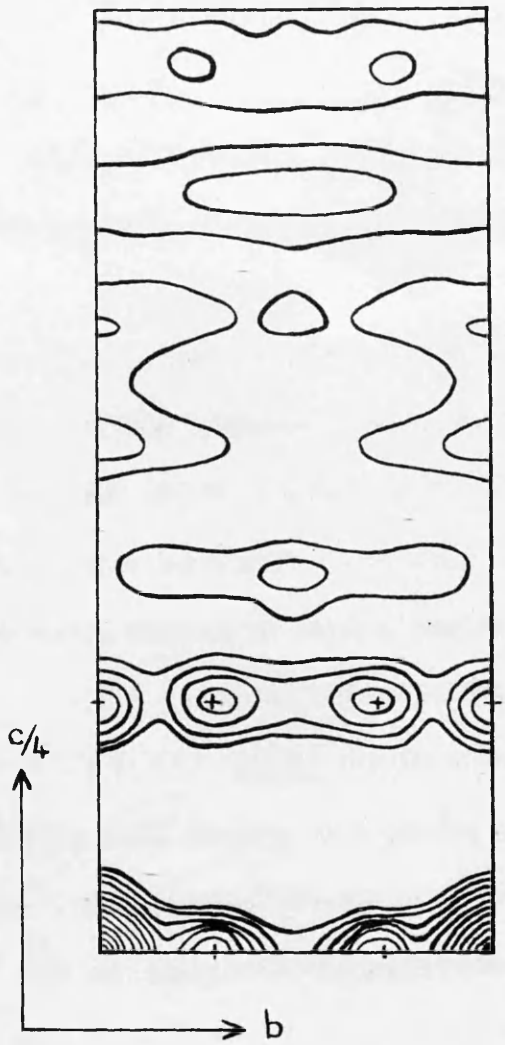

Fig. 33. Patterson projection on (100). Contours at equal, arbitrary levels. Peaks due to Br - Br vectors are marked by crosses.

smoothly with $\sin\theta$ in the way shown in Fig. 31. This scaling curve was used to place all the F_o' values on an absolute scale.

3.6. Progress of Refinement

When all these factors had been allowed for the percentage discrepancy for the 249 observed ($h0\ell$) structure factors dropped to 15.0.

Final values of F_o and F_c are listed in Appendix 3.

At this stage another electron-density projection on (010) was prepared using the final signs which had been obtained for the structure factors. This is shown in Fig. 32 and, as expected, shows a marked improvement over the electron-density projection shown in Fig. 29.

3.7. Analysis of the Projection on (100)

A Patterson projection along the a axis was prepared and is shown in Fig. 33. The heaviest peaks, due to Br - Br vectors, were located and coordinates assigned to the bromine atom.

A choice between the two alternative z coordinates, differing by a quarter of the cell side, was made by calculating ($0k\ell$) structure factors for the bromine atoms only and comparing these with the observed structure factors for planes with ℓ odd. The correct alternative was found to be the

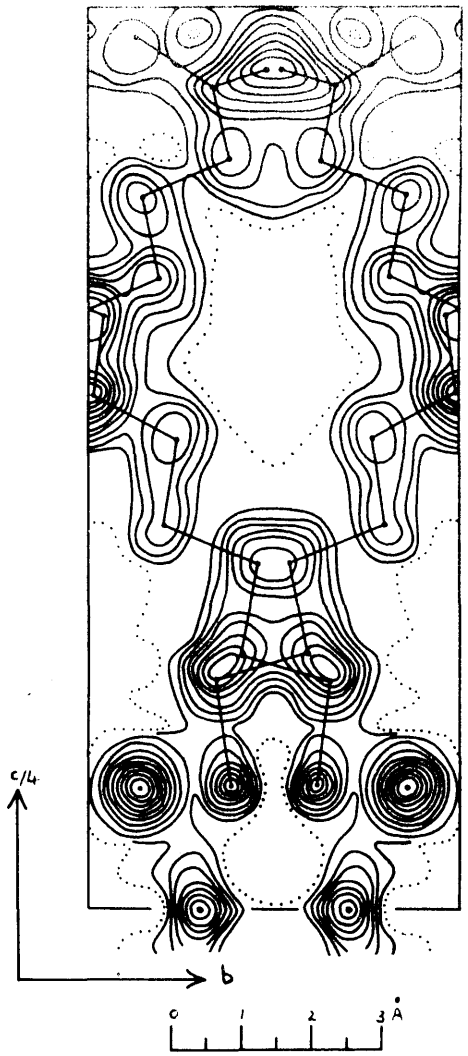

Fig. 34. Final electron-density projection on (100). Contours as in Fig. 32.

choice which had been made for the b axis projection, so that z coordinates derived from that projection did not require to be altered.

Using the signs of the bromine atom contributions an electron-density projection along the a axis was computed from the observed (0kℓ) structure factors. From this projection coordinates for the light atoms were chosen and the refinement continued by Fourier and difference Fourier syntheses. The final electron-density projection on (100) is shown in Fig. 34.

No indications of anisotropic thermal vibration by the bromine atom were found in either the difference-synthesis or electron-density projections on (100).

The scaling factor used to place the relative F_o values on an absolute scale was investigated in the manner described earlier but was not found to vary with $\sin\theta$.

The final percentage discrepancy for the 108 observed (0kℓ) structure factors is 13.9. Calculated and observed structure factors are listed in Appendix 3.

3.8. Choice of Origin

In the (010) projection the origin had been chosen on the water molecule. An inspection of the electron-density projection shown in Fig. 34 reveals that this choice is incorrect, for the water molecule is not situated on the origin of the

Table 20

Atomic coordinates expressed as fractions of the axial lengths.

Atom	x	y	z
N	0.103	1.623	0.0342
C_{11}	0.130	1.660	0.0630
C_{10}	0.197	1.410	0.0700
C_9	0.270	1.450	0.0950
C_8	0.340	1.200	0.1050
C_7	0.417	1.238	0.1300
C_6	0.486	1.008	0.1400
C_5	0.556	1.055	0.1650
C_4	0.626	0.813	0.1730
C_3	0.705	0.864	0.1970
C_2	0.780	0.625	0.2050
C_1	0.860	0.667	0.2290
O_1	0.942	0.520	0.2333
O_2	0.860	0.870	0.2400
H_2O	0.250	0.300	0
Br	-0.087	0.140	0.0328

(100) projection. The water molecule is in fact situated on a two-fold rotation axis and the projection of this axis is an effective centre of symmetry for the (010) projection. The true origin is really situated at a quarter of the unit cell side a along from the water molecule.

The x coordinates of the atoms were changed accordingly and the signs of the ($h0\ell$) structure factors, when h is not a multiple of 4, were also changed.

The electron-density projection on (010) shown in Fig. 32 has been drawn with the correct choice of origin.

4. COORDINATES, MOLECULAR DIMENSIONS, AND ESTIMATION OF ACCURACY

4.1. Coordinates and Molecular Dimensions

The final coordinates of the atoms are shown in Table 20 and the various interatomic distances and angles calculated from these coordinates are listed in Table 21.

The average C - C bond length is 1.539 Å.

4.2. Calculation of the Average Vector between Alternate Carbon Atoms

The hydrocarbon chain was assumed to be a periodic structure so that the coordinates of the even and odd carbon atoms satisfy linear equations. Assuming that the atomic coordinates can all be given equal weight, a least-squares calculation was made of the components of the average vector

Table 21

Interatomic distances and angles

The letters associated with some of the atoms refer to the following equivalent positions:

b .... $\bar{x},\bar{y},\bar{z}$; c .... $\frac{1}{2}+x,\bar{y},z$; d .... $\bar{x},\frac{1}{2}-y,\frac{1}{2}-z$;

e .... $\frac{1}{2}-x,\frac{1}{2}+y,\frac{1}{2}-z$; f .... $\frac{1}{2}-x,y,\bar{z}$.

Intramolecular		Intermolecular		Interbond angles	
N-C_{11}	1.50 Å	N-Br	3.30, 3.44 Å	C-C-C	112° 44'
C_{11}-C_{10}	1.56	N-Br (b)	3.62	O_1-C_1-O_2	119°
C_{10}-C_9	1.52	N-Br (c)	3.66	C_2-C_1-O_1	119°
C_9-C_8	1.61	N-H_2O	2.92	C_2-C_1-O_2	120°
C_8-C_7	1.54	H_2O-Br(c)	3.38, 3.84	C_1-O_1-O_2(d)	125°
C_7-C_6	1.52	H_2O-Br	4.17	C_1-O_2-O_1(d)	116°
C_6-C_5	1.51	Br-Br(b)	4.11	C_{11}-N-Br	104°, 92°
C_5-C_4	1.55	N-N(b)	4.34	C_{11}-N-Br(b)	151°
C_4-C_3	1.52	C_2-C_5(c)	4.04	C_{11}-N-H_2O	123°
C_3-C_2	1.56	C_4-C_7(c)	3.90	Br(c)-H_2O-Br(b)	93°
C_2-C_1	1.52	C_6-C_9(c)	4.57	N-H_2O-N(f)	109°
C_1-O_1	1.22	C_8-C_{11}(c)	3.92		
C_1-O_2	1.21	C_{10}-Br(c)	3.86		
		C_2-C_6(c)	4.45		
		C_2-O_2(e)	3.46		
		C_1-O_2(d)	3.48		
		C_{11}-H_2O	3.94		
		C_{11}-Br	3.80, 3.95		
		O_1-C_3(c)	4.00		
		O_1-O_2(d)	2.64		
		O_2-O_2(e)	3.73		

between alternate carbon atoms. The calculation was made separately for the even and odd sets of carbon atoms and the estimates were then averaged. The values found are given in Table 22.

From these components the modulus of the vector $\underline{s}$ between two alternate carbon atoms was found to be 2.563 Å. From this value of $\underline{s}$ and the value of 1.539 Å found for the average C - C bond length the average interbond angle was calculated to be 112° 44'.

4.3. Accuracy of Bond Lengths

The standard deviation of length of a C - C bond was estimated by the method of Cruickshank to be 0.040 Å, so that the standard deviation of the average C - C bond is $0.040/\sqrt{10} = 0.012_6$ Å.

The difference, $\Delta\ell$, between the length of each C - C bond and the expected value of 1.545 Å was used to confirm the correctness of the estimate of the C - C bond standard deviation. It is to be expected that $\{\overline{\Delta\ell^2}\}^{\frac{1}{2}}$ should give a reasonable estimate of $\sigma(\ell)$, for there are ten independent values of $\Delta\ell$. The value found in this way is 0.030 Å, which is rather smaller than the value of 0.040 Å deduced by Cruickshank's method.

Table 22

Components of the average vector $\underline{s}$ between two alternate carbon atoms.

Coordinate	Fractional component	Rectangular component (Å)
x	0.1454	1.612
y	-0.1965	-1.036
z	0.03363	1.702

5. DISCUSSION

5.1. The C-C Bond Lengths

The C-C bond lengths appear at first sight to fall into two series, one having an average value of 1.560 Å and the other 1.519 Å. The standard deviation of each value, however, is $0.040/\sqrt{5} = 0.018$ Å, and the total standard deviation of the difference, $\sigma(t)$, is then $0.018\sqrt{2(1-\cos 112^\circ 44')} = 0.030$ Å. In consequence $\Delta/\sigma(t)$, where Δ is the difference between the two average bond lengths, has a value of 1.33 and the difference cannot be regarded as significant.

The average C-C bond length of 1.539 Å, with standard deviation of 0.012_6 Å, does not differ significantly from the accepted value of 1.545 Å.

5.2. The Vector s between Alternate Carbon Atoms

For a hydrocarbon chain in which the average carbon bond length is 1.545 Å and the interbond angle tetrahedral, a value of s equal to 2.522 Å is to be expected. The distance of 2.563 Å found in this analysis is 0.041 Å greater. This difference is significant, for $\Delta/\sigma(t) = 0.041/0.012_6 = 3.26$.

Similar enlargements of this distance have been found by Morley & Vand in strontium laurate[106], with $s = 2.610$ Å, and by Vand, Lomer & Lang in potassium caprate[97], with

$\underline{s} = 2.598$ Å. The value found by Vand, Morley & Lomer in the case of lauric acid[94], however, is 2.521 Å.

The enlargement of $\underline{s}$ in the present case from 2.522 to 2.563 Å is connected with an enlargement of the interbond angle from the normal tetrahedral value of 109° 28' to 112° 44'. Since 11-amino-undecanoic acid differs from lauric acid only in having a nitrogen atom substituted for the terminal carbon atom, it seems probable that this expansion of the interbond angle is caused by intermolecular rather than by intramolecular forces. More definite evidence on this point could perhaps be obtained by structure analyses of other derivatives of 11-amino-undecanoic acid.

5.3. Planarity of the Acid Molecule

It was found that the coordinates, expressed in Ångstrom units, of the atoms C_1, C_2, ... C_{11} of the hydrocarbon chain could be fitted to an equation of the form

$$X = AY + BZ + C.$$

A, B and C were determined by the method of least squares to be -0.3394, 0.7413 and 1.9964 respectively. The average displacement of a carbon atom from this plane is 0.050 Å and the largest (C_1) is 0.106 Å, so that atoms C_1, C_2 .... C_{11} may be regarded as coplanar and the deviations of these atoms from the common plane are due solely to experimental errors.

The terminal nitrogen atom, however, departs significantly from this plane with a displacement of 0.593 Å. The carboxyl group also appears to be twisted out of the plane of the hydrocarbon chain, but the magnitude of this effect is rather uncertain since the coordinates of the oxygen atoms are less accurate than those of the carbon atoms due to the considerable lack of resolution, in both projections, of the atoms of the carboxyl group.

5.4. Hydrogen Bonding between Carboxyl Groups

The length of the hydrogen bonds between adjacent carboxyl groups is 2.64 Å and is normal for this type of hydrogen bonding where values ranging from 2.53 Å found by Goodwin & Thomson in furoic acid[101] to 2.69 Å found by Morrison & Robertson in glutaric acid[102] are known.

The two molecules which are connected by this hydrogen bonding between carboxyl groups are not coplanar, the perpendicular distance between the two planes being 1.62 Å. In this respect the structure is similar to that of pimelic acid[103] and contrasts with carboxylic acids of the benzene series[31,81] in which the two molecules constituting the dimer are very nearly coplanar.

5.5. Packing and Tilt of the Hydrocarbon Chains

The electron-density projection on (100) shown in Fig. 34

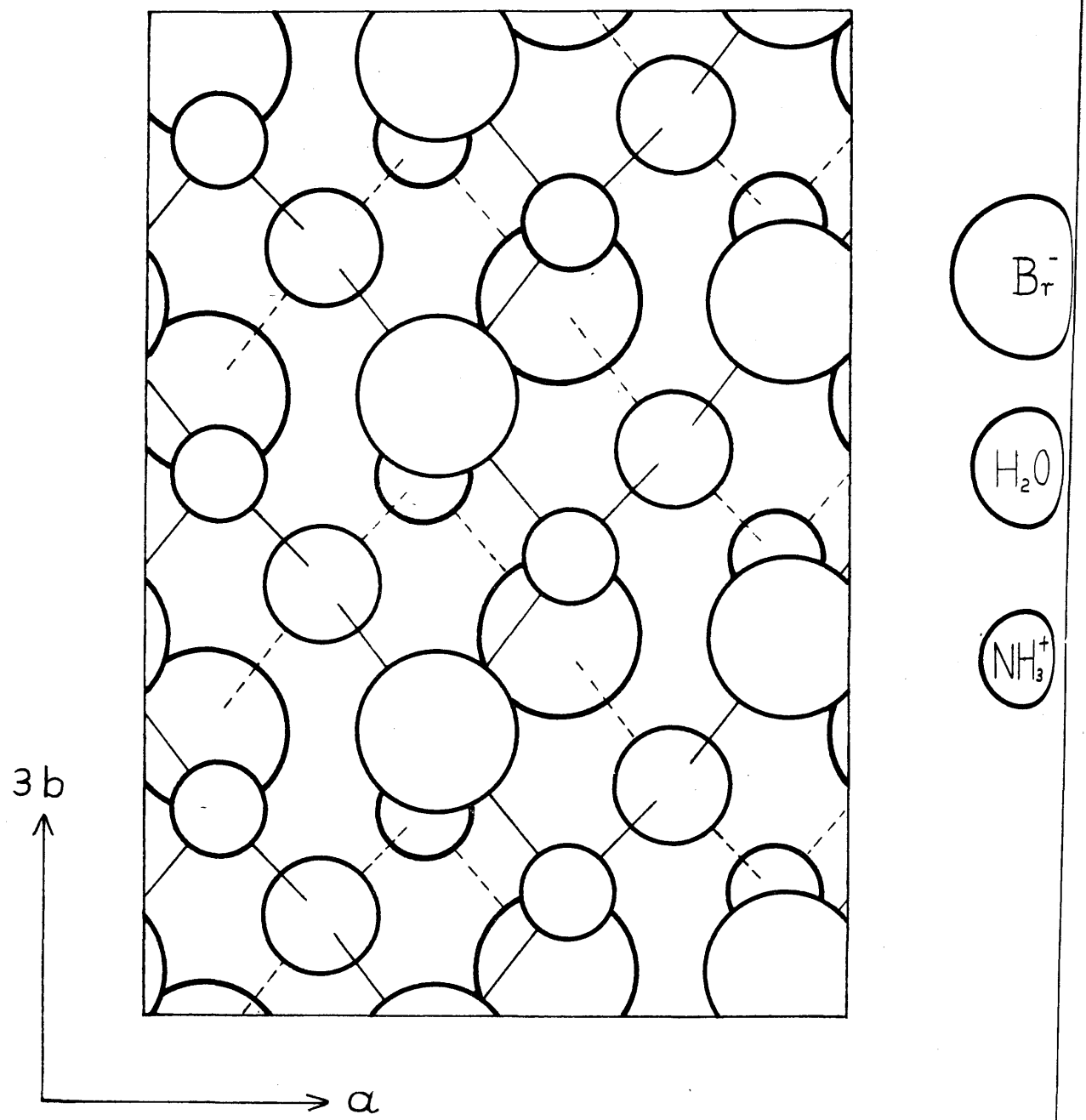

Fig. 35. Section through the plane of the water molecules, parallel to (001), showing the packing of the NH_3^+ and Br^- ions around the water molecules. Full lines represent hydrogen bonds above the plane of the water molecules, while broken lines represent hydrogen bonds below this plane.

reveals clearly that alternate hydrocarbon chains are tilted in opposite directions and cross each other. This type of packing of the hydrocarbon chains is unusual and is similar to that found for form A of potassium caprate[97].

Normally hydrocarbon chains pack together with their chain axes parallel and so far the only structures which have been found to have hydrocarbon chains crossing each other are all ionic in type.

The inclination of the chain axes to the (001) plane was calculated from the components of the vector between alternate carbon atoms. The result obtained is

$$\sin\tau = (\Delta Z)/\underline{s} \quad \ldots\ldots\ldots\ldots\ldots\ldots\ldots \quad (69)$$

and so $\sin\tau = 0.6640$. Consequently $\tau = 41^{\circ}\ 36'$, a value which is considerably smaller than that found for any known form of straight chain fatty acid and is very close to the value of 43°-45° found for the branched chain fatty acid, isopalmitic acid[95], discussed in a later chapter.

The effective cross-section of the molecules at right angles to the chain axis was calculated from the expression

$$S = \tfrac{1}{2}\, \underline{a}.\underline{b} \sin\tau \quad \ldots\ldots\ldots\ldots\ldots\ldots\ldots \quad (70)$$

and a value of 19.4 $\mathring{A}^2$ obtained. This value agrees with similar determinations made on other long chain compounds[104].

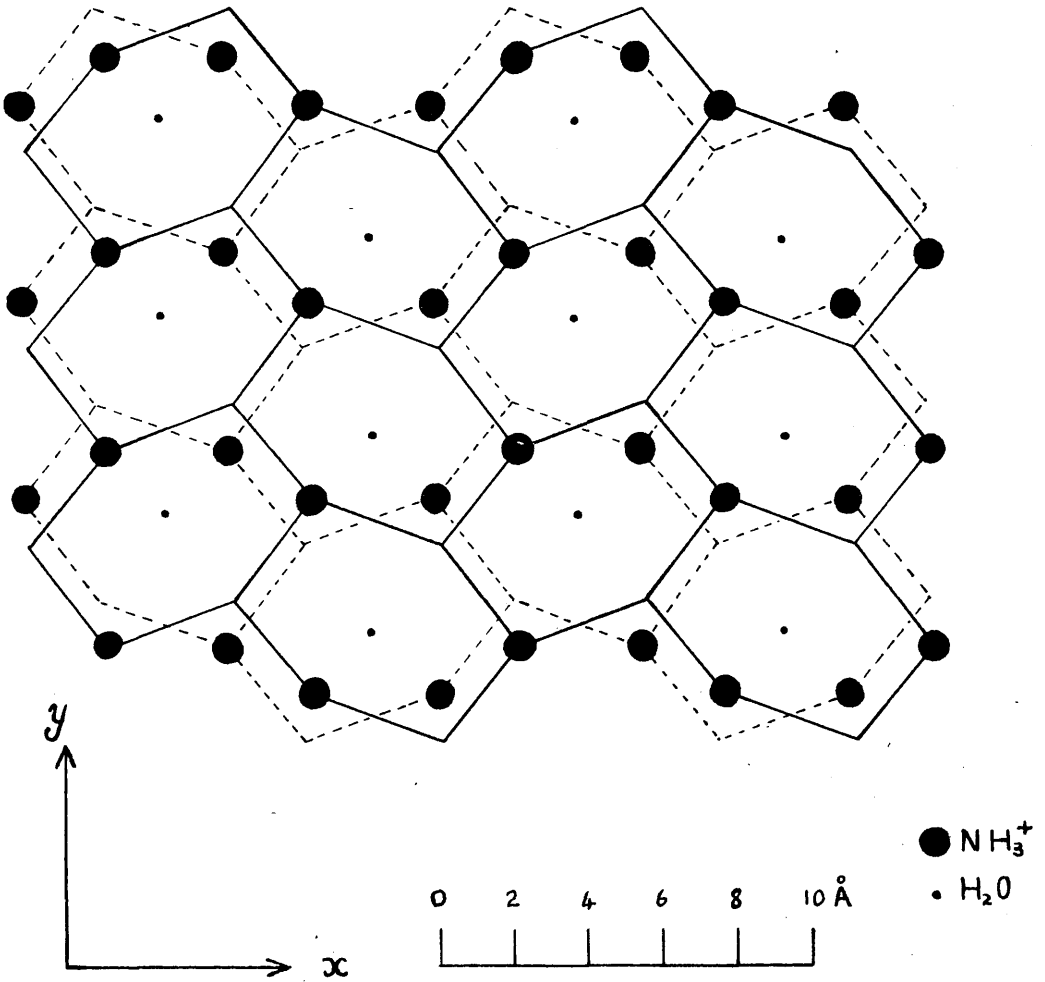

Fig. 36. Representation of the double ionic layer. The corners of the hexagonal network which are dotted are occupied by NH_3^+ ions: those not dotted, by Br^- ions. Ions above the plane of the water molecules are joined by full lines, those below by broken lines.

It is slightly larger than the value of 18.43 $\mathring{A}^2$ found by Vand[105] for n-hexatriacontane at 20°C.

5.6. Hydrogen Bonds Involving the Nitrogen and Bromine Atoms

The terminal nitrogen atom forms three hydrogen bonds, two to bromine atoms of lengths 3.30 and 3.44 Å, and one to a water molecule of length 2.92 Å. These bonds are directed approximately tetrahedrally, the angles which the C_{11}-N bond makes with the hydrogen bonds being 104°, 92° and 123° respectively.

The water molecules, situated on twofold axes, are involved in four hydrogen bonds, two to nitrogen atoms and two to bromine atoms. These bonds are also directed nearly tetrahedrally, the angles $\angle$Br-H_2O-Br and $\angle$N-H_2O-N being 93° and 109° respectively The bonds from the water molecule to the bromine atoms are 3.38 Å in length and presumably the hydrogen atoms of the water molecule are directed towards the bromine atoms.

As it has not been possible to locate the hydrogen atoms directly in this analysis, it is not possible to decide definitely which of the systems $-NH_3^+ \ldots\ldots Br^-$ or $-NH_2 \ldots\ldots HBr$ exists in the crystal. It is probable, however, that the first is correct and that Br^- and NH_3^+ ions are packed together in the structure.

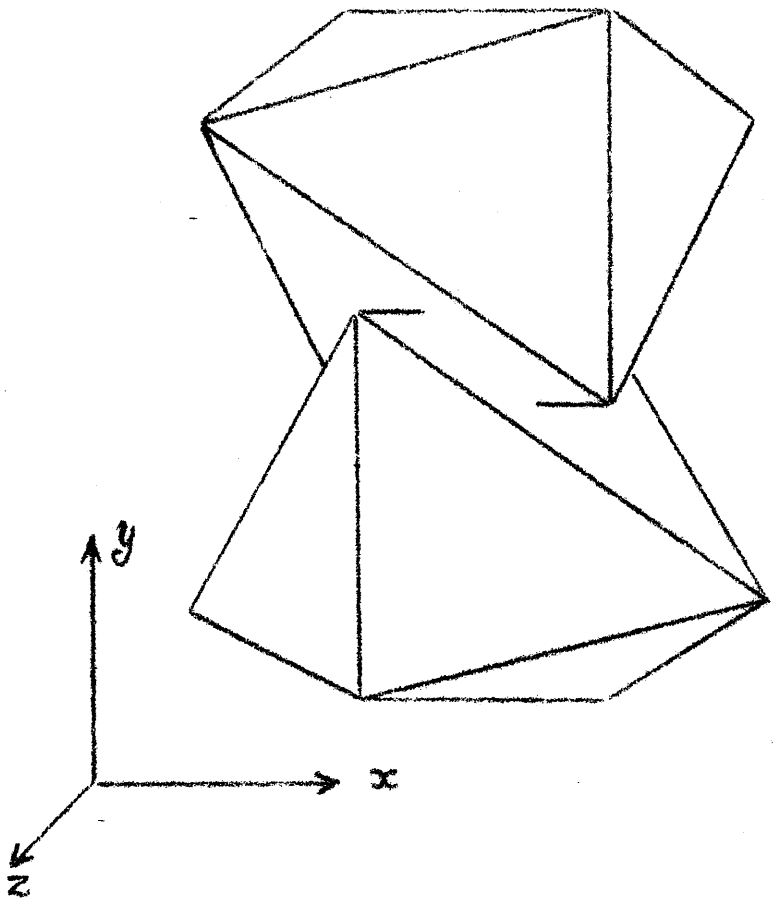

Fig. 37. Relative orientations of the two interpenetrating systems of octahedra formed by the NH_3^+ and Br^- ions. The corners of the upper octahedron are occupied by Br^- ions, while those of the lower are occupied by NH_3^+ ions.

5.7. Arrangement of the Br^- and NH_3^+ Ions

A section of the structure in the plane of the water molecules, parallel to (001), showing the arrangement of the water molecules, NH_3^+ and Br^- ions is shown in Fig. 35. The NH_3^+ and Br^- ions are at heights of 1.73 and 1.66 Å respectively, both above and below the plane of the water molecules.

There is an almost planar, distorted hexagonal arrangement of alternate Br^- and NH_3^+ ions arranged in two sheets, one above and the other below the plane of the water molecules, with the Br^- ions of the lower sheet fitting approximately below the NH_3^+ ions of the upper sheet. The separation of the two sheets is 3.4 Å. The water molecules pack into the channels which run vertically through the hexagonal network. This arrangement is illustrated in Fig. 36.

While the surroundings of a water molecule may be regarded as symmetrical, having NH_3^+ and Br^- ions both above and below, the surroundings of a Br^- or NH_3^+ ion cannot be so regarded. Each Br^- ion is surrounded by three NH_3^+ ions (at 3.30, 3.44 and 3.66 Å), the four ions being approximately in the one plane, and by three water molecules (at 3.38, 3.84 and 4.17 Å) in a plane 1.7 Å below. These six neighbours form a distorted octahedron. Below the face formed by the water molecules there is a fourth NH_3^+ ion (at 3.62 Å), so that each Br^- ion

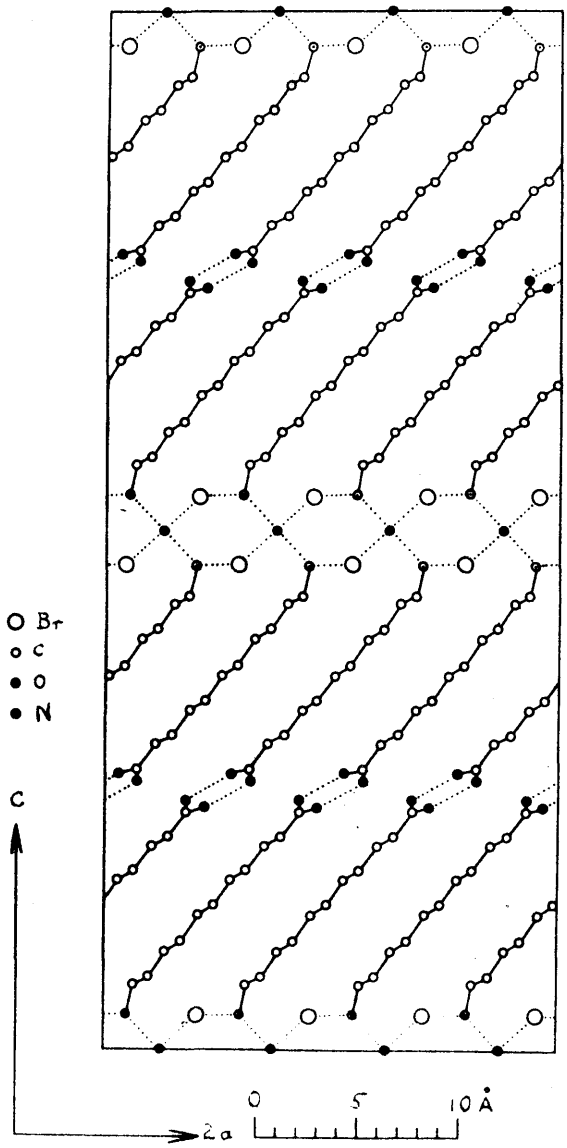

Fig. 38. Arrangement of the molecules in the (010) projection. Dotted lines represent hydrogen bonding. Hydrogen atoms are not shown.

has an unsymmetrical arrangement of four oppositely charged NH_3^+ ions to one side of it. The environment of an NH_3^+ ion is similar.

The surroundings of a water molecule may also be described in terms of two interpenetrating systems of distorted octahedra, the corners of which are occupied by Br^- and NH_3^+ ions respectively. The relative orientations of these systems are illustrated in Fig. 37.

5.8. Intermolecular Approach Distances

The approach distances between carbon atoms of neighbouring chains are approximately 4 Å and correspond to normal van der Waals interactions. Some of the shorter of these distances are listed in Table 21.

The arrangements of the molecules in the (010) and (100) projections are indicated in Figs. 38 and 39.

6. THE HYDROCHLORIDE OF 11-AMINO-UNDECANOIC ACID

Crystals of the hydrochloride, obtained by crystallising 11-amino-undecanoic acid from hydrochloric acid solution, have the form of very thin flat plates. They show orthorhombic symmetry, with a unit cell of dimensions $\underline{a} = 8.54$, $\underline{b} = 9.07$, $\underline{c} = 35.3$ Å.

The systematic absences suggest Pbca or Pbcn for the space group. There are eight molecules in the unit cell.

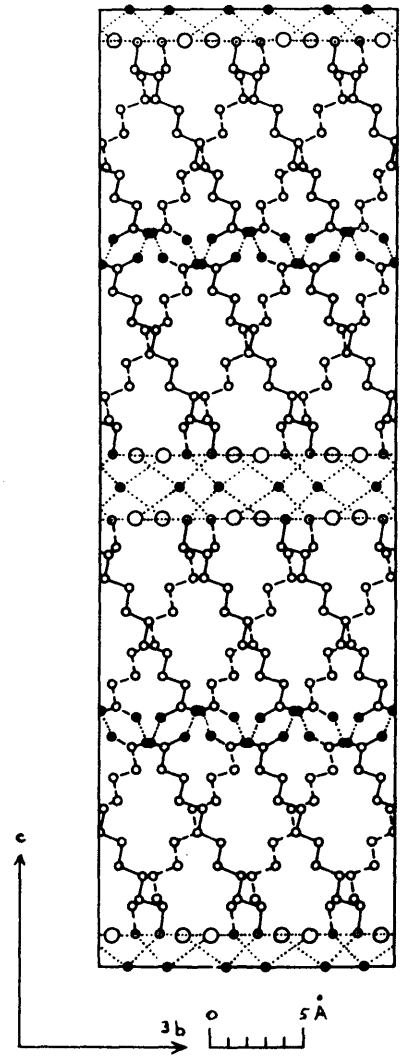

Fig. 39. Arrangement of the molecules in the (100) projection. Molecules on a lower relative level are indicated by broken lines. Hydrogen bonding is indicated by dotted lines. Hydrogen atoms are not shown.

A Patterson projection along the b axis was prepared and from this two possible positions for the chlorine atom were deduced. Corresponding to these alternatives, electron-density projections using the signs of the chlorine atom contributions to the structure factors were prepared. No obvious position for the molecule was found in either.

Lack of time has prevented any further attempt to determine the structure but the presence of a very strong (0,0,28) reflexion with spacing 1.26 Å, i.e. half of 2.52 Å, suggests that the chain axis must be parallel to the c axis. If the molecules, then, are assumed to pack together perpendicular to the (001) plane the average cross-section of each molecule is 19.4 $Å^2$, in satisfactory agreement with the value deduced from the structure of the hydrobromide.

CHAPTER VI

EXAMINATION OF THE SIGN DETERMINING POWER OF THE HEAVY ATOM TECHNIQUE

1. INTRODUCTION

Many crystal structure determinations depend on the presence of a heavy atom in the molecule. This atom will, depending on the number of electrons associated with it and on the number and weight of the other atoms present, determine the signs of a certain number of the reflexions given by the crystal. When this atom is located its contribution to each structure factor can be evaluated, signs allotted to the observed structure factors and a Fourier synthesis prepared. If sufficient of the signs have been determined correctly by the heavy atom contributions the Fourier synthesis should give a recognisable picture of the molecule.

An example of this technique has been given in the previous chapter.

Luzzati[107] has developed a relationship between the true electron density and the electron density calculated from the moduli of the observed structure factors with phase angles corresponding to only some of the atoms in the structure. The expressions he derives are, however, somewhat complicated.

The problem examined in this chapter is rather simpler, being that of calculating the fraction of the reflexions for a given structure which are determined in sign by the contributions of a heavy atom or, more generally, by the contributions of a group of atoms.

The treatment which is adopted here was worked out with the help of Dr. M.M. Woolfson, without whose advice and criticism it would not have been completed.

Attention will be confined to structures having space group $P\bar{1}$ or to projections of other space groups which possess this symmetry only.

2. RELATIVE CONTRIBUTIONS OF TWO GROUPS OF ATOMS

Let the total number of atoms in the unit cell be divided into two groups A and B. Let the contributions of groups A and B to a particular structure factor be F_1 and F_2 respectively so that

$$F_1 = 2\sum_i f_i \cos 2\pi(hx_i + ky_i + lz_i)$$

$$F_2 = 2\sum_j f_j \cos 2\pi(hx_j + ky_j + lz_j).$$

Consequently,

$$F_1^2 = 4\sum f_i^2 \cos^2 2\pi(hx_i + ky_i + lz_i) + 4\sum_{i\neq k} f_i f_k \cos 2\pi(hx_i + ky_i + lz_i) \cos 2\pi(hx_k + ky_k + lz_k)$$

and since

$$\overline{\cos^2 2\pi(hx_i + ky_i + lz_i)} = 0.5$$

$$\overline{\cos 2\pi(hx_i + ky_i + lz_i)} = 0$$

we have

$$\overline{F_1^2} = 2\sum f_i^2 \quad \ldots\ldots\ldots\ldots\ldots\ldots\ldots\ldots\ldots\ldots\ldots\ldots\ldots\ldots (71)$$

and consequently

$$\overline{F_1^2} / \overline{F_2^2} = \Sigma f_i^2 / \Sigma f_j^2 \quad \ldots\ldots\ldots\ldots\ldots\ldots\ldots\ldots (72)$$

That is, the ratio of the average squared contributions of each group at any particular value of $\sin\theta$ is equal to the ratio of the sum of the squares of the scattering factors of each group.

Let the root-mean-square contributions of groups A and B be p and q respectively and let the ratio p/q equal r, so that at any particular value of $\sin\theta$

$$r = (\Sigma f_i^2 / \Sigma f_j^2)^{\frac{1}{2}} \quad \ldots\ldots\ldots\ldots\ldots\ldots\ldots\ldots (73)$$

The factor r will in general vary with $\sin\theta$ because of the differing relative variation of scattering factors with increasing $\sin\theta$. In any small range of $\sin\theta$, however, r may be treated as a constant.

3. THE CASE OF TWO 'LARGE' GROUPS OF ATOMS

3.1. Theoretical Treatment

If A and B both contain more than about five or six atoms then in any given small range of $\sin\theta$ the contributions F_1 and F_2 of these groups are distributed according to a Gaussian law.

For a particular reflexion let the contribution F_1 be X. Then the probability that F_2 exceeds X in magnitude and differs from it in sign is given by

$$P_1 = \frac{1}{q\sqrt{2\pi}} \int_X^\infty \exp\left(-\frac{X^2}{2q^2}\right) dX \quad \ldots\ldots\ldots\ldots\ldots\ldots (74)$$

We may put

$$\Phi(z) = \frac{1}{\sqrt{2\pi}} \int_o^z \exp\left(-\tfrac{1}{2}t^2\right) dt \quad \ldots\ldots\ldots\ldots\ldots\ldots (75)$$

which is a common statistical integral tabulated in various books (e.g. Uspensky[100]), allowing P_1 to be expressed as

$$P_1 = \tfrac{1}{2} - \Phi(X/q) \quad \ldots\ldots\ldots\ldots\ldots\ldots\ldots\ldots (76)$$

Since values of F_1 are assumed to have a Gaussian distribution the fraction which make a contribution X to values of F is given by

$$n = \frac{1}{p\sqrt{2\pi}} \exp\left(-X^2/2p^2\right) dX \quad \ldots\ldots\ldots\ldots\ldots\ldots (77)$$

and the fraction of these which are outweighed by a contribution from F_2 of greater magnitude and opposite sign is given by

$$n' = \frac{1}{p\sqrt{2\pi}} \left\{\tfrac{1}{2} - \Phi(X/q)\right\} \exp\left(-X^2/2p^2\right) dX$$

In consequence, the total fraction N of all the reflexions which do not have their signs determined by F_1 is given by

$$N = \frac{1}{p\sqrt{2\pi}} \int_{-\infty}^{+\infty} \left\{\tfrac{1}{2} - \Phi(X/q)\right\} \exp\left(-X^2/2p^2\right) dX$$

On putting $y = X/p$ the expression reduces to

$$N = \frac{1}{\sqrt{2\pi}} \int_{-\infty}^{+\infty} \left\{\tfrac{1}{2} - \Phi(ry)\right\} \exp\left(-\tfrac{1}{2}y^2\right) dy$$

and as the function which is to be integrated is symmetrical about $y = 0$, the expression becomes

$$N = \frac{2}{\sqrt{2\pi}} \int_0^\infty \left\{\tfrac{1}{2} - \wp(ry)\right\} \exp\left(-\tfrac{1}{2}y^2\right) dy \quad \ldots\ldots\ldots\ldots \quad (78)$$

If it is required to evaluate the fraction of reflexions in a given range of $\sin\theta$ having a contribution $F_1 > k$ which do not have their signs determined by F_1, the expression to be evaluated is

$$N_k = \frac{2}{\sqrt{2\pi}} \int_k^\infty \left\{\tfrac{1}{2} - \wp(ry)\right\} \exp\left(-\tfrac{1}{2}y^2\right) dy \quad \ldots\ldots\ldots\ldots \quad (79)$$

Equations (78) and (79) allow us to determine the fraction of reflexions not determined in sign by F_1 as a function of r, i.e. as a function of the ratio of the root-mean-square contributions of the two sets of atoms. Unfortunately, however, it is not possible to evaluate the double integral involved in these equations other than by graphical or numerical methods.

Since both the functions $\left\{\frac{1}{2} - \wp(ry)\right\}$ and $\exp\left(-\frac{1}{2}y^2\right)$ decrease with increasing y, their product decreases quite rapidly and a reasonably accurate numerical integration may be accomplished readily.

3.2. Discussion

Three simple cases may first be considered.

(a) When $r = \infty$ $\quad \wp(ry) = 0.5$ so that

$$N = 0.$$

(b) When $r = 0$ $\quad \wp(ry) = 0$ so that

$$N = \frac{1}{\sqrt{2\pi}} \int_0^\infty \exp\left(-\tfrac{1}{2}y^2\right) dy = 0.5.$$

Table 23

Calculation of N for the case r = 1.

y	$\frac{1}{2} - \phi(y)$	$\exp(-\frac{1}{2}y^2)$	Product	ℓ_x Product
0	0.5000	1.0000	0.5000	0.5000
0.2	0.4207	0.9802	0.4124	1.6496
0.4	0.3446	0.9231	0.3181	0.6362
0.6	0.2743	0.8353	0.2291	0.9164
0.8	0.2119	0.7261	0.1539	0.3078
1.0	0.1587	0.6065	0.0963	0.3852
1.2	0.1151	0.487	0.0561	0.1122
1.4	0.0808	0.373	0.0301	0.1204
1.6	0.0548	0.279	0.0153	0.0306
1.8	0.0359	0.198	0.0071	0.0284
2.0	0.0228	0.135	0.0031	0.0031
			Total	4.6899

$$N = \frac{2}{\sqrt{2\pi}} \times \frac{0.2}{3} \times 4.6899$$

$$= \frac{2}{2.507} \times 0.667 \times 0.469$$

$$= 0.250.$$

(c) When $r = 1$

$$N = \frac{2}{\sqrt{2\pi}} \int_0^{\infty} \{\tfrac{1}{2} - \varphi(y)\} \exp(-\tfrac{1}{2}y^2)\, dy$$

For $y = 0.0, 0.2, 0.4 \ldots 2.0$ the functions $\{\tfrac{1}{2} - \varphi(y)\}$ and $\exp(-\tfrac{1}{2}y^2)$ were evaluated and multiplied together. The numerical integration was then accomplished using Simpson's Rule:

$$N = \frac{2}{\sqrt{2\pi}} \times \frac{h}{3} \{ y_0' + 4y_1' + 2y_2' + \ldots\ldots 4y_{n-1}' + y_n' \} .$$

In this expression h is the interval at which y values are selected and y' is the value of a product of the two functions. The actual evaluation of N for this particular case is given in Table 23, the value obtained being 0.25.

These results are all in agreement with expectation.

The cases of 11-amino-undecanoic acid hydrobromide and hydrochloride were examined. In the case of the hydrobromide since the scattering curves of bromine and carbon change in a different manner with increasing $\sin\theta$ the evaluation of N should really be made in various ranges of $\sin\theta$. To simplify the calculation, however, an estimate of the average value of r, where r is the ratio of the root-mean-square contributions of the bromine and light atoms, was made by assuming that in the range $\sin\theta = 0 - 0.9$, $\overline{f_{Br}} / \overline{f_c}$ is about 40/6 and that all the light atoms can be treated as carbon atoms, apart from the

hydrogen atoms which were neglected. The water molecule was also neglected since it does not occupy a general position. It was then found that r is about 1.78.

The functions $\{\frac{1}{2} - \wp(1.78y)\}$ and $\exp(-\frac{1}{2}y^2)$ were evaluated for y = 0.0, 0.1, 0.2 .... etc. Their products fell off rapidly and for y = 1.2 had become very small. Simpson's rule was then applied to the thirteen products in order to obtain the integral in equation (78). The value so obtained is N = 0.162, so that the bromine atom contribution to the structure factors should determine the signs of 83.8% of the reflexions.

A survey was made of the 340 F_c values for the (h0ℓ) zone. It was found that in 32 cases the combined contribution of the atoms of the 11-amino-undecanoic acid molecule exceeded the corresponding bromine contribution and differed in sign. This is equivalent to 9.4% of the reflexions against the theoretical value of 16.2%.

There are two reasons for this discrepancy. In the first place, it is difficult to arrive at a completely satisfactory average value of r since the ratio f_{Br}/f_c increases with $\sin\theta$. If a value of r greater than 1.78 is assumed then the theoretical number of sign determination failures will decrease. The most satisfactory method of overcoming this difficulty would be to

evaluate N in different ranges of $\sin\theta$ but this would involve an increase in the amount of computation.

Secondly, and this is the more important reason, a Gaussian distribution of both F_1 and F_2 values has been assumed in deriving equations (78) and (79). This is a poor approximation for the distribution of F_1 values since these are contributed to by only one independent atom. Even F_2 cannot really be assumed to have an exactly Gaussian distribution since the coordinates of the atoms of the hydrocarbon chain are not really random. If one atom is fixed, the remaining carbon atoms of the chain are given in terms of multiples of only two vectors.

When applying the calculation to the case of the hydrochloride, the average value of r was taken to be 0.71 approximately, leading to a value of $N = 0.302$. Consequently only 69.8% of the reflexions in this compound should have their signs determined by the chlorine atom contributions.

Equation (79) could probably be usefully employed in cases where a group of atoms does not determine the signs of more than about 65 - 80% of all the reflexions. A value of $y = k$ could be found such that, say, about 90% of those reflexions for which $F_1 > k$ are determined in sign by F_1.

4. THE CASE OF ONE HEAVY ATOM AND A 'LARGE' NUMBER OF LIGHT ATOMS

4.1. Theoretical Treatment

Let us consider a centrosymmetric crystal, space group $P\bar{1}$, with 2 atoms with scattering factor f_H and 2m atoms each with scattering factor f_L. Then the ratio of the root-mean-square contributions of each group is

$$r = p/q = (f_H^2/m f_L^2)^{\frac{1}{2}} = f_H/f_L\sqrt{m}$$

As before r may be treated as a constant in any small range of $\sin\theta$.

For a particular reflexion in this range of $\sin\theta$ let the contribution F_1 of the heavy atom be X. Then the probability, assuming a Gaussian distribution of F_2 values, that the contribution F_2 of the light atoms exceeds X in magnitude and differs from it in sign is given by

$$P = \frac{1}{q\sqrt{2\pi}} \int_X^\infty \exp(-X^2/2q^2)\, dX$$

$$= \tfrac{1}{2} - \Phi(X/q).$$

The fraction of F_1 values which make a contribution X to F is given by

$$n = \frac{dX}{\pi\sqrt{f_H^2 - X^2}} \qquad \ldots\ldots\ldots\ldots\ldots\ldots\ldots\ldots\ldots \quad (80)$$

and the fraction of these not sign-determined by F_1 will be

$$n' = \frac{\{\tfrac{1}{2} - \phi(X/q)\}\, dX}{\pi\sqrt{(f_H^2 - X^2)}}$$

Consequently the total fraction of the reflexions in the small range of $\sin\theta$ which do not have their signs determined by the contributions of the heavy atoms is given by

$$N = \frac{2}{\pi}\int_0^{f_H} \frac{\{\tfrac{1}{2} - \phi(X/q)\}\, dX}{\sqrt{(f_H^2 - X^2)}}$$

On putting $y = X/f_H$ this becomes

$$N = \frac{1}{\pi}\int_o^1 \frac{dy}{\sqrt{(1-y^2)}} - \frac{2}{\pi}\int_o^1 \phi\left(\frac{f_H}{q}\, y\right) \frac{dy}{\sqrt{(1-y^2)}}$$

As $f_H/q = \sqrt{2}\, r$ this becomes

$$N = \tfrac{1}{2} - \frac{2}{\pi}\int_o^1 \frac{\phi(\sqrt{2}\, ry)\, dy}{\sqrt{(1-y^2)}}$$

$$= \tfrac{1}{2} - \frac{2}{\pi}\,\frac{1}{\sqrt{2\pi}}\int_{y=0}^{1}\int_{t=o}^{\sqrt{2}ry} \frac{\exp(-\frac{t^2}{2})}{\sqrt{(1-y^2)}}\, dy\, dt$$

$$= \tfrac{1}{2} - \frac{2}{\pi}\,\frac{1}{\sqrt{2\pi}}\int_{y=0}^{1}\int_{t=o}^{\sqrt{2}ry} \sum_{n=o}^{\infty}(-1)^n\, \frac{(t/\sqrt{2})^{2n}}{n!\,\sqrt{(1-y^2)}}\, dy\, dt$$

$$= \tfrac{1}{2} - \frac{2}{\pi}\,\frac{1}{\sqrt{2\pi}}\int_o^1 \sum_{n=o}^{\infty}(-1)^n\, \frac{(\sqrt{2}\, ry)^{2n+1}}{2^n\, n!\,(2n+1)\sqrt{(1-y^2)}}\, dy$$

$$= \tfrac{1}{2} - \frac{2}{\pi\sqrt{\pi}}\int_o^1 \sum_{n=o}^{\infty} a_n\, \frac{(ry)^{2n+1}}{\sqrt{(1-y^2)}}\, dy$$

where $a_n = (-1)^n/n!(2n+1)$.

Now let $y = \sin\theta$ and

$$N = \tfrac{1}{2} - \frac{2}{\pi\sqrt{\pi}} \int_0^{\pi/2} \sum_{n=0}^{\infty} a_n \, r^{2n+1} \sin^{2n+1}\theta \; d\theta$$

Since

$$\int_0^{\pi/2} \sin^{2n+1}\theta \; d\theta = \frac{2n}{(2n+1)} \cdot \frac{(2n-2)}{(2n-1)} \cdots\cdots\cdots \frac{2}{3}$$

the expression becomes

$$N = \tfrac{1}{2} - \frac{2}{\pi\sqrt{\pi}} \sum_{n=0}^{\infty} \frac{(-1)^n}{n!(2n+1)} \cdot \frac{2n}{(2n+1)} \cdot \frac{(2n-2)}{(2n-1)} \cdots \frac{2}{3} r^{2n+1} \qquad \text{.....(81)}$$

Evaluating the first few coefficients gives us

$$N = \tfrac{1}{2} - \frac{2}{\pi\sqrt{\pi}} \left(r - 0.2222r^3 + 0.0533r^5 - 0.0109r^7 + 0.0019r^9 \cdots\cdots\right).$$

The series in equation (81) must converge since there is a factor of n! in the denominator and the limit of $\frac{r^{2n+1}}{n!}$ as $n \to \infty$ is zero. For $r > 1$, however, the convergence is not very rapid.

Dr. Woolfson suggested that this difficulty could be overcome by expressing N in a form suitable for numerical integration as in section 3.1. This is done as follows:

$$N = \frac{2}{\pi} \int_0^{f_H} \frac{\{\tfrac{1}{2} - \rho(X/a)\}}{\sqrt{(f_H^2 - X^2)}} \, dX$$

and on making the substitution $\sin\theta = X/f_H$ we obtain

$$N = \frac{2}{\pi} \int_0^{\pi/2} \{\tfrac{1}{2} - \rho(\sqrt{2}\, r \sin\theta)\} \; d\theta \qquad \text{..... (82)}$$

This expression can be integrated fairly accurately by Simpson's

rule on splitting the range $\theta = 0 - \pi/2$ into ten intervals. The expression obtained is

$$N = \tfrac{1}{2} - 0.1333\{\varphi(0.2211r) + \varphi(0.6420r) + \varphi(0.9998r) + \varphi(1.2599r) + \varphi(1.3966r)\} - 0.0667\{\varphi(0.4369r) + \varphi(0.8311r) + \varphi(1.1439r) + \varphi(1.3449r)\} - 0.0333\varphi(1.4140r) \quad \ldots\ldots\ldots\ldots\ldots\ldots (83)$$

4.2. Discussion

Equations (81) and (83) are equivalent. The former holds exactly, though a considerable number of terms may require to be evaluated unless $r < 1$, while the latter is a good approximation.

That equation (83) gives reliable results may be seen by comparing the results obtained from this equation with those obtained from equation (81) for the cases $r = 0.71$ and $r = 1.00$. The actual values obtained are

	$r =$ 0.71	1.00
Equation (81)	$N =$ 0.270	0.204
Equation (83)	$N =$ 0.270	0.205

The case $r = 0.71$ refers to the hydrochloride of 11-amino-undecanoic acid. For this compound the chlorine atom contributions to the structure factors should determine the signs of about 73% of all the reflexions. For the heavy atom technique to work easily this is probably not a sufficiently

large percentage, though it is difficult to be precise about this since individual circumstances are bound to vary.

The result for the case r = 1.00 is interesting, for it means that a single atom which has the same root-mean-square contribution to the total structure factor as a group of light atoms will determine the signs of 79.5% of the reflexions, as against the value of 75% which might have been expected. This is because of the different distribution functions of the contributions of a single atom and a group of atoms.

In the case of 11-amino-undecanoic acid hydrobromide where r = 1.78, equation (81) cannot be employed readily because of the slow convergence of the series. It is much more convenient to use equation (83), the result obtained being N = 0.109. For this compound, then, the bromine atom contributions to the structure factors should determine the signs of 89.1% of the reflexions. In actual fact 90.6% of the reflexions have the same sign as the bromine atom contributions, a figure which agrees remarkably well with the theoretical prediction.

It is possible to use the equations in a slightly different manner in order to calculate the minimum contribution of the heavy atom such that a certain percentage of the reflexions are determined in sign by the heavy atom contributions. It is

not possible to set down an explicit formula for this but the method would be as follows.

Let us decide that, say, 90% of the reflexions which we wish to choose must be determined in sign by the heavy atom contributions. Then the minimum contribution of the heavy atom which will result in this is $2f_H \cos 2\pi(h_i x_H + k_i y_H + \ell_i z_H)$. Let $k = \cos 2\pi(h_i x_H + k_i y_H + \ell_i z_H)$.

Then the fraction of reflexions having $F_1 > 2kf_H$ which are not determined in sign by F_1 is given by

$$N_k = \frac{2}{\pi} \int_{\sin^{-1} k}^{\pi/2} \{ \tfrac{1}{2} - \phi(\sqrt{2}\, r \sin\theta) \} d\theta \quad \ldots\ldots\ldots\ldots\ldots (84)$$

For the appropriate value of r the function $\{ \frac{1}{2} - \phi(\sqrt{2}\, r \sin\theta) \}$ is evaluated at suitable intervals of θ and the results plotted in the form of a graph. By dividing the total area under the graph between $\theta = 0$ and $\theta = \frac{\pi}{2}$ into strips and evaluating the area in each (or by numerical integration) a value of $\sin^{-1} k$ may be found readily such that $N_k = 0.10$.

By selecting only those planes for which $\cos 2\pi(h_i x_H + k_i y_H + \ell_i z_H)$ is greater than this value of k we can be sure that 90% of the reflexions will be determined in sign by the heavy atom contribution.

Such a process might be of value when the heavy atom determines the signs of only about 65%-80% of the total

reflexions. By selecting those reflexions which satisfy the condition that 90% of them are determined in sign by the heavy atom, a better approximation to the electron density in the crystal may perhaps be achieved than by using all the available reflexions with the signs of the heavy atom contributions.

CHAPTER VII

THE CRYSTAL STRUCTURE OF ISOPALMITIC ACID

1. INTRODUCTION

The study of the crystal structure of this compound was undertaken originally for the preparation of a thesis submitted to Glasgow University in partial satisfaction of the requirements for the B.Sc. degree.

The structure was solved by means of trial and error methods and refined to some extent by Fourier methods. Details of this analysis are available elsewhere[95].

Owing to the poor nature of the crystals only a small number of reflexions were available for use in that analysis so that the first problem to be tackled was that of obtaining rather more detailed intensity data.

2. EXPERIMENTAL DETAILS

2.1. Preparation of Single Crystals

The crystals, which had been grown from light petroleum, were in the form of thin elongated plates with well developed {001} faces. All the crystals were found to be twinned in one way or another on the (001) plane. Twinning is common with long-chain compounds, having been reported by von Sydow[96] and Muller[108].

It was found possible to obtain single crystals by splitting the twins parallel to (001), though as the crystals are very

soft this process caused the single crystal specimens to be rather distorted.

2.2. Crystal Data

Molecular formula, $C_{16}H_{32}O_2$. Molecular weight, 256.4. The crystal is triclinic with dimensions

$$\underline{a} = 5.09, \quad \underline{b} = 5.68, \quad \underline{c} = 48.1 \text{ Å},$$

$$\alpha = 140.0^\circ, \quad \beta = 111.1^\circ, \quad \gamma = 72.7^\circ.$$

There are two molecules per unit cell. Density calc. 1.020 g.cm.$^{-3}$. Density meas. 1.012 g.cm.$^{-3}$. No systematic absences. Space group P1 or $P\bar{1}$; the Fourier analysis indicates $P\bar{1}$.

2.3. Evaluation of Intensities

The intensity data which were collected using single crystals consisted of the (0kℓ) and (h0ℓ) reflexions. These were collected on equatorial layer moving-film photographs using the multiple film technique[7].

By using long exposures it was possible to collect rather more intensity data for the (0kℓ) zone than had been available in the earlier work. Owing to the poor nature of the crystals reflexions in different parts of the film differed considerably in shape and were very irregular in appearance. This effect probably causes the measured intensities to be less accurate than visually estimated intensities usually are.

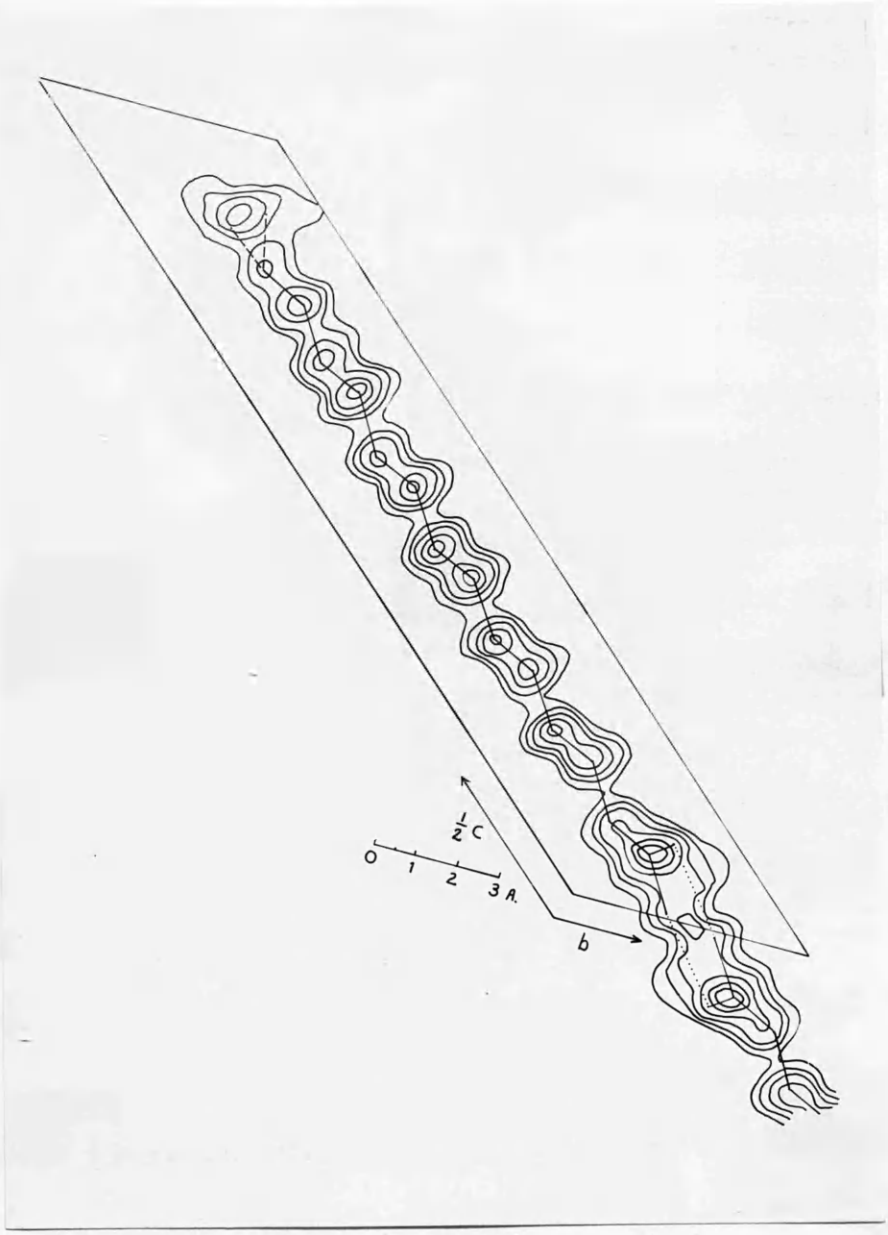

Fig. 40. Final a axis electron-density projection of the earlier analysis.

The intensities were converted to F_o values in the usual way.

3. STRUCTURE REFINEMENT

3.1. State of Previous Work

In the earlier work on this compound the percentage discrepancy for 42 observed planes had been reduced to 29.0 by Fourier methods. The final electron-density map which was prepared is shown in Fig. 40. The carboxyl group and the terminal branched group are only poorly resolved on this map and the coordinates of the atoms concerned were of necessity rather approximate.

3.2. Use of the New F_o Values

Using the atomic coordinates deduced from the electron-density projection shown in Fig. 40 structure factors were recalculated and compared with the more extensive F_o data which were now available. For the 80 observed reflexions it was found that the percentage discrepancy had risen to over 40.0.

Using those reflexions whose signs seemed reasonably well established an electron-density projection along the a axis was then prepared and new atomic coordinates were selected. The percentage discrepancy for the structure factors calculated on this basis was 43.0.

The main trouble was that the atoms of the branched group

at the end of the chain were not at all well defined on the electron-density projection and their coordinates were very uncertain.

The strong 'subcell'[14] reflexions are not affected to any great extent by the branched group but depend mainly on the periodic repetition of the hydrocarbon chain so that their signs could be fixed relatively easily. Many of the weaker planes, however, have only a small contribution from the atoms of the regular portion of the hydrocarbon chain and their signs are much more dependent on the contributions of the atoms of the branched group than are the strong reflexions. Because of this the signs of many of these reflexions were uncertain at this stage.

3.3. Use of (F_o-F_c) Syntheses

In order to speed up the refinement process the use of (F_o-F_c) syntheses was adopted. These difference maps showed that the atomic coordinates required considerable adjustment and, in addition, peaks which could reasonably be assigned to some of the hydrogen atoms were located.

Up to this stage of the analysis an empirical scattering curve derived by Vand, Morley & Lomer for lauric acid[94] was used for both oxygen and carbon atoms. It was decided to use

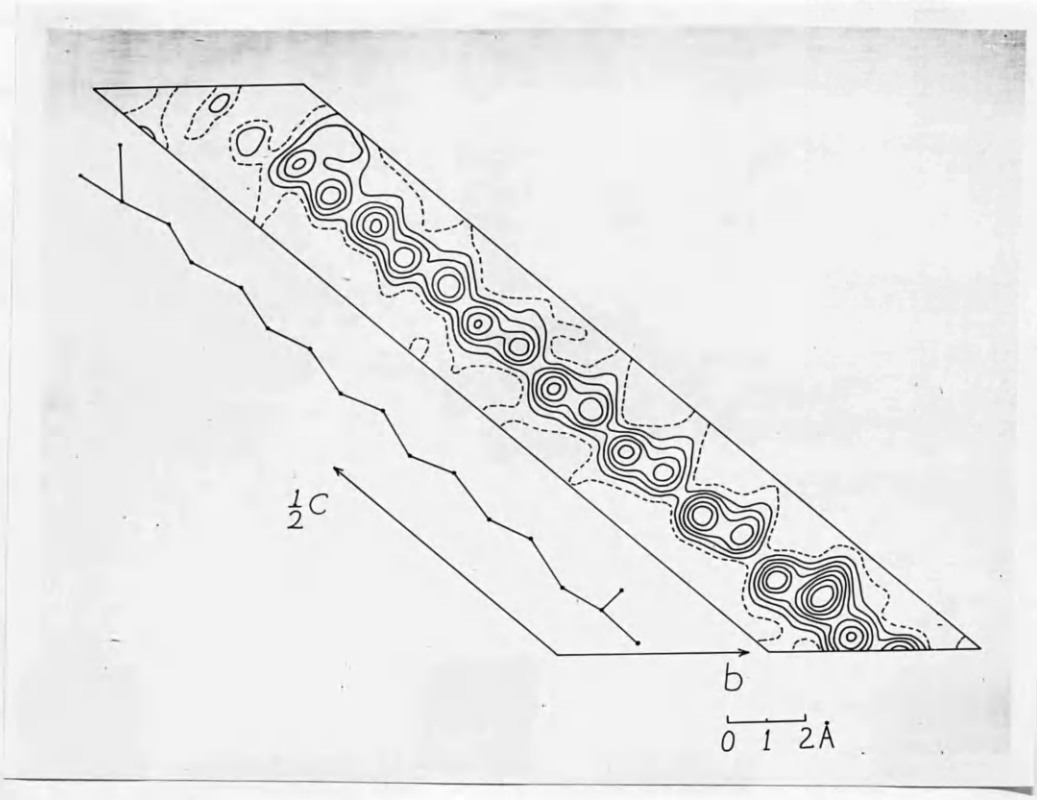

Fig. 41. Electron-density projection on (100). Contours at intervals of 1 e.Å^{-2}, the one electron line being broken. The outline of the molecule corresponds to coordinates deduced from the final difference synthesis.

scattering factors with a better theoretical basis and, in consequence, McWeeny scattering factors[2] for oxygen, carbon and hydrogen atoms were employed. They were multiplied by a temperature factor exp $(-B \sin^2\theta/\lambda^2)$, the constant B being determined from a plot of log F_o/F_c against $\sin^2\theta/\lambda^2$ to be 4.5.

After five successive difference-synthesis projections followed by structure-factor calculations on the basis of the corrected coordinates, it was found that the percentage discrepancy had dropped to 26.0 for the observed reflexions.

At this stage another electron-density projection along the a axis was prepared and is shown in Fig. 41. While most of the atoms are clearly revealed the resolution of one of the atoms in the terminal branched group is very poor.

3.4. Discussion

The appearance of the last (F_o-F_c) synthesis was rather disappointing. Although the electron-density slope at each atomic centre had become nearly zero suggesting that the refinement process was complete, there still remained relatively large peaks of heights about 0.6 - 0.8 e.Å^{-2} in regions away from the atomic centres, particularly near the branched-chain terminal group. These could be caused by several factors

(a) Inaccurate F_o values.

(b) Anisotropic thermal vibration of the atoms.

(c) The use of terms with incorrect signs.

The nature of the crystals which were used for the collection of intensity data was such that the F_o values used in this analysis are probably not quite as accurate as such visually estimated F_o values usually are. Even if the errors in the intensities, however, were three or four times as large as those in the case of benzoic acid (Chapter III) the final value of the percentage discrepancy would still be expected to be lower than 26.0.

The possible importance of anisotropic thermal vibration is difficult to assess. One might expect a long molecule such as isopalmitic acid to vibrate preferentially at right angles to its length, though if this motion consisted of an oscillation in its own plane about the origin, the effect on the a axis projection, apart from the terminal atoms, might not be very great because of the large angle (about 70°) between the plane of the hydrocarbon chain and the plane of projection. Moreover, the residual peaks on the difference map did not appear to be in such positions that they could readily be explained by anisotropic vibration.

It seems more probable to the author that some of the signs of the structure factors are wrong and that instead of the coordinates refining to the true ones they have refined

Table 24

Atomic coordinates deduced from the final difference synthesis on (100).

Atom	y	z
O_1	0.434	0.010
O_2	0.652	0.056
C_1	0.459	0.039
C_2	0.390	0.058
C_3	0.518	0.103
C_4	0.430	0.119
C_5	0.533	0.161
C_6	0.415	0.175
C_7	0.547	0.216
C_8	0.451	0.231
C_9	0.560	0.271
C_{10}	0.473	0.289
C_{11}	0.575	0.325
C_{12}	0.487	0.348
C_{13}	0.600	0.381
C_{14}	0.507	0.401
C_{15}	0.457	0.425
C_{16}	0.810	0.451

to positions giving the best agreement between F_o and F_c values for that set of signs which is slightly incorrect. This view is supported by the electron-density projection shown in Fig. 41, for the peak representing one of the terminal carbon atoms is very poorly defined, suggesting that the refinement of the structure is still incomplete.

The coordinates of the terminal carbon atoms deduced from the difference maps also seem rather incorrect, for they do not fit a tetrahedral arrangement of bonds from C_{14}: see, for example, the outline of the molecule given in Fig. 41.

The final coordinates derived from the difference syntheses are listed in Table 24 and final values of the structure factors are listed in Appendix 4.

3.5. Application of the Fourier Transform Method

It was felt that a rather different approach was required to establish the correctness or otherwise of the signs of some of the higher-angle reflexions.

If it is assumed, to a first approximation, that the molecules occur as coplanar dimers of the form shown in Fig. 42, then it should be possible to find the set of signs which gives best agreement between the F_o values placed on a reciprocal-lattice net and values of the transform of such a dimer.

It was assumed that if C_{16} is neglected then the remainder

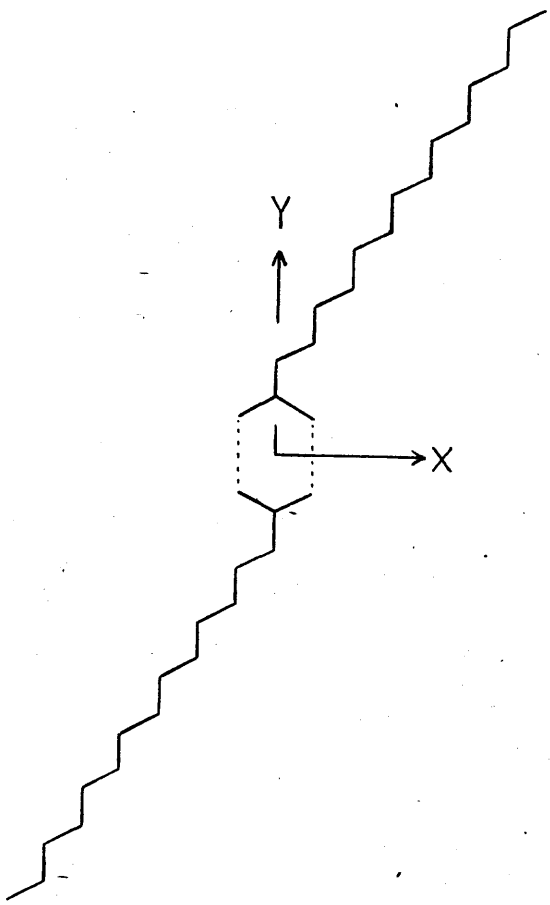

Fig. 42. Idealised dimer used as the basis on which to calculate the Fourier transform of isopalmitic acid. C_{16} has been neglected.

of the molecule can be treated as a periodic structure in which all the C-C and C-O bonds are approximately equal. It was also assumed that the O .... O distance between molecules is twice the length of one of the bonds in the molecule. If the bond lengths are taken as 1.5 Å and the interbond angles as 120° then the approximate positions of the atoms with reference to the origin at the centre of the dimer, should be correct to within 0.1 or 0.2 Å.

Axes X and Y were chosen in the plane of the idealised dimer as shown in Fig. 42 and the coordinates of the atoms were chosen with respect to these axes. When evaluating the transform, which is everywhere real because of the centre of symmetry at the origin, the oxygen and carbon atoms were weighted in the ratio 45:30.

The function evaluated is

$$
\begin{aligned}
T(XY) = 45 \{ & \cos(X+2Y) + \cos(2Y-X) \} \\
& + 30 \{ \cos 3Y + \cos 5Y + \cos(X+6Y) \\
& + \cos(X+8Y) + \cos(2X+9Y) \\
& + \cos(2X+11Y) + \cos(3X+12Y) \\
& + \cos(3X+14Y) + \cos(4X+15Y) \\
& + \cos(4X+17Y) + \cos(5X+18Y) + \cos(5X+20Y) \\
& + \cos(6X+21Y) + \cos(6X+23Y) + \cos(7X+24Y) \} .
\end{aligned}
$$

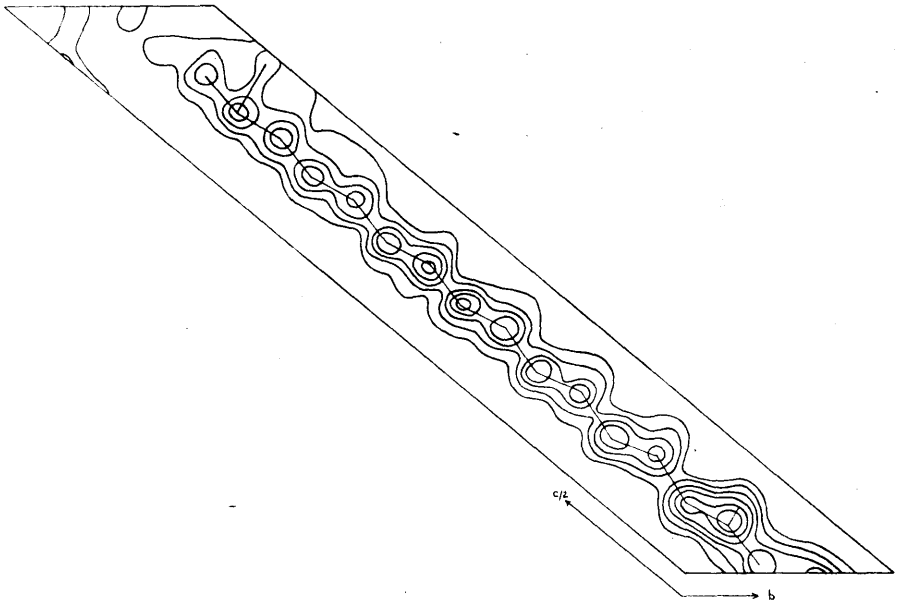

Fig. 43. Electron-density projection along the a axis prepared using the signs deduced from the Fourier transform. Contours at equal arbitrary intervals.

This function was evaluated on a Hollerith machine and contoured in the usual way.

The orientation of the (0kℓ) section of the reciprocal lattice of isopalmitic acid was found readily on the transform and the signs of the majority of the structure factors obtained directly. Those signs which seemed fairly certain from the transform are listed in Appendix 4, the signs of planes with k odd being reversed so that they refer to a dimer centred about $y = \frac{1}{2}$, $z = 0$, in the unit cell and are thus directly comparable with the signs obtained previously. Several of these signs differ.

Using the signs obtained from the transform, an electron-density projection along the a axis was prepared and is shown in Fig. 43. The resolution of most of the atoms is good, that of the terminal carbon atoms being very encouraging for C_{16} had been neglected when calculating the transform. On comparing this projection with that shown in Fig. 41 it will be seen that the coordinates of C_{15} and C_{16} have changed quite appreciably and there is now a tetrahedral arrangement of bonds from C_{14}.

Although it has not yet been possible to calculate structure factors on the basis of coordinates taken from the electron-density projection shown in Fig. 43, it seems possible that these coordinates may provide a starting point from which the refinement may be successfully accomplished.

CHAPTER VIII

ATTEMPTS TO SOLVE THE CRYSTAL STRUCTURE OF p-HYDROXYBENZOIC ACID

1. EXPERIMENTAL DETAILS

1.1. Preparation of Crystals

The crystals of p-hydroxybenzoic acid were grown from acetone/petroleum ether solution. They were obtained in the form of needles with a as needle axis. For photographs taken with the crystal rotating around the a axis, specimens about 0.2 mm. in diameter perpendicular to the rotation axis were used.

The crystals showed very marked cleavage parallel to a, so that on attempting to cut them at right-angles to a they usually split along a into very fine needles. This made the preparation of crystals suitable for b axis photographs very difficult, but eventually a specimen of approximate dimensions 0.5 x 0.2 mm. perpendicular to b was obtained and was used for all b axis photographs.

1.2. Unit Cell Dimensions

Rotation, oscillation and moving-film photographs around the a and b axes were taken with copper $K\alpha$ radiation. From these the following unit cell was deduced:

$a = 6.78, \quad b = 6.47, \quad c = 17.73$ Å;
$\beta = 105^{\circ}\ 30'$.

The absent spectra are $(h0\ell)$ when ℓ is odd, and $(0k0)$ when k is odd, so that the space group is $P2_1/c$.

Table 25

Relative unitary structure factors, $U/\bar{U}$, for p-hydroxybenzoic acid (0kℓ) reflexions.

ℓ/k	0	1	2	3	4	5	6	7	8
0			1.2		0.2		0.9		3.2
1		1.6	0.4	0.5	0.3	0.0	0.0	1.7	0.0
2	0.6	2.0	0.2	1.2	0.9	0.3	0.9	1.0	1.0
3		0.5	1.4	2.2	0.3	2.0	0.6	0.0	1.5
4	1.7	0.3	1.5	1.5	0.8	2.2	1.8	1.3	1.4
5		0.6	0.5	0.0	0.4	1.7	0.0	1.0	0.0
6	1.4	0.2	1.4	2.1	2.9	3.2	0.5	1.3	
7		0.0	1.4	0.0	0.6	3.4	1.6	0.0	
8	2.1	0.0	0.1	1.2	0.9	2.2	2.0	0.0	
9		1.7	0.9	0.0	1.0	0.5	2.3	0.0	
10	0.8	0.2	2.3	0.4	0.7	1.4	1.0	2.5	
11		1.1	0.0	0.0	0.4	0.0	1.3	0.0	
12	0.5	1.7	0.9	1.2	0.8	0.9	1.3		
13		1.2	1.7	1.3	0.5	0.0	0.0		
14	0.4	2.0	0.4	0.0	0.5	1.0	0.0		
15		0.0	0.5	0.9	0.8	0.8			
16	1.6	0.8	1.3	1.8	1.2				
17		1.1	1.1	0.0	1.3				
18	0.0	0.8	1.8	1.4	0.0				
19		2.0	0.9	1.6					
20	1.1	0.0	0.7	0					
21		0.0	0.9						

Assuming that there are four molecules per unit cell, the density was calculated to be 1.22 g./cc.

1.3. Measurement of Intensities

The X-ray data were obtained from equatorial layer moving-film photographs around the a and b axes. Since the Weissenberg camera used had a radius of 2 cm. it was impossible to use the multiple-film technique. Exposures of varying times were used and the intensities measured by comparison with a calibrated scale. A correlation ratio between films of different exposure times was determined by comparing the sum of the measured intensities for each film of those reflexions which had been measured on both. By this method it was possible to place the intensities of all reflexions on the same scale.

From the intensities structure factors were derived by application of the usual mosaic crystal formula.

2. ATTEMPTS AT STRUCTURE DETERMINATION

2.1. Application of the Method of Cochran & Douglas

The method for determining signs proposed by Cochran & Douglas gave, among others, the correct set of signs for a number of the reflexions of salicylic acid. Since that compound is of the same order of complexity as p-hydroxybenzoic acid, it was decided to apply their method to the (0kℓ) data of p-hydroxybenzoic acid.

Table 26

The letters A_0, A_1, etc. are used to denote the S(h) according to the manner given in this table. The signs of two structure factors were assumed positive, so fixing the origin, and the sign of another was found by means of equation 85

A_0	S(057)	B_0	S(0,1,19)
A_1	S(046)	B_1	S(053)
A_2	S(0,7,10)	B_2	S(068)
A_3	S(0,2,10)	B_3	S(064)
A_4	S(054)	B_4	S(019)
A_5	S(058)	B_5	S(0,1,12)
A_6	S(033)	B_6	S(034)
A_7	S(036)	+	S(056)
A_8	S(012)	+	S(069)
A_9	S(0,1,14)	+	S(080)

From the observed structure factors a set of relative unitary structure factors ($U/\bar{U}$) were calculated and are listed in Table 25.

The strong (080) reflexion was found to be positive by application of the expression

$$S(0,2k,0) = |U(0,2k,0)| \sum_{\ell} (-1)^{k+\ell} \; U^2(0k\ell) \quad \ldots\ldots\ldots \quad (85)$$

and two other reflexions, (056) and (069), were allotted positive signs to fix the origin of the cell. From the remaining reflexions the seventeen with largest values of $U/\bar{U}$ were selected and arranged in order of magnitude. The signs, $S(h)$, of these reflexions were labelled A_0, A_1, ... A_9, B_0, ... B_6 as shown in Table 26.

From these twenty reflexions it was found possible to derive thirty values of $Y(h,h')$ and $P(h,h')$ given by the equations

$$Y(h,h') = S(h)\,S(h')\,S(h+h')$$

$$P(h,h') = |U(h)\,U(h')\,U(h+h')|\,/\,|\bar{U}|^3 .$$

Values of $Y(h,h')$ and $P(h,h')$ are listed in Table 27 along with the serial number assigned to each. In the group with serial numbers 1 ..... 17 it was decided to allow up to two values of Y to be negative and in the group with serial numbers 18 .... 30 it was decided to allow up to three values of Y to be negative.

Table 27

Values of $P(h,h')$ and $Y(h,h')$

Column I Serial number of each term $P(h,h')\ Y(h,h')$.

Column II Values of $Y(h,h')$.

Column III Values of $P(h,h')$

I	II	III	I	II	III
1	$-A_7$	21.5	16	$A_1A_2B_6$	10.9
2	$A_0A_3A_6$	16.5	17	A_6A_7	10.7
3	A_1B_5	15.8	18	$-A_3A_4A_7$	10.6
4	A_0A_8	15.7	19	$-A_4B_6$	10.5
5	A_6B_1	14.1	20	$-A_1A_7B_5$	10.4
6	$-A_9B_2$	12.8	21	$A_2A_8B_2$	10.0
7	A_8B_2	12.8	22	$A_1B_1B_4$	9.9
8	$A_1A_5A_9$	12.8	23	$A_2A_9B_3$	9.0
9	$A_1A_5A_8$	12.8	24	$A_1A_8B_6$	8.7
10	$-A_1A_4A_8$	12.8	25	B_1B_5	7.8
11	$A_1A_3B_3$	12.0	26	$A_3B_0B_4$	7.8
12	$-A_8B_3$	11.5	27	$-A_3A_8B_5$	7.8
13	$-A_2B_0$	11.5	28	$-A_4B_2B_5$	7.5
14	$-A_3B_6$	11.0	29	$A_3A_9B_6$	6.9
15	$A_1A_6B_4$	10.9	30	$-A_5B_3B_5$	6.7

A negative value of Y corresponds to the sign relationship $S(h)S(h') = S(h+h')$ not holding.

These data were punched in the appropriate manner on EDSAC tape and the machine, by computing values of

$$\chi = \sum_{h} \sum_{h'} P(h,h')\ Y(h,h') \quad \ldots\ldots\ldots\ldots\ldots\ldots \quad (22a)$$

selected all possible sets of signs for A_0, A_1, etc. which allow up to five values of Y to be negative. The results obtained are listed in Table 28.

Forty-one sets of signs for the seventeen reflexions were deduced by the machine and, along with the three other signs which were known, were used to calculate forty-one electron-density projections by means of a programme designed for the EDSAC by Dr. M.M. Woolfson. Although almost all of them showed the number of peaks to be expected if the atoms are resolved in projection, it was not possible to fit a model of the molecule on to any of the maps. It appears, then, that the correct set of signs has not been deduced by this method.

It is not altogether unexpected for the method to fail, since out of thirty equations of the form $S(h)S(h') = S(h+h')$ only up to five have been allowed to fail in the sets of signs which have been deduced. In the corresponding case of salicylic acid, twenty-nine equations were deduced for sixteen

Table 28

Sets of signs for p-hydroxybenzoic acid.
Column I Serial number of each set of signs.
Column II Sets of signs produced by EDSAC.
Column III Serial numbers of those Y which are negative.

I	II																	III				
	A_0	A_1	A_2	A_3	A_4	A_5	A_6	A_7	A_8	A_9	B_0	B_1	B_2	B_3	B_4	B_5	B_6					
1	+	+	+	−	−	−	−	−	+	−	−	−	+	−	−	+	+	9	25	26	30	
2	+	+	+	−	−	+	−	−	+	−	−	−	+	−	−	+	+	8	25	26		
3	−	+	−	+	+	−	−	−	−	−	+	−	+	+	−	+	−	7	25	26	28	
4	−	+	−	+	+	−	−	−	−	−	+	−	−	+	−	+	−	6	21	25	26	
5	+	+	+	−	−	+	−	−	+	+	−	−	+	−	−	+	+	6	23	25	26	29
6	+	−	+	+	+	+	+	−	+	−	−	+	+	−	−	−	−	9	17	25	30	
7	+	−	+	+	+	−	+	−	+	−	−	+	+	−	−	−	−	8	17	25		
8	−	−	−	−	−	+	+	−	−	−	+	+	+	+	−	−	+	7	17	25	28	
9	−	−	−	−	−	+	+	−	−	−	+	+	−	+	−	−	+	6	17	21	25	
10	+	−	+	+	+	−	+	−	+	+	−	+	+	−	−	−	−	6	17	23	25	29
11	−	+	+	+	+	+	−	−	−	+	−	−	−	+	−	+	−	9	16	25	29	30
12	+	+	−	−	−	+	−	−	+	−	+	−	+	−	−	+	+	8	16	21	23	25
13	−	+	+	+	+	−	−	−	−	+	−	−	−	+	−	+	−	8	16	25	29	
14	+	+	−	−	−	+	−	−	+	+	+	−	−	−	−	+	+	7	16	25	28	29
15	−	+	+	+	+	−	−	−	−	−	−	−	−	+	−	+	−	6	16	23	25	
16	+	+	−	−	−	+	−	−	+	+	+	−	+	−	−	+	+	6	16	21	25	29
17	+	+	+	−	−	−	−	−	+	−	−	−	+	−	+	+	+	9	15	22	25	30
18	+	+	+	−	−	+	−	−	+	−	−	−	+	−	+	+	+	8	15	22	25	
19	−	+	−	+	+	−	−	−	−	−	+	−	+	+	+	+	−	7	15	22	25	28
20	−	+	−	+	+	−	−	−	−	−	+	−	−	+	+	+	−	6	15	21	22	25
21	−	+	+	+	+	−	−	−	−	+	−	−	−	+	−	+	+	8	14	19	24	25
22	+	+	+	−	−	−	−	−	+	−	+	−	+	−	−	+	+	9	13	25	30	
23	+	+	+	−	−	+	−	−	+	−	+	−	+	−	−	+	+	8	13	25		
24	−	+	−	+	+	−	−	−	−	−	−	−	+	+	−	+	−	7	13	25	28	
25	−	+	−	+	+	−	−	−	−	−	−	−	−	+	−	+	−	6	13	21	25	
26	+	+	+	−	−	+	−	−	+	+	+	−	+	−	−	+	+	6	13	23	25	29
27	+	+	+	−	−	−	−	−	+	−	−	+	+	−	−	+	+	5	9	22	26	30
28	−	−	+	+	+	+	−	−	+	−	−	−	+	−	+	−	−	4	9	26	30	
29	+	−	+	+	+	+	−	−	+	−	−	−	+	−	+	−	−	2	9	26	30	
30	+	+	+	−	−	+	−	−	+	−	−	+	+	−	−	+	+	5	8	22	26	
31	−	−	+	+	+	−	−	−	+	−	−	−	+	−	+	−	−	4	8	26		
32	+	−	+	+	+	−	−	−	+	−	−	−	+	−	+	−	−	2	8	26		
33	+	−	+	+	+	−	+	+	+	−	−	+	+	−	−	−	−	1	8	18	20	25
34	−	+	−	+	+	−	−	−	−	−	+	+	+	+	−	+	−	5	7	22	26	28
35	+	−	−	−	−	+	−	−	−	−	+	−	+	+	+	−	+	4	7	26	28	
36	−	−	−	−	−	+	−	−	−	−	+	−	+	+	+	−	+	2	7	26	28	
37	−	+	−	+	+	−	−	−	−	−	+	+	−	+	−	+	−	5	6	21	22	26
38	+	−	−	−	−	+	−	−	−	−	+	−	−	+	+	−	+	4	6	21	26	
39	−	−	+	+	+	−	−	−	+	+	−	−	+	−	+	−	−	4	6	23	26	29
40	−	−	−	−	−	+	−	−	−	−	+	−	−	+	+	−	+	2	6	21	26	
41	+	−	+	+	+	−	−	−	+	+	−	−	+	−	+	−	−	2	6	23	26	29

reflexions and the correct set of signs gave five negative values of Y. If the sign relationship equations were to hold even slightly less well in the case of p-hydroxybenzoic acid, then the correct set of signs could easily correspond to one allowing six or even seven sign relations to fail.

If, however, the EDSAC were allowed to deduce sets of signs allowing up to six negative Y values the number of sets would probably be very large, probably over a hundred, and the labour involved in examining all the corresponding electron-density projections would be very time-consuming unless some very rapid method of inspection was available. The method would probably work most successfully if facilities such as provided by the XRAC computer were available for assessing the sets of signs.

2.2. Application of the Fourier Transform Method

The Fourier transform of an idealised dimer, similar to that postulated for benzoic acid, was evaluated in the usual way. The resulting map was very similar to that of the benzoic acid dimer shown in Fig. 2.

A prolonged attempt was made to fit an ($h0\ell$) reciprocal-lattice net on the transform so that good agreement would be achieved between the observed structure factors and structure factors obtained from the transform. All the efforts were

unsuccessful, the disagreement for low-order (00ℓ) reflexions being marked.

This suggests that molecules of p-hydroxybenzoic acid do not crystallize as simple dimers like benzoic acid but that the terminal hydroxyl groups are involved in some hydrogen bonding system holding the molecules together.

References

1. James, R.W. & Brindley, G.W. (1931). Phil. Mag. 12, 81.
2. McWeeny, R. (1951). Acta Cryst. 4, 513.
3. Hoerni, J.A. & Ibers, J.A. (1954). Acta Cryst. 7, 744.
4. Bragg, W.L. & West, J. (1930). Phil. Mag. 10, 823.
5. International Tables for X-Ray Crystallography (1952). Vol. 1. Birmingham: Kynoch Press.
6. Bragg, W.H. (1915). Trans. Roy. Soc. (London) A215, 253.
7. Bragg, W.L. (1929). Proc. Roy. Soc. (London) A123, 537.
8. Boyes-Watson, J., Davidson, E. & Perutz, M.F. (1947). Proc. Phys. Soc. A191, 83.
9. Knott, G. (1940). Proc. Phys. Soc. (London) 52, 229.
10. Klug, A. (1950). Acta Cryst. 3, 176.
11. Patterson, A.L. (1935). Z. Krist. A90, 517.
12. Morse, P.M. & Feshbach, H. (1953). Methods of Theoretical Physics, Vol. 1, p. 464. New York: McGraw-Hill Book Company.
13. Lipson, H. & Cochran, W. (1953). The Determination of Crystal Structures, p. 15. London: G. Bell & Sons.
14. Vand, V. (1951). Acta Cryst. 4, 104.
15. Abrahams, S.C. & Robertson, J.M. (1948). Acta Cryst. 1, 252.
16. Robertson, J.M. & White, J.G. (1945). J. Chem. Soc. 607.
17. Harker, D. & Kasper, J.S. (1948). Acta Cryst. 1, 70.
18. Karle, J. & Hauptmann, H. (1950). Acta Cryst. 3, 181.
19. Sayre, D. (1952). Acta Cryst. 5, 60.
20. Cochran, W. (1952). Acta Cryst. 5, 65.
21. Zachariasen, W.H. (1952). Acta Cryst. 5, 68.
22. Cochran, W. & Douglas, A.S. (1955). Proc. Roy. Soc. A227, 486.
23. Oddo, G. & Puxeddu, E. (1906). Gazz. chim. ital. 36, ii, 1.
24. Moore, T.S. & Winmill, T.F. (1907). J. Chem. Soc. 91, 1373; and (1912), 101, 1635.

25. Sidgwick, N.V., Spurrell, W.S. & Davies, T.E. (1915). J. Chem. Soc. 107, 1202.

Sidgwick, N.V. & Aldous, W.M. ibid, (1921) 119, 1001.

26. Hilbert, Wulf, Hendricks & Liddel (1936). J. Amer. Chem. Soc. 58, 548.

27. Pauling, L. (1928). Proc. Nat. Acad. Sci. U.S., 14, 359; and (1931) J. Amer. Chem. Soc. 53, 1367.

28. Gillette, R.H. & Sherman, A. (1936). J. Amer. Chem. Soc. 58, 1135.

29. Bacon, G.E. & Pease, R.S. (1953). Proc. Roy. Soc. A220, 397.

30. Hughes, E.W. (1941). J. Amer. Chem. Soc. 63, 1737.

31. Cochran, W. (1953). Acta Cryst. 6, 260.

32. Penfold, B.R. (1953). Acta Cryst. 6, 591.

33. Speakman, J.C. (1949). J. Chem. Soc. p. 3357.

34. Skinner, J.M. & Speakman, J.C. (1951). J. Chem. Soc. p. 185.

35. Brown, C.J., Peiser, H.S. & Turner-Jones, A. (1949). Acta Cryst. 2, 167.

36. Davies, M. & Thomas, O. (1951). J. Chem. Soc. p. 2858.

37. Bacon, G.E. & Curry, N.A. (1955). Nature (London) 175, 894.

38. Helmholz, L. & Rogers, M. (1939). J. Amer. Chem. Soc. 61, 2590.

39. Bauer, S.H., Beach, J.Y. & Simons, J.H. (1939). J. Amer. Chem. Soc. 61, 19.

40. Donohue, J. (1952). J. Phys. Chem. 56, 502.

41. Pauling, L. (1947). J. Amer. Chem. Soc. 69, 542.

42. Westrum, E.F. & Pitzer, K.S. (1949). J. Amer. Chem. Soc. 71, 1940.

43. Ketelaar, J.A.A. (1941). Rec. trav. Chim. Pays-Bas 60, 523.

44. Peterson, S.W. & Levy, H.A. (1952). J. Chem. Phys. 20, 704.

45. McDonald, T.R.R. Personal communication.

46. Rundle, R.E. & Parasol, M. (1952). J. Chem. Phys. 20, 1487.

47. Coulson, C.A. & Danielsson, U. (1954). Ark. Fys. 8, 239.

48. Coulson, C.A. & Danielsson, U. (1954). Ark. Fys. 8, 245.

49. Abrahams, S.C. & Robertson, J.M. (1948). Acta Cryst. 1, 252.

50. Goodwin, T.H., Przybylska, M. & Robertson, J.M. (1950). Acta Cryst. 3, 279.

51. Bertinotti, F., Giacomello, G. & Liquori, A.M. (1954). Acta Cryst. 7, 808.

52. Brown, C.J. & Corbridge, D.E.C. (1954). Acta Cryst. 7, 711.

53. Bragg, W.H. (1921). Proc. Phys. Soc. 34, 33; and (1922). J. Chem. Soc. p. 2766.

54. Robertson, J.M. & Ubbelohde, A.R. (1939). Proc. Roy. Soc. A170, 222.

55. Steinmetz, H. (1914). Z. Kristallogr. 53, 463.

56. Bodewig, C. (1880). Z. Kristallogr. 4, 57.

57. Robertson, J.M. (1943). J. Sci. Instrum. 20, 175.

58. Lipson, H. & Beevers, C.A. (1936). Proc. Phys. Soc. 48, 772.

59. Booth, A.D. (1946). Proc. Roy. Soc. A188, 77.

60. Hughes, E.W. (1941). J. Amer. Chem. Soc. 63, 1737.

61. Booth, A.D. (1947). Nature (London) 160, 196.

62. Cochran, W. (1948). Acta Cryst. 1, 138.

63. Finback, C. & Norman, H. (1948). Acta Chem. Scand. 2, 813.

64. Cochran, W. (1951). Acta Cryst. 4, 81.

65. Booth, A.D. (1948). Nature (London) 161, 765.

66. Cochran, W. (1951). Acta Cryst. 4, 408.

67. Bacon, G.E. (1952). Acta Cryst. 5, 492.

68. March, N.H. (1952). Acta Cryst. 5, 187.

69. Wheatley, P.J. (1953). Acta Cryst. 6, 369.

70. Cruickshank, D.W.J. (1949). Acta Cryst. 2, 65.

71. Cruickshank, D.W.J. & Rollet, J.S. (1953). Acta Cryst. 6, 705.

72. Cruickshank, D.W.J. (1954). Acta Cryst. 7, 519.

73. Ahmed, F.R. & Cruickshank, D.W.J. (1953). Acta Cryst. 6, 385.

74. Parry, G.S. (1954). Acta Cryst. 7, 313.

75. Donohue, J. (1950). J. Amer. Chem. Soc. 72, 949.

76. Donohue, J. & Trueblood, K.N. (1952). Acta Cryst. 5, 419.

77. Cochran, W. & Penfold B.R. (1952). Acta Cryst. 5, 644.

78. Coulson, C.A. (1948). Contribution a l'etude de la structure moleculaire, p. 17 (Victor Henri Memorial Volume). Liege: Desoer.

79. Sutor, D.J., Llewellyn, F.J. & Maslen, H.S. (1954). Acta Cryst. 7, 145.

80. Wright, W.B. & King, G.S.D. (1953). Acta Cryst. 6, 305.

81. Sim, G.A., Robertson, J.M. & Goodwin, T.H. (1955). Acta Cryst. 8, 157.

82. Cochran, W. (1950). Acta Cryst. 3, 268.

83. Weisz, O. & Cole, W.F. (1948). J. Sci. Instr. 25.

84. Ross, P.A. (1928). J. Opt. Soc. Amer. 16, 433.

85. Taylor, J. & Parrish, W. (1955). Rev. Sci. Instr. 26, 367.

86. Albrecht, G. (1939). Rev. Sci. Instr. 10, 221.

87. International Tables, 1935: Internationale Tabellen zur Bestimmung von Kristallstrukturen Berlin: Borntraeger.

88. Clews, C.J.B. & Cochran, W. (1947). Nature (London) 159, 264.

89. Hendricks, S.B. (1933). Z. Krist. 84, 85.

90. Holleman, (1910). Die direkte Einfuhrung von Substituenten in den Benzolkern, Leipzig: Veit.

91. Ri & Eyring (1940). J. Chem. Phys. 8, 433.

92. King, M.V. & Lipscomb, W.N. (1950). Acta Cryst. 3, 222.

93. Gordon, M., Stenhagen, E. & Vand, V. (1953). Acta Cryst. 6, 739.

94. Vand, V., Morley, W.M. & Lomer, T.R. (1951). Acta Cryst. 4, 324

95. Stenhagen, E., Vand, V. & Sim, A. (1952). Acta Cryst. 5, 695.

96. Sydow, E. von (1954). Acta Cryst. 7, 529 and 823.

97. Vand, V., Lomer, T.R., & Lang, A. (1949). Acta Cryst. 2, 214.

98. Daniel, V. (1953). Advances in Physics, 2, 450.

99. Clews, C.J.B. & Cochran, W. (1949). Acta Cryst. 2, 46.

100. Uspensky, J.V. (1937). Introduction to Mathematical Probability, p. 407. New York: McGraw-Hill Book Company.

101. Goodwin, T.H. & Thomson, C.M. (1954). Acta Cryst. 7, 166.

102. Morrison, J.D. & Robertson, J.M. (1949). J. Chem. Soc. p. 1001.

103. MacGillavry, C.H., Hoogschagen, G. & Sixma, F.L.J. (1948). Rec. trav. chim. Pays-Bas. 67, 869.

104. Lingafelter, E.C. & Jensen, L.H. (1950). Acta Cryst. 3, 257.

105. Vand, V. (1953). Acta Cryst. 6, 797.

106. Morley, W.M. & Vand, V. (1949). Nature (London) 163, 285.

107. Luzzati, V. (1953). Acta Cryst. 6, 142.

108. Muller, A. (1927). Proc. Roy. Soc. A114, 542.

APPENDIX 1

Observed and calculated structure factors for the (h0ℓ) and (0kℓ) zones of benzoic acid. The F_o values are derived from visually estimated intensities and the F_c values are derived from the crystal-structure analysis described in Chapter III.

hkℓ	F_o	F_c
000	-	256
002	34.3	32.5
004	31.3	-31.8
006	8.9	8.7
008	22.3	-21.9
0,0,10	10.2	8.6
0,0,12	5.6	3.9
0,0,14	11.0	11.3
0,0,16	8.5	9.2
0,0,18	<2.0	1.2
0,0,20	11.9	11.9
0,0,22	2.8	-2.1
0,0,24	9.0	-10.9
100	36.0	41.3
102	37.3	-38.3
104	26.8	27.7
106	18.7	-16.1
108	21.9	-21.1
1,0,10	25.7	-25.0
1,0,12	25.5	-25.1
1,0,14	3.9	3.3
1,0,16	3.3	1.4
1,0,18	10.9	10.5
1,0,20	3.4	2.7
1,0,22	15.3	-16.5
1,0,24	5.3	-4.5
$10\bar{2}$	74.8	83.7
$10\bar{4}$	3.0	3.4
$10\bar{6}$	6.9	8.3
$10\bar{8}$	34.1	-35.0
1,0,$\overline{10}$	5.2	-4.0
1,0,$\overline{12}$	38.8	37.5
1,0,$\overline{14}$	15.0	15.5
1,0,$\overline{16}$	13.3	13.1
1,0,$\overline{18}$	8.5	10.7
1,0,$\overline{20}$	5.6	5.2
1,0,$\overline{22}$	4.2	5.1
200	7.0	5.2
202	6.7	-3.9
204	16.8	-15.4
206	8.6	-9.0
208	14.0	-15.1
2,0,10	34.2	-35.0
2,0,12	4.6	-5.2
2,0,14	8.8	8.5
2,0,16	<2.7	2.0
2,0,18	2.9	4.3
2,0,20	3.1	-3.9
2,0,22	2.7	-1.9
$20\bar{2}$	18.7	-18.3
$20\bar{4}$	36.2	-40.0
$20\bar{6}$	9.5	-8.8
$20\bar{8}$	4.8	-2.4
2,0,$\overline{10}$	24.9	-25.7
2,0,$\overline{12}$	2.1	0.7
2,0,$\overline{14}$	11.9	11.8
2,0,$\overline{16}$	<2.5	-3.3
2,0,$\overline{18}$	3.1	-2.9
2,0,$\overline{20}$	5.3	5.4
2,0,$\overline{22}$	4.0	3.9

hkℓ	F_o	F_c
300	9.7	-11.1
302	22.3	-23.2
304	10.8	11.0
306	8.8	10.1
308	5.9	-5.2
3,0,10	<2.6	-0.8
3,0,12	6.7	5.4
30$\bar{2}$	<1.9	-0.7
30$\bar{4}$	17.4	-15.6
30$\bar{6}$	8.7	-8.1
30$\bar{8}$	7.9	-8.2
3,0,$\overline{10}$	6.4	-6.2
3,0,$\overline{12}$	2.4	-3.8
3,0,$\overline{14}$	7.4	-8.1
3,0,$\overline{16}$	8.6	-8.9
3,0,$\overline{18}$	11.8	-13.8
3,0,$\overline{20}$	6.7	-8.6
3,0,$\overline{22}$	<2.3	0.4
400	12.7	-12.8
402	6.5	5.1
404	14.9	13.2
406	4.6	3.8
408	6.7	6.9
4,0,10	<2.7	-0.1
4,0,12	3.4	2.3
4,0,14	4.0	3.9
40$\bar{2}$	7.4	-5.1
40$\bar{4}$	6.7	-6.0
40$\bar{6}$	17.4	16.1
40$\bar{8}$	20.3	20.4
4,0,$\overline{10}$	6.5	-7.0
4,0,$\overline{12}$	<2.7	-0.4
4,0,$\overline{14}$	<2.7	0.8
4,0,$\overline{16}$	5.5	-5.6
4,0,$\overline{18}$	4.6	-4.0
4,0,$\overline{20}$	6.5	-7.0
500	3.0	-2.7
50$\bar{2}$	<2.7	-0.7
50$\bar{4}$	3.0	-3.1
50$\bar{6}$	3.0	-4.0
50$\bar{8}$	21.2	19.9
5,0,$\overline{10}$	13.1	12.8
6,0,$\overline{10}$	5.0	5.2
011	11.7	-12.9
012	20.5	19.5
013	21.8	18.0
014	79.1	-72.7
015	26.5	26.5
016	27.6	-27.8
017	11.7	-11.7
018	21.1	-18.9
019	12.8	-12.4
0,1,10	<1.1	-0.4
0,1,11	7.9	-8.3
0,1,12	11.4	12.2
0,1,13	<1.3	-0.1
0,1,14	5.0	-4.3
0,1,15	13.5	15.2
0,1,16	<1.4	2.5

hkℓ	F_o	F_c
0,1,17	5.5	4.7
0,1,18	11.0	-10.4
0,1,19	8.9	-8.9
0,1,20	11.8	-13.7
0,1,21	2.6	-1.6
0,1,22	<1.5	-1.2
0,1,23	2.0	2.3
0,1,24	2.5	-2.8
020	27.9	-27.5
021	< 1.0	2.4
022	18.4	-21.1
023	20.7	-21.0
024	31.7	-32.4
025	27.7	-25.6
026	11.6	-9.2
027	3.7	4.8
028	11.1	9.1
029	9.8	10.3
0,2,10	2.9	-3.0
0,2,11	4.3	5.8
0,2,12	4.0	3.6
0,2,13	<1.4	-1.6
0,2,14	7.3	-9.6
0,2,15	2.9	-3.7
0,2,16	11.9	-12.1
0,2,17	<1.6	1.5
0,2,18	2.5	3.2
0,2,19	2.2	-2.5
0,2,20	<1.6	0.1
0,2,21	2.2	-2.6

hkℓ	F_o	F_c
031	17.5	-17.6
032	2.4	4.2
033	9.8	9.7
034	8.0	8.1
035	3.6	2.9
036	5.9	4.0
037	8.7	-8.7
038	7.6	7.7
039	6.5	4.5
0,3,10	3.6	2.2
0,3,11	2.8	2.9
0,3,12	2.5	3.1
0,3,13	3.1	-4.6
0,3,14	3.0	4.6
0,3,15	<1.6	-2.2
040	4.8	6.0
041	<1.5	0.5
042	3.4	2.6
043	<1.5	-0.3
044	3.0	4.1
045	5.3	3.3
046	7.7	7.5
047	< 1.6	-0.1
048	7.7	6.6
049	3.7	-5.7
0,4,10	< 1.6	1.1
0,4,11	4.8	5.3
0,4,12	< 1.6	-0.5
0,4,13	2.8	4.0

APPENDIX 2

Structure factors and values of θ and ϕ for the $(h0\ell)$ and $(0k\ell)$ zones of benzoic acid. The F_o values are derived from Geiger-counter measured intensities and the F_c values are derived from the crystal-structure analysis described in Chapter IV.

hkℓ	θ	φ	F_o	F_c
000	-	-	-	256
002	4°4'	82°52'	32.2	30.0
004	8°10'	"	30.7	-33.2
006	12°18'	"	8.3	8.8
008	16°30'	"	20.3	-20.6
0,0,10	20°48'	"	9.6	10.5
0,0,12	25°13'	"	5.5	6.3
0,0,14	29°48'	"	11.0	11.3
0,0,16	34°37'	"	8.6	8.6
0,0,18	39°43'	"	2.2	2.2
0,0,20	45°14'	"	13.4	13.5
0,0,22	51°21'	"	4.4	-2.1
100	8°6'	0°	39.3	40.8
102	9°32'	25°11'	34.4	-37.2
104	12°15'	41°37'	26.6	25.9
106	15°39'	51°36'	17.2	-17.6
108	19°24'	57°58'	19.3	-20.8
1,0,10	23°27'	62°17'	22.2	-21.5
1,0,12	27°43'	65°21'	23.2	-23.1
1,0,14	32°13'	67°39'	3.7	3.5
1,0,16	37°0'	69°25'	2.0	2.2
1,0,18	42°10'	70°50'	9.9	9.6
1,0,20	47°48'	71°59'	2.8	2.1
$10\bar{2}$	8°37'	-28°3'	72.1	84.3
$10\bar{4}$	10°48'	-48°47'	2.8	3.7
$10\bar{6}$	13°55'	-61°32'	6.5	7.8
$10\bar{8}$	17°31'	-69°27'	34.7	-34.7
$1,0,\overline{10}$	21°26'	-74°37'	4.4	-3.4

hk ℓ	θ	ϕ	F_o	F_c
1,0,$\bar{12}$	25°35'	-78°14'	35.0	35.8
1,0,$\bar{14}$	29°58'	-80°52'	15.5	16.0
1,0,$\bar{16}$	34°37'	-82°52'	12.1	11.9
1,0,$\bar{18}$	39°34'	-84°27'	7.0	7.9
1,0,$\bar{20}$	44°57'	-85°43'	5.9	5.9
1,0,$\bar{22}$	50°55'	-86°45'	3.9	5.2
200	16°23'	0°	6.3	6.3
202	17°25'	13°37'	6.1	-5.6
204	19°20'	25°11'	17.0	-15.5
206	21°57'	34°25'	8.2	-9.2
208	25°6'	41°37'	14.9	-15.2
2,0,10	28°41'	47°14'	34.5	34.1
2,0,12	32°37'	51°37'	5.0	-5.2
2,0,14	36°56'	55°7'	10.0	9.0
2,0,16	41°39'	57°58'	0.7	-0.5
2,0,18	46°51'	60°19'	3.2	2.2
2,0,20	52°43'	62°16'	4.1	-3.7
20$\bar{2}$	16°23'	-14°28'	19.3	-18.4
20$\bar{4}$	17°26'	-28°3'	38.8	-37.4
20$\bar{6}$	19°22'	-39°34'	8.7	-8.1
20$\bar{8}$	22°0'	-48°47'	4.3	-4.6
2,0,$\bar{10}$	25°9'	-55°58'	24.6	-23.7
2,0,$\bar{12}$	28°44'	-61°33'	2.5	1.7
2,0,$\bar{14}$	32°42'	-65°56'	11.8	11.0
2,0,$\bar{16}$	37°1'	-69°26'	1.0	-2.6
2,0,$\bar{18}$	41°44'	-72°17'	2.9	-3.1
2,0,$\bar{20}$	46°56'	-74°37'	5.1	5.3
300	25°2'	0°	13.5	-13.7
302	25°57'	9°16'	23.7	-23.7

hkℓ	θ	φ	F_o	F_c
304	27°33'	17°44'	11.6	11.1
306	29°46'	25°11'	8.8	8.2
308	32°33'	31°35'	6.2	-5.5
3,0,10	35°48'	37°1'	1.0	-1.2
3,0,12	39°31'	41°37'	6.2	5.5
3,0,14	43°45'	45°29'	0	-0.2
3,0,16	48°30'	48°47'	0	-0.7
$30\bar{2}$	24°50'	-9°39'	1.4	-1.7
$30\bar{4}$	25°25'	-19°9'	16.5	-18.0
$30\bar{6}$	26°42'	-28°3'	8.7	-8.8
$30\bar{8}$	28°38'	-36°0'	7.9	-8.0
$3,0,\bar{10}$	31°10'	-42°54'	5.6	-6.1
$3,0,\bar{12}$	34°11'	-48°48'	2.0	-3.7
$3,0,\bar{14}$	37°42'	-53°45'	6.3	-7.2
$3,0,\bar{16}$	41°40'	-57°58'	8.1	-7.9
$3,0,\bar{18}$	46°9'	-61°32'	13.3	-13.2
$3,0,\bar{20}$	51°16'	-64°34'	7.6	-8.3
400	34°20'	0°	12.2	-13.6
402	35°16'	7°1'	6.5	6.2
404	36°46'	13°37'	13.3	12.9
406	38°50'	19°42'	4.7	4.7
408	41°27'	25°11'	6.7	6.7
4,0,10	44°38'	30°5'	0.6	0.1
4,0,12	48°24'	34°25'	3.5	3.4
4,0,14	52°48'	38°14'	3.4	3.6
$40\bar{2}$	34°2'	-7°14'	6.3	-7.5
$40\bar{4}$	34°21'	-14°28'	6.7	-7.0
$40\bar{6}$	35°17'	-21°27'	16.9	15.4
$40\bar{8}$	36°49'	-28°3'	21.4	20.1

hk ℓ	θ	ϕ	F_o	F_c
4,0,$\overline{10}$	38°54'	-34°6'	7.0	-7.1
4,0,$\overline{12}$	41°33'	-39°35'	1.8	-0.6
4,0,$\overline{14}$	44°45'	-44°28'	1.1	0.2
4,0,$\overline{16}$	48°30'	-48°47'	6.0	-6.4
500	44°50'	0°	2.3	-2.2
502	45°50'	5°38'	1.2	1.8
504	47°24'	11°2'	0.4	-0.5
506	49°35'	16°7'	2.7	3.9
508	52°22'	20°50'	0.7	1.3
50$\overline{2}$	44°24'	-5°47'	0	-0.6
50$\overline{4}$	44°34'	-11°35'	3.2	-3.4
50$\overline{6}$	45°18'	-17°18'	3.3	-3.4
50$\overline{8}$	46°36'	-22°49'	22.4	21.0
5,0,$\overline{10}$	48°30'	-28°3'	14.9	13.9
5,0,$\overline{12}$	51°0'	-32°56'	2.2	-2.3
011	8°53'	13°17'	12.7	-12.9
012	9°34'	25°17'	18.7	19.5
013	10°37'	35°19'	21.4	18.0
014	11°56'	43°22'	69.8	-72.7
015	13°27	49°45'	24.5	26.5
016	15°7'	54°48'	23.6	-27.8
017	16°53'	58°50'	11.1	-11.7
018	18°45'	62°7'	18.5	-18.9
019	20°40'	64°48'	13.1	-12.4
0,1,10	22°41'	67°3'	0.4	-0.4
0,1,11	24°44'	68°57'	9.0	-8.3
0,1,12	26°51'	70°34'	12.7	12.2
0,1,13	29°2'	71°58'	1.4	-0.1

hkl	θ	φ	F_o	F_c
0,1,14	31°17'	73°10'	5.3	-4.3
0,1,15	33°36'	74°14'	14.6	15.2
0,1,16	35°59'	75°11'	2.2	2.5
0,1,17	38°27'	76°1'	6.1	4.7
0,1,18	41°1'	76°46'	10.6	-10.4
0,1,19	43°43'	77°26'	10.1	-8.9
0,1,20	46°31'	78°3'	14.0	-13.7
0,1,21	49°30'	78°36'	4.1	-1.6
0,1,22	52°41'	79°6'	2.4	-1.2
020	17°30'	0°	27.0	-27.5
021	17°37'	6°44'	1.3	2.4
022	18°0'	13°17'	17.3	-21.1
023	18°36'	19°31'	19.9	-21.0
024	19°25'	25°17'	32.0	-32.4
025	20°26'	30°34'	25.4	-25.6
026	21°37'	35°19'	12.1	-9.2
027	22°58'	39°35'	3.9	4.8
028	24°25'	43°22'	10.7	9.1
029	26°1'	46°45'	10.0	10.3
0,2,10	27°43'	49°45'	2.8	-3.0
0,2,11	29°31'	52°25'	4.9	5.8
0,2,12	31°26'	54°48'	4.3	3.6
0,2,13	33°25'	56°55'	0.6	-1.6
0,2,14	35°30'	58°50'	8.2	-9.6
0,2,15	37°42'	60°33'	3.8	-3.7
0,2,16	40°0'	62°7'	14.0	-12.1
0,2,17	42°24'	63°31'		1.5
0,2,18	44°55'	64°48'		3.2
0,2,19	47°36'	65°59'		-2.5
0,2,20	50°26'	67°4'		0.1

hkℓ	θ	φ	F_o	F_c
031	26°56'	4°30'	17.4	-17.6
032	27°8'	8°57'	2.9	4.2
033	27°38'	13°17'	10.1	9.7
034	28°15'	17°29'	7.8	8.1
035	29°0'	21°29'	3.5	2.9
036	29°56'	25°17'	5.3	4.0
037	30°59'	28°52'	8.4	-8.7
038	32°12'	32°12'	7.4	7.7
039	33°32'	35°19'	6.1	4.5
0,3,10	35°0'	38°13'	3.6	2.2
0,3,11	36°38'	40°54'	2.8	2.9
0,3,12	38°21'	43°22'	2.8	3.1
0,3,13	40°10'	45°40'	3.7	-4.6
0,3,14	42°8'	47°47'	3.4	4.6
0,3,15	44°14'	49°45'	1.1	-2.2
0,3,16	46°30'	51°33'	0	
0,3,17	48°51'	53°14'	0.9	
0,3,18	51°29'	54°48'	1.9	
040	37°0'	0°	4.9	6.0
041	37°3'	3°23'	0.9	0.5
042	37°17'	6°44'	3.6	2.6
043	37°38'	10°3'	1.0	-0.3
044	38°11'	13°17'	3.3	4.1
045	38°49'	16°27'	5.7	3.3
046	39°39'	19°30'	7.3	7.5
047	40°34'	22°27'	1.9	-0.1
048	41°40'	25°17'	7.1	6.6
049	42°56'	28°0'	4.0	-5.7

hkℓ	θ	φ	F_o	F_c
0,4,10	44°19'	30°34'	1.6	1.1
0,4,11	45°48'	33°0'	5.1	5.3
0,4,12	47°28'	35°19'	0.6	-0.5
0,4,13	49°19'	37°31'	3.7	4.0
0,4,14	51°18'	39°35'	0	
051	48°48'	2°42'	3.1	
052	49°2'	5°24'	4.9	
053	49°22'	8°4'	3.1	
054	49°54'	10°42'	0.9	
055	50°36'	13°17'	0.2	
056	51°21'	15°50'	0.6	
057	52°20'	18°18'	3.1	

APPENDIX 3

Observed and calculated structure factors for the (h0ℓ) and (0kℓ) zones of 11-amino-undecanoic acid hydrobromide hemihydrate.

hkℓ	F_o	F_c	hkℓ	F_o	F_c
000		1224	200	51	17
004	151	177	202	125	131
006	16	10	204	165	113
008	< 8	-13	206	214	202
0,0,10	137	-136	208	112	102
0,0,12	155	-153	2,0,10	138	143
0,0,14	175	-198	2,0,12	43	-34
0,0,16	178	-178	2,0,14	< 11	-6
0,0,18	128	-149	2,0,16	174	-179
0,0,20	121	-103	2,0,18	140	-148
0,0,22	18	-20	2,0,20	300	-349
0,0,24	16	16	2,0,22	< 14	-14
0,0,26	97	76	2,0,24	63	-87
0,0,28	126	103	2,0,26	36	-35
0,0,30	228	252	2,0,28	17	5
0,0,32	103	76	2,0,30	24	19
0,0,34	88	82	2,0,32	56	52
0,0,36	41	26	2,0,34	60	63
0,0,38	24	-4	2,0,36	73	74
0,0,40	20	-28	2,0,38	48	49
0,0,42	49	-46	2,0,40	44	47
0,0,44	54	-62	2,0,42	< 15	6
0,0,46	50	-48	2,0,44	< 15	-15
0,0,48	42	-41	2,0,46	37	-36
0,0,50	27	-28	2,0,48	30	-37
0,0,52	< 10	-10	2,0,50	26	-34
0,0,54	< 10	6	2,0,52	60	-44
0,0,56	20	21	2,0,54	32	-23
0,0,58	25	24	2,0,56	< 16	-16
0,0,60	16	22	2,0,58	< 16	3
0,0,62	21	20	2,0,60	< 16	-1

hkℓ	F_o	F_c
$20\bar{2}$	30	13
$20\bar{4}$	32	-96
$20\bar{6}$	35	59
$20\bar{8}$	67	66
$2,0,\overline{10}$	566	-602
$2,0,\overline{12}$	150	-171
$2,0,\overline{14}$	230	-212
$2,0,\overline{16}$	54	-67
$2,0,\overline{18}$	31	16
$2,0,\overline{20}$	50	35
$2,0,\overline{22}$	90	98
$2,0,\overline{24}$	90	79
$2,0,\overline{26}$	96	100
$2,0,\overline{28}$	56	53
$2,0,\overline{30}$	56	60
$2,0,\overline{32}$	< 15	-9
$2,0,\overline{34}$	< 15	-7
$2,0,\overline{36}$	22	-12
$2,0,\overline{38}$	44	-31
$2,0,\overline{40}$	101	-116
$2,0,\overline{42}$	64	-50
$2,0,\overline{44}$	51	-51
$2,0,\overline{46}$	40	-30
$2,0,\overline{48}$	< 16	8
$2,0,\overline{50}$	< 16	1
$2,0,\overline{52}$	25	28
$2,0,\overline{54}$	22	16
$2,0,\overline{56}$	22	25
$2,0,\overline{58}$	< 16	6
$2,0,\overline{60}$	< 16	14
$2,0,\overline{62}$	< 16	-1
400	167	-180
402	14	2
404	20	-20
406	183	192
408	125	129
4,0,10	306	320
4,0,12	28	31
4,0,14	153	173
4,0,16	150	118
4,0,18	76	62
4,0,20	< 16	-12
4,0,22	64	-60
4,0,24	88	-108
4,0,26	106	-118
4,0,28	68	-96
4,0,30	84	-83
4,0,32	22	-22
4,0,34	22	12
4,0,36	44	44
4,0,38	46	52
4,0,40	60	60
4,0,42	103	91
4,0,44	60	51
4,0,46	22	28
4,0,48	24	7
4,0,50	< 16	-3
4,0,52	< 16	-22

hkℓ	F_o	F_c
4,0,54	23	-19
4,0,56	24	-30
4,0,58	21	-14
4,0,60	21	-20
4,0,62	< 15	-2
40$\bar{2}$	140	-127
40$\bar{4}$	231	-233
40$\bar{6}$	150	-96
40$\bar{8}$	98	-124
4,0,$\overline{10}$	< 16	10
4,0,$\overline{12}$	83	53
4,0,$\overline{14}$	160	190
4,0,$\overline{16}$	56	40
4,0,$\overline{18}$	48	25
4,0,$\overline{20}$	201	220
4,0,$\overline{22}$	83	117
4,0,$\overline{24}$	82	86
4,0,$\overline{26}$	28	47
4,0,$\overline{28}$	< 16	-44
4,0,$\overline{30}$	38	-22
4,0,$\overline{32}$	65	-58
4,0,$\overline{34}$	60	-45
4,0,$\overline{36}$	58	-74
4,0,$\overline{38}$	38	-17
4,0,$\overline{40}$	< 18	-32
4,0,$\overline{42}$	< 18	36
4,0,$\overline{44}$	< 17	26
4,0,$\overline{46}$	< 17	15

hkℓ	F_o	F_c
4,0,$\overline{48}$	20	-2
4,0,$\overline{50}$	42	56
4,0,$\overline{52}$	22	12
4,0,$\overline{54}$	< 16	30
4,0,$\overline{56}$	< 16	6
4,0,$\overline{58}$	< 15	-4
4,0,$\overline{60}$	< 15	-6
600	178	-166
602	100	-130
604	109	-107
606	102	-92
608	< 17	15
6,0,10	46	37
6,0,12	100	117
6,0,14	102	100
6,0,16	129	143
6,0,18	87	68
6,0,20	101	88
6,0,22	< 17	-16
6,0,24	< 16	-7
6,0,26	69	-82
6,0,28	65	-63
6,0,30	83	-107
6,0,32	97	-96
6,0,34	64	-70
6,0,36	< 16	-1
6,0,38	24	-18
6,0,40	22	27

hkℓ	F_o	F_c	hkℓ	F_o	F_c
6,0,42	22	26	6,0,$\overline{44}$	34	35
6,0,44	38	44	6,0,$\overline{46}$	37	34
6,0,46	39	39	6,0,$\overline{48}$	25	27
6,0,48	34	32	6,0,$\overline{50}$	< 16	21
6,0,50	26	22	6,0,$\overline{52}$	< 16	-5
6,0,52	< 15	6	6,0,$\overline{54}$	< 15	-23
6,0,54	< 15	-6	6,0,$\overline{56}$	< 15	-4
6,0,56	< 15	-5	6,0,$\overline{58}$	< 15	-1
60$\overline{2}$	148	-154	800	< 16	-20
60$\overline{4}$	148	-115	802	57	-51
60$\overline{6}$	45	-72	804	67	-69
60$\overline{8}$	< 17	9	806	86	-84
6,0,$\overline{10}$	67	36	808	65	-64
6,0,$\overline{12}$	101	110	8,0,10	66	-63
6,0,$\overline{14}$	126	103	8,0,12	18	-9
6,0,$\overline{16}$	123	129	8,0,14	< 16	3
6,0,$\overline{18}$	108	75	8,0,16	42	46
6,0,$\overline{20}$	41	78	8,0,18	66	63
6,0,$\overline{22}$	20	-20	8,0,20	71	85
6,0,$\overline{24}$	82	-79	8,0,22	88	94
6,0,$\overline{26}$	39	-62	8,0,24	53	50
6,0,$\overline{28}$	40	-13	8,0,26	< 16	2
6,0,$\overline{30}$	98	-104	8,0,28	38	37
6,0,$\overline{32}$	51	-51	8,0,30	< 15	-10
6,0,$\overline{34}$	51	-70	8,0,32	< 15	-21
6,0,$\overline{36}$	27	-27	8,0,34	33	-37
6,0,$\overline{38}$	< 16	-2	8,0,36	45	-48
6,0,$\overline{40}$	< 16	10	8,0,38	38	-40
6,0,$\overline{42}$	34	36	8,0,40	36	-35

hkℓ	F_o	F_c
8,0,42	< 15	-10
8,0,44	< 15	-2
8,0,46	< 14	13
8,0,48	18	17
8,0,50	25	25
8,0,52	36	28
8,0,54	< 14	4
80$\bar{2}$	< 16	18
80$\bar{4}$	70	40
80$\bar{6}$	62	68
80$\bar{8}$	79	81
8,0,$\overline{10}$	83	71
8,0,$\overline{12}$	70	74
8,0,$\overline{14}$	42	40
8,0,$\overline{16}$	< 16	28
8,0,$\overline{18}$	< 16	-15
8,0,$\overline{20}$	24	-12
8,0,$\overline{22}$	36	-52
8,0,$\overline{24}$	48	-33
8,0,$\overline{26}$	49	-51
8,0,$\overline{28}$	44	-23
8,0,$\overline{30}$	30	-40
8,0,$\overline{32}$	< 15	2
8,0,$\overline{34}$	39	36
8,0,$\overline{36}$	< 15	34
8,0,$\overline{38}$	< 15	8
8,0,$\overline{40}$	34	32
8,0,$\overline{42}$	20	12
8,0,$\overline{44}$	20	21

hkℓ	F_o	F_c
8,0,$\overline{46}$	< 15	5
8,0,$\overline{48}$	< 15	2
8,0,$\overline{50}$	< 15	-1
8,0,$\overline{52}$	< 15	-6
8,0,$\overline{54}$	< 15	-7
10,0,0	41	37
10,0,2	27	28
10,0,4	< 16	-17
10,0,6	26	-26
10,0,8	75	-74
10,0,10	64	-64
10,0,12	89	-88
10,0,14	46	-38
10,0,16	20	-21
10,0,18	46	-48
10,0,20	< 16	5
10,0,22	29	36
10,0,24	48	46
10,0,26	62	64
10,0,28	46	46
10,0,30	37	44
10,0,32	18	8
10,0,34	< 15	4
10,0,36	< 15	-24
10,0,38	24	-24
10,0,40	27	-37
10,0,42	35	-26
10,0,44	15	-13
10,0,46	< 15	-3

hkℓ	F_o	F_c
10,0,$\bar{2}$	70	76
10,0,$\bar{4}$	68	54
10,0,$\bar{6}$	57	72
10,0,$\bar{8}$	37	25
10,0,$\bar{10}$	<16	26
10,0,$\bar{12}$	<16	32
10,0,$\bar{14}$	<16	-14
10,0,$\bar{16}$	56	-59
10,0,$\bar{18}$	54	-48
10,0,$\bar{20}$	56	-53
10,0,$\bar{22}$	53	-40
10,0,$\bar{24}$	38	-27
10,0,$\bar{26}$	<15	-6
10,0,$\bar{28}$	<15	8
10,0,$\bar{30}$	25	20
10,0,$\bar{32}$	25	26
10,0,$\bar{34}$	25	26
10,0,$\bar{36}$	22	16
10,0,$\bar{38}$	21	12
10,0,$\bar{40}$	<15	10
10,0,$\bar{42}$	<15	6
10,0,$\bar{44}$	<15	-18
10,0,$\bar{46}$	<15	-12
10,0,$\bar{48}$	<15	-12
12,0,0	35	39
12,0,2	44	39
12,0,4	32	28
12,0,6	<16	7
12,0,8	30	40
12,0,10	<16	-20
12,0,12	30	-30
12,0,14	35	-42
12,0,16	33	-36
12,0,18	30	-34
12,0,20	19	-19
12,0,22	<15	-5
12,0,24	<15	5
12,0,$\bar{2}$	37	40
12,0,$\bar{4}$	<16	22
12,0,$\bar{6}$	<16	13
12,0,$\bar{8}$	<15	-4
12,0,$\bar{10}$	16	-14
12,0,$\bar{12}$	30	-32
12,0,$\bar{14}$	24	-27
12,0,$\bar{16}$	24	-34
12,0,$\bar{18}$	19	-22
12,0,$\bar{20}$	<15	-13
12,0,$\bar{22}$	<15	14
12,0,$\bar{24}$	<15	1
011	87	87
013	< 7	-1
015	93	102
017	188	179
019	108	-99
0,1,11	76	-71
0,1,13	130	-147

hkℓ	F_o	F_c
0,1,15	122	-115
0,1,17	113	-104
0,1,19	68	-72
0,1,21	21	-33
0,1,23	< 13	17
0,1,25	38	45
0,1,27	42	36
0,1,29	53	67
0,1,31	37	38
0,1,33	32	27
0,1,35	48	37
0,1,37	44	56
0,1,39	28	-31
0,1,41	22	-13
0,1,43	34	-50
0,1,45	35	-35
0,1,47	27	-37
0,1,49	18	-17
0,1,51	< 11	-9
0,1,53	25	-11
0,1,55	< 11	7
020	38	-28
022	80	-42
024	25	-26
026	50	-20
028	< 8	-7
0,2,10	14	-28
0,2,12	46	59
0,2,14	40	45
0,2,16	37	-12
0,2,18	< 10	-4
0,2,20	36	21
0,2,22	< 10	6
0,2,24	20	-12
0,2,26	< 10	-10
0,2,28	29	-29
0,2,30	12	-14
0,2,32	26	-20
0,2,34	< 12	-10
0,2,36	< 12	-10
0,2,38	< 13	-10
0,2,40	< 13	-15
0,2,42	36	34
0,2,44	< 13	20
031	86	-91
033	56	-71
035	44	-42
037	< 10	0
039	< 10	11
0,3,11	33	30
0,3,13	120	111
0,3,15	129	131
0,3,17	67	68
0,3,19	87	78
0,3,21	12	12
0,3,23	16	7
0,3,25	33	-36
0,3,27	31	-38
0,3,29	49	-60

hkℓ	F_o	F_c
0,3,31	40	-48
0,3,33	33	-49
0,3,35	21	-20
0,3,37	< 13	-8
0,3,39	< 13	5
0,3,41	< 13	7
0,3,43	45	49
0,3,45	31	34
0,3,47	22	25
0,3,49	34	37
0,3,51	< 10	6
0,3,53	< 10	4
040	93	-93
042	79	-71
044	82	-96
046	< 12	-5
048	35	37
0,4,10	30	32
0,4,12	68	66
0,4,14	69	69
0,4,16	73	60
0,4,18	66	65
0,4,20	38	31
0,4,22	28	33
0,4,24	14	-16
0,4,26	38	-48
0,4,28	47	-51
0,4,30	49	-55

hkℓ	F_o	F_c
0,4,32	40	-48
0,4,34	37	-47
0,4,36	< 12	-11
0,4,38	< 12	9
0,4,40	< 12	12
0,4,42	25	26
0,4,44	28	28
0,4,46	25	21
0,4,48	18	21
0,4,50	< 9	9
0,4,52	< 9	6
051	< 11	-2
053	25	-23
055	25	-17
057	< 11	5
059	< 11	-8

APPENDIX 4

Observed and calculated values for the (0kℓ) structure factors of isopalmitic acid. Signs deduced from the Fourier transform are also listed.

0kℓ	F_o	F_c	Transform Sign	0kℓ	F_o	F_c	Transform Sign
003	23.8	30.2	+	01$\bar{4}$	6.1	8.8	+
004	2.1	-7.0	-	01$\bar{5}$	17.4	-24.9	-
005	19.1	20.1	+	01$\bar{6}$	<1.2	7.3	
006	11.2	-10.7	-	01$\bar{7}$	<1.5	-8.7	
007	9.7	7.9		01$\bar{8}$	3.5	5.4	
008	14.7	-13.0		01$\bar{9}$	10.9	5.0	+
009	2.1	-3.0		0,1,$\overline{10}$	4.2	2.6	
0,0,10	11.6	-8.1	-	0,1,$\overline{11}$	20.1	17.5	+
0,0,11	2.4	-6.3	-	0,1,$\overline{12}$	2.6	5.9	+
0,0,12	13.1	-6.0	-	0,1,$\overline{13}$	25.3	26.2	+
0,0,13	5.5	-3.1		0,1,$\overline{14}$	<1.7	-1.4	
0,0,14	7.1	-1.0	-	0,1,$\overline{15}$	21.8	20.5	
0,0,15	8.2	0.8		0,1,$\overline{16}$	3.6	1.5	+
0,0,16	<1.5	1.2		0,1,$\overline{17}$	18.8	-13.5	-
0,0,17	14.9	15.2	+	0,1,$\overline{18}$	37.7	-37.5	-
0,0,18	24.1	29.2	+	0,1,$\overline{19}$	10.9	-14.8	-
0,0,19	6.0	8.7	+	0,1,$\overline{20}$	12.5	5.8	
010	138.8	-145.5	-	0,1,36	9.1	10.0	
011	16.6	-22.1	-	020	47.5	47.1	+
012	7.0	-5.7	-	021	7.5	5.2	+
013	7.7	-15.8	-	022	<2.3	-2.6	
014	12.7	5.7	-	023	8.2	9.1	+
015	4.7	-7.1	-	024	4.6	-9.1	-
016	9.0	2.0		025	4.2	9.6	
01$\bar{1}$	42.0	-38.2	-	026	5.3	-3.1	-
01$\bar{2}$	24.9	31.4	+	02$\bar{1}$	4.9	8.8	+
01$\bar{3}$	34.0	-36.6	-	02$\bar{2}$	13.1	-15.8	-

0kℓ	F_o	F_c	Transform Sign
$02\bar{3}$	<3.0	5.2	
$02\bar{4}$	6.0	6.8	-
$02\bar{5}$	<2.0	3.7	
$02\bar{6}$	6.1	8.8	-
$02\bar{7}$	<2.3	3.4	
$02\bar{8}$	9.5	10.0	-
$02\bar{9}$	3.6	1.4	-
$0,2,\bar{10}$	9.6	4.1	-
$0,2,\bar{11}$	<2.3	-5.8	
$0,2,\bar{12}$	8.7	-7.4	
$0,2,\bar{13}$	<2.0	-14.5	
$0,2,\bar{14}$	6.4	-4.8	-
$0,2,\bar{15}$	6.1	-15.2	-
$0,2,\bar{16}$	6.4	-12.9	-
$0,2,\bar{17}$	9.9	1.8	-
$0,2,\bar{18}$	5.9	-11.1	
$0,2,\bar{19}$	10.6	8.4	+
$0,2,\bar{20}$	3.5	-9.6	+
$0,2,\bar{21}$	6.4	2.0	+
$0,2,\bar{36}$	18.2	-23.4	
030	11.2	-14.7	-
$03\bar{1}$	4.2	4.2	+
$03\bar{2}$	10.2	9.9	+
$0,3,\bar{18}$	21.4	22.5	+
$0,3,\bar{19}$	8.1	11.0	+
$0,3,\bar{20}$	<2.9	-5.8	
$0,3,\bar{21}$	11.7	12.3	
$0,3,\bar{22}$	3.2	0.7	
$0,3,\bar{23}$	8.2	1.6	-
$0,3,\bar{24}$	<2.3	2.7	
$0,3,\bar{25}$	7.1	-6.0	-
$0,3,\bar{26}$	<2.3	-4.4	
$0,3,\bar{27}$	3.9	-1.3	-
$0,3,\bar{28}$	<2.3	-2.1	
$0,3,\bar{29}$	<2.3	1.1	
$0,3,\bar{30}$	5.7	-0.9	-
$0,3,\bar{31}$	<2.9	0.5	
$0,3,\bar{32}$	9.4	2.3	
$0,3,\bar{33}$	<2.9	6.0	
$0,3,\bar{34}$	16.2	9.6	-
$0,3,\bar{35}$	6.8	10.0	+
$0,3,\bar{36}$	32.3	32.2	+
$0,4,\bar{18}$	14.6	-13.3	-
$0,4,\bar{36}$	33.9	-25.9	-